UCRL-10757

1963

# University of California

# Ernest O. Lawrence Radiation Laboratory

TWO-WEEK LOAN COPY

This is a Library Circulating Copy which may be borrowed for two weeks. For a personal retention copy, call Tech. Info. Division, Ext. 5545

## SOME PROPERTIES OF SOLID HYDROGEN AT SMALL MOLAR VOLUMES

Berkeley, California

## DISCLAIMER

This document was prepared as an account of work sponsored by the United States Government. While this document is believed to contain correct information, neither the United States Government nor any agency thereof, nor the Regents of the University of California, nor any of their employees, makes any warranty, express or implied, or assumes any legal responsibility for the accuracy, completeness, or usefulness of any information, apparatus, product, or process disclosed, or represents that its use would not infringe privately owned rights. Reference herein to any specific commercial product, process, or service by its trade name, trademark, manufacturer, or otherwise, does not necessarily constitute or imply its endorsement, recommendation, or favoring by the United States Government or any agency thereof, or the Regents of the University of California. The views and opinions of authors expressed herein do not necessarily state or reflect those of the United States Government or any agency thereof or the Regents of the University of California.

Research and Development

UCRL-10757

UC-4 Chemistry
TID-4500 (24th Ed.)

UNIVERSITY OF CALIFORNIA

Lawrence Radiation Laboratory
Berkeley, California

AEC Contract No. W-7405-eng-48

# SOME PROPERTIES OF SOLID HYDROGEN AT SMALL MOLAR VOLUMES

Guenter Ahlers

(Ph. D. Thesis)

September 24, 1963

Printed in USA. Price $2.50. Available from the
Office of Technical Services
U. S. Department of Commerce
Washington 25, D.C.

# SOME PROPERTIES OF SOLID HYDROGEN AT SMALL MOLAR VOLUMES

## Contents


Abstract . . . . . v

I. Introduction . . . . . 1

II. Apparatus . . . . . 3

A. General Description . . . . . 3

1. Sample-Preparation Units . . . . . 3

2. Pressure System . . . . . 3

3. Cryostat . . . . . 5

4. Sample-Analysis Units . . . . . 7

B. Changes from the Original Design . . . . . 7

1. Sample-Preparation Units . . . . . 7

2. Pressure System . . . . . 7

3. Pressure Cells . . . . . 8

4. Cryostat . . . . . 15

5. Sample-Analysis Units . . . . . 19

III. Experimental Aspects

A. Preparation for Experiments . . . . . 24

B. Thermometer Calibration . . . . . 25

C. Heat Capacity Measurements . . . . . 29

D. The Effect of the Capillary on Afterdrifts . . . . . 29

E. Measurement of Sample Volume and Density . . . . . 32

F. Measurements at High Ortho Hydrogen Concentrations . 38

G. Preliminary Measurements

1. The Heat Capacity of Copper . . . . . 40

2. The Heat Capacity of the Empty Calorimeter . . . 44

IV. The Lattice Heat Capacity of Hydrogen

A. General Comments . . . . . 51

B. Experimental Measurements

1. The Heat Capacity of Para Hydrogen at Constant Pressure . . . . . 52

2. The Heat Capacity of 2% Ortho Hydrogen at 22.56 cc/M . . . . . 54

3. The Heat Capacity of Para Hydrogen at 19.83 cc/M . . . . . 63
4. The Heat Capacity of 6% Ortho Hydrogen at 18.73 cc/M . . . . . 68
C. The Debye Characteristic Temperature and the Grüneisen Gamma of Hydrogen . . . . . 70
D. The Thermodynamic Properties of Solid Para Hydrogen . . . . . 76
V. The Anomalous Heat Capacity of Ortho Hydrogen . . . . . 90
A. The Anomalous Heat Capacity at Low Ortho-Hydrogen Concentrations. . . . . 90
B. The λ Anomaly
1. Thermal Equilibrium . . . . . 97
2. The λ Anomaly at Zero Pressure . . . . . 104
3. The λ Anomaly at Constant Volume . . . . . 112
4. Discussion of Results . . . . . 123
VI. The Kinetics of the Ortho-Para Conversion. . . . . 126
Acknowledgments . . . . . 130
References . . . . . 131

# SOME PROPERTIES OF SOLID HYDROGEN AT SMALL MOLAR VOLUMES

Guenter Ahlers

Inorganic Materials Research Division
of Lawrence Radiation Laboratory
and Department of Mineral Technology
University of California, Berkeley, California

September 24, 1963

## ABSTRACT

Apparatus and experimental procedures are described for the measurements of properties of solid hydrogen over the volume range from 15 cc/M to 23 cc/M and the temperature range from 1.3 °K to 20 °K.

The lattice heat capacity of hydrogen was measured at constant pressure, and at 22.56, 19.83, and 18.73 cc/M. The results are compared with simple theories, and with the lattice properties of other solids. Some thermodynamic properties of solid hydrogen are deduced from the heat-capacity measurements.

The effect of volume changes on the λ anomaly in ortho hydrogen was measured over the volume range from 15.8 cc/M to 22.6 cc/M. The results are in agreement with qualitative predictions based on the intermolecular potential, but the detailed nature of the anomaly is found to be rather complicated.

The kinetics of the ortho-para conversion in solid hydrogen was studied over the volume range from 16 cc/M to 22.6 cc/M and the temperature range from 1.6 °K to 20 °K.

# I. INTRODUCTION

In many respects solid hydrogen is one of the simplest known solids, and a study of its properties may be expected to lead to an improved understanding of the nature of solids in general. In its ground state (para hydrogen), the hydrogen molecule has a spherically symmetric rotational-wave function, and in this respect resembles the inert gases argon and krypton whose properties in the solid state have been studied to some extent both theoretically[1] and experimentally.[2,3] However, it differs from these so-called ideal solids in that it has a rather high compressibility in the solid state. It can therefore be studied over a considerable volume range. Associated with this advantage is, however, the complicating fact that hydrogen has a rather large zero-point energy, and that it may be expected to show some deviations from classical behavior. But these deviations in themselves are of great interest, and a comparison of the properties of solid hydrogen with the predictions of classical theories may result in their better understanding.

In addition to offering the opportunity to study the properties of a relatively simple lattice, hydrogen can also be studied in its first excited rotational level (ortho hydrogen) because of the existence of symmetric and antisymmetric nuclear-spin states between which transition is forbidden in the absence of external perturbations. Ortho hydrogen has an antisymmetric rotational-wave function, and it can exist in solid solution in the para modification. It has three degenerate rotational states in the absence of external perturbations, and the degeneracy is removed by the interaction between neighbors in the crystal. The effect of these rather interesting interactions in the crystal on the rotational states can thus be studied. It was found experimentally that the perturbation depends on the occupation of the rotational states, and that the heat capacity shows an anomalous contribution of the $\lambda$ type, which is characteristic of cooperative phenomena.[4,5] Again because of its great compressibility, hydrogen offers the opportunity to study a cooperative transition over a large volume range.

The magnetic interactions between neighbors in a crystal containing ortho hydrogen result in a nonzero transition probability between the ortho and para modifications, and conversion occurs. But the transition probability is small enough to make experimental study possible over a large volume range. The kinetics of the ortho-para conversion is thus a third interesting problem to be studied in solid hydrogen.

In spite of these opportunities to investigate the properties of relatively simple systems, little is known about solid hydrogen. Orttung recently reviewed the literature on the subject rather extensively,[6] so this review will not be repeated here.

The purpose of this work is to describe investigations of the lattice properties of solid hydrogen, the anomalous contribution to the heat capacity from ortho hydrogen, and the ortho-para conversion in the solid. The apparatus and experimental techniques used during this work are also discussed.

## II. APPARATUS

The apparatus used was designed and built by Orttung.[6] However, a number of changes had to be made before measurements were possible. A brief general description of the apparatus is given here, and is followed by a detailed discussion of those aspects which differ from Orttung's original design.

### A. General Description

Basically the apparatus consisted of four parts: the sample-preparation units, the pressure-generating system, the cryostat, and the sample-analysis units. A schematic diagram is given in Fig. II-1.

#### 1. Sample-Preparation Units

The hydrogen samples used were prepared electrolytically, purified over silica gel at 78 °K, and stored at about 2000 psi in steel cylinders. Before use the gas at 1 atm pressure was passed over copper at 600 °C, and then through a liquid nitrogen cold trap. The sample was then passed through a ferric oxide catalyst at room temperature, 78 °K, or 20 °K depending on the concentration of ortho hydrogen desired. This procedure yielded 75%, 50%, or 0.2% ortho hydrogen concentrations respectively. Other concentrations between 0.2% and 75% could be made by appropriate mixing. After preparation the samples were stored in four 5-liter glass bulbs.

#### 2. Pressure System

The pressure system consisted of a condensing bomb, a series of three U-tubes (each half-filled with mercury), and the cell. The sample was first condensed out of the 5-liter bulbs in the sample-preparation system into a bomb surrounded by solid hydrogen. It was then allowed to expand into one arm of a U-tube half filled with mercury. This was accomplished by warming the bomb above the normal boiling point. The pressure obtained in this manner was about 10 atm. Oil pressure was then applied to the other arm of the U-tube, and the sample was pushed into a second U-tube of smaller volume and

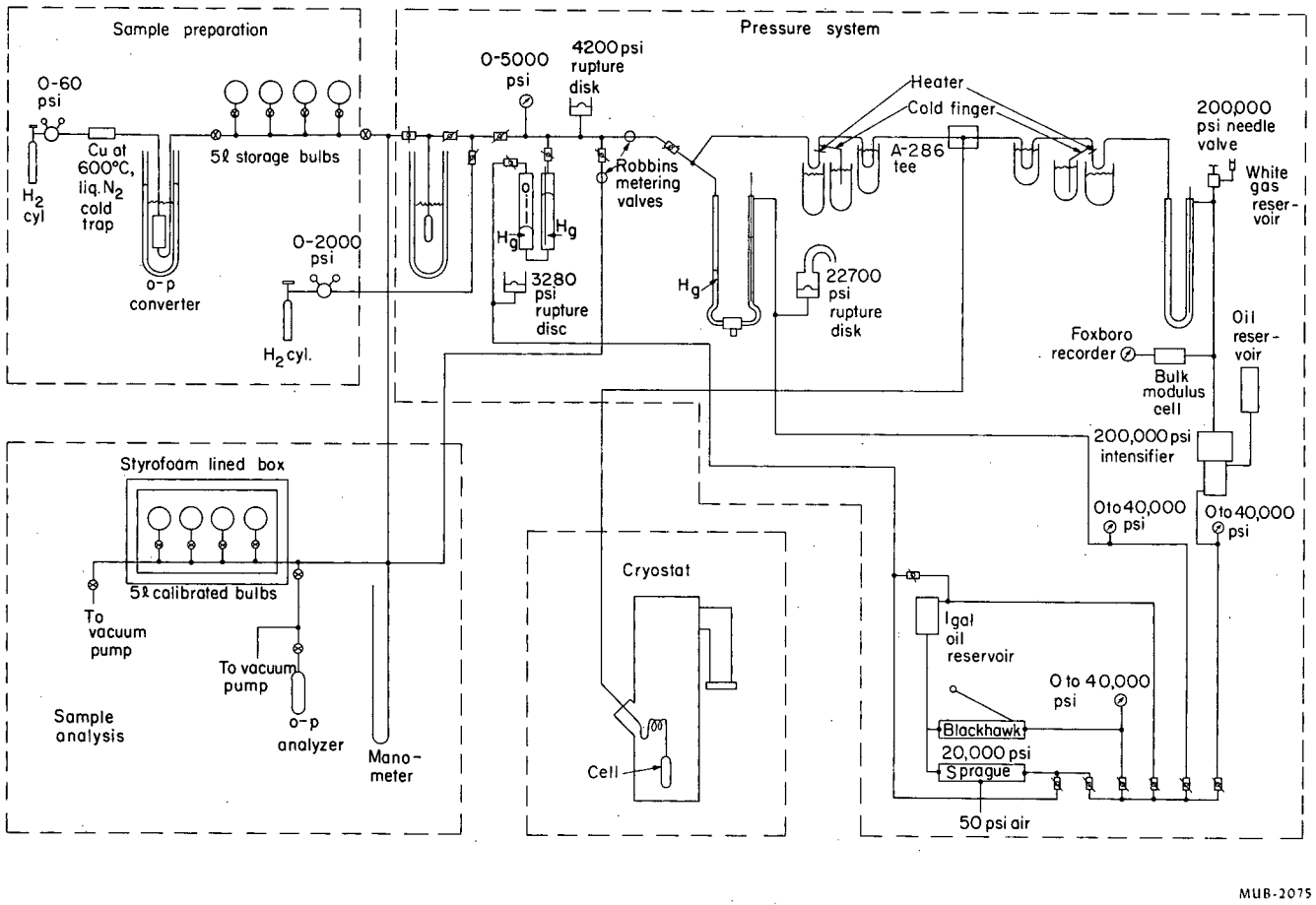


Fig. II-1. Schematic diagram of the apparatus.

heavier design. By a similar procedure the sample was pushed into a third U-tube, and finally into the high-pressure cell in which the thermal measurements were made. The pressure increased approximately by a factor of 10 in each stage, so that a final pressure of about 10 000 atm could be reached.

Mechanical valves were used to confine the sample in the various stages as far as the inlet to the second U-tube. Beyond that point, the successive pressure gradients were supported by mercury frozen in stainless steel capillaries.

The mercury level in the U-tubes was indicated by means of an insulated wire dipped into the mercury. This wire served as a capacitor in one arm of an ac bridge. The bridge unbalance, and therefore the mercury level, was indicated on an ac voltmeter.

The pressure was generated by a Sprague Engineering Corporation S-440-200 air-operated pump, and transmitted by LX-21 Blackhawk hydraulic oil to the first and second U-tubes, and to an intensifier. Pressures above 20 000 psi were needed in the last U-tube, and were generated in a Harwood Engineering Company A-25J intensifier. White gasoline (hexanes) was used as a pressure-transmitting fluid between the intensifier and the last U-tube. A Blackhawk model P-228 hand pump was also in the system and could be used instead of the Sprague pump.

The parts of the system exposed to pressures above 20 000 psi were connected by means of cold-worked 316 stainless steel capillary tubing, 1/8 inch and 0.5 mm i.d.

The sample was sealed in the high-pressure cell by the solid hydrogen plug in the capillary.

### 3. Cryostat

A schematic diagram of the cryostat is given in Fig. II-2. The cryostat had one vacuum system composed of the outer casing A, an MCF 300 diffusion pump B, a gate valve C, a water-cooled baffle D, and a forepump line E. The bottom section of the casing was removable at flange F for access to the high-pressure cell.

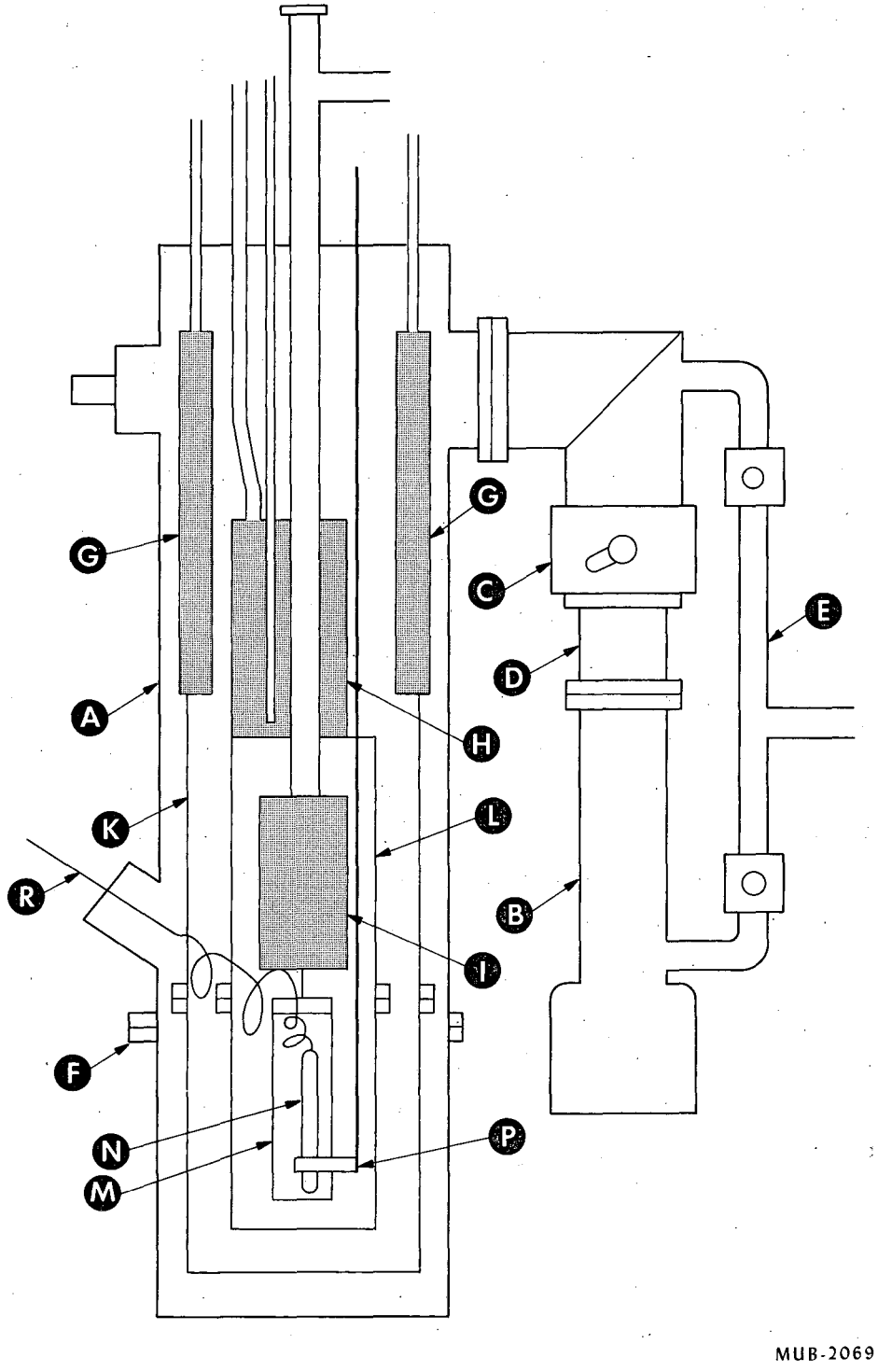


Fig. II-2. Schematic diagram of the cryostat.

Inside the vacuum system were three baths--G, H, and I for liquid nitrogen, hydrogen, and helium respectively. The inner bath (I) was suspended by its pump tube from the outer bath (H). Separate Kinney pumps were used to pump down baths H and I.

Copper shields K and L were attached to the liquid nitrogen (G) and hydrogen (H) baths respectively to thermally protect the lower region of the calorimeter. The bottom sections of these shields were detachable for access to the high-pressure cell. A third shield M protected the cell; its temperature could be regulated above the helium-bath temperature in order to control the heat leak out of the cell N. The cell could be cooled to the helium-bath temperature by means of a mechanical heat switch P. The capillary R was thermally attached to the various shields and connected the cell to the high-pressure system.

### 4. Sample-Analysis Units

The ortho-hydrogen concentration was determined by measuring the thermal conductivity of the gas. The amount of sample used in an experiment was determined by expanding the sample into calibrated 5-liter glass bulbs, thermostated at room temperature, and then measuring the pressure of the gas after expansion.

## B. Changes From the Original Design

### 1. Sample-Preparation Units

There were no changes in the sample-preparation units. The ortho-para converters and the storage bulbs functioned well. The ortho-hydrogen separators described by Orttung were not suitable for enriching the ortho contents above 75%. However, in view of the fact that no measurements at ortho-hydrogen concentrations above 75% were planned, no attempt to modify them was made.

### 2. Pressure System

Several changes from the original design were necessary in the pressure-generating system, and extensive changes in the cell design were required. It was inconvenient to control the low-pressure U-tube

with nitrogen-gas pressure, so oil was used, with the same Sprague Engineering Corporation No. S-440-200 pump that operated the medium- and high-pressure U-tubes. An appropriate rupture disk was installed in the oil line as a safety device. Pressures as high as 3000 psi could be generated in the low-pressure system.

Teflon-insulated No. 22 wire (American Super-Temperature Wires, Inc.) was used for all mercury depth gauges instead of the Formvar-insulated wires. The wire was doubled, and the uninsulated end was at the tops of the U-tubes, thus serving as a short that strongly unbalanced the bridge when the mercury reached that level.

It was found that the safety U-tubes in the high-pressure capillaries did not adequately protect the cell from mercury contamination when cooled with acetone and dry ice. Liquid nitrogen was used instead, except on the high-pressure U-tube side, where acetone and dry ice were used when pressures in excess of 78 000 psi were desired. Even with these precautions, it was necessary to avoid pressure surges in the system. For this reason a Robbins Aviation Inc. INS G 103-1P needle valve was installed on the low-pressure side of the valve separating the medium- and low-pressure system. This made it possible to slowly fill the medium- and high-pressure system with gas up to 3000 psi.

Some difficulties were experienced with the packing head in the intensifier. Pinch-off seemed to occur after repeated use. However, the lifetime of a packing head was long enough to require only occasional replacement.

### 3. Pressure Cells

The pressure cells used in these experiments were made of beryllium-copper. Orttung discussed the properties of this material. It was decided that measurements at low pressures (up to 3500 atm) on the lattice heat capacity should be made in a relatively thin-walled cell to reduce the heat capacity of the empty calorimeter and therefore increase the accuracy of the measurements. Two heavier-walled cells were used for measurements on normal hydrogen over the entire pressure range.

In the low-pressure cell designed by Orttung, the threaded soft-soldered seals always leaked at about 3000 atm. It was decided to develop an unsupported-area type of seal for the low-pressure cell as well as the high-pressure ones. The general design of the cells is shown in Fig. II-3, and dimensions are given in Table II-1. The discussion of the properties of cells given by Orttung is generally applicable to the present design. According to the formulas developed there, the pressure limits for elastic flow of the low-pressure cell should be between 53 000 and 70 000 psi, and the burst pressure should be between 91 000 and 126 000 psi. The cell was tested at pressures as high as 60 000 psi. Since the sample had to be introduced at the liquid nitrogen boiling point, a pressure of 4000 atm resulted only in a pressure of about 2000 atm at 0 °K. The corresponding volume decrease is of the order of 29% of the normal volume of the solid.

The high-pressure cells have a theoretical burst pressure in excess of 150 000 psi.[6] They were tested to 140 000 psi, but were used only at considerably lower pressures. The smallest volume accessible to measurements is not primarily limited by the maximum available pressure, but rather by the freezing pressure of solid hydrogen. At 78 °K, the most convenient temperature for filling the bomb, hydrogen freezes at about 5250 atm. The PVT (pressure-volume-temperature) properties in this region are not known at all; but it can be estimated that this pressure corresponds approximately to a molar volume of 15 cc. Even if one were to fill the bomb at a higher temperature, little would be gained because the freezing temperature increases rapidly with decreasing molar volume. At 10 000 atm, which is about the highest safe operating pressure for the apparatus, hydrogen would melt in the vicinity of 110 °K. The molar volume would be about 14 cc/M. This small gain was not considered worth the additional experimental effort. The high-pressure cells were therefore used only to about 6000 atm. The change in volume of solid hydrogen was about 34%.

The design of a high-pressure seal usable at low temperatures involves some special problems. A general description of the

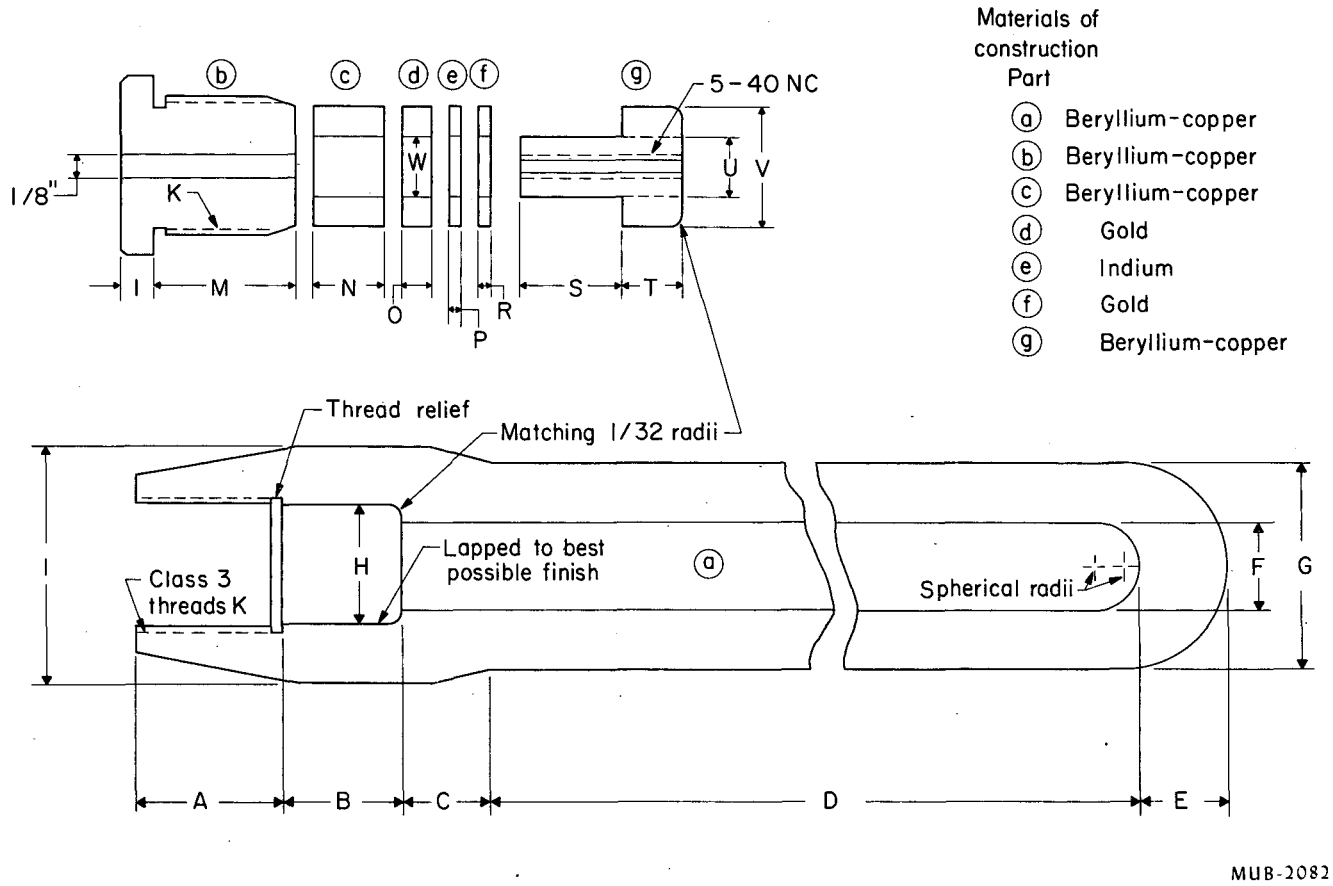


Fig. II-3. High-pressure cell and seal. For dimensions see Table II-1.

Table II-1. Pressure cell dimensions. The symbols refer to Fig. II-3.

| Cell | I (Inches) | II (Inches) | III (Inches) |
|---|---|---|---|
| A | 5/8 | 1/2 | 1/2 |
| B | 1/2 | 1/2 | 1/2 |
| C | 3/8 | 3/8 | 3/8 |
| D | 4-1/4 | 3/4 | 3-5/8 |
| E | 1/4 | 4-3/4 | 1/4 |
| F | 3/8 | 1/4 | 0.094 |
| G | 5/8 | 3/4 | 5/8 |
| H | 0.5000 ± 0.0005 | 0.3440 ± 0.0005 | 0.2500 ± 0.0005 |
| I | 15/16 | 1 | 3/4 |
| K | 9/16-28 | 7/16-28 | 5/16-27 |
| L | 3/16 | 3/16 | 3/16 |
| M | 5/8 | 1/2 | 1/2 |
| N | 1/4 | 1/4 | 1/4 |
| O | 1/8 | 1/8 | 1/8 |
| P | 1/32 or less | 1/32 or less | 1/32 or less |
| R | 1/32 | 1/32 | 1/32 |
| S | 13/32 | 0 | 0 |
| T | 3/32 | 3/32 | 3/32 |
| U | 5/16 | — | — |
| V | H± 0.0002 | H± 0.002 | H± 0.002 |
| W | U± 0.0002 | 1/8 | 1/8 |

unsupported-area type of seal was given by Bridgman.[7] This seal utilizes a soft packing material contained by hard backing washers. By supporting the packing over an area smaller than that over which the inside pressure is applied, a hydrostatic pressure greater than the sample pressure is generated in the packing. Therefore a seal is maintained regardless of the sample pressure. However, the seal will work only if initially it is prepressurized well beyond the yield point of the packing material. This pre-tightening is accomplished by the bolt b (Fig. II-3) and must of course be done at room temperature. In general, a soft packing material will have larger volume changes due to cooling than the surrounding beryllium-copper. Thus there will be a tendency to lose some of the initial compression of the seal. It is therefore necessary to minimize the thickness of the packing, and to use a larger initial seal pressure than one would use at room temperature. Due also to the temperature range is the fact that many materials that are soft enough at room temperature become much harder at low temperatures and thus require a larger initial seal. It was not possible to obtain a seal using lead, although lead seals performed very well at room temperature. Indium, however, was usable at the temperatures of interest. In this work 99.999% pure indium was used. Impurities are believed to affect the flow properties of the metals at low temperatures; however, only the high-purity material was tried.

The use of indium presented an additional problem. Whereas it is difficult enough to contain lead in the seal area, indium is even more difficult to contain. The backing washers had a clearance of less than 0.0005 in. This was not adequate to prevent extrusion of indium. A dead soft-gold washer was therefore placed on each side of the indium. The gold is soft enough to be pushed against the walls and therefore contains the indium. Gold also has a slightly smaller thermal-expansion coefficient than beryllium-copper, and therefore tends to retain the initial seal on cooling. For this reason the gold washer on one side of the indium was made rather

thick. Another advantage of having thick backing washers is that a longer section of the surrounding beryllium-copper is under tension, thus acting like a spring as the indium cools. These general considerations lead to the seal dimensions given in Table II-1. After application of the initial seal, the thickness of the indium washer had been considerably reduced owing to extrusion before the gold washers began to flow. One seal was taken apart after some pressure testing, and the indium washer was found to be only 0.01 in. thick; but this thickness was adequate to make a seal.

We first attempted to use only the capillary cross section as unsupported area. This has the advantage that the indium seal works against the capillary as well as against the wall, and one does not depend on the threaded soft-solder joint to be leaktight; but in the low-pressure cell the unsupported area was only about 7% and this was not enough. The design shown in Fig. II-3 with the dimensions in Table II-1 was therefore adopted. This design required that the soft-soldered threads on the capillary not leak. The method used to seal the threads is illustrated in Fig. II-4. The threads C on the capillary B are made to fit the threads in the washer A as well as possible. The capillary was drilled out at the cell end so that it became a thin-walled cylinder for about 3/32 inch. The top of this cylinder was spread by center punching. It was hoped that the sample pressure would stretch the capillary enough to seal against the soft solder. A thin copper plate D was then soft-soldered against the capillary end, and a fillet of solder E was applied. The author is indebted to Dr. Leonard X. Finegold for the idea of using the copper plate. Although it is not understood which features make this seal work, it has been used successfully at pressures as high as 3500 atmospheres, and it may hold at higher pressures.

In the high-pressure cells, it was possible to use only the capillary cross section as unsupported area because of the smaller seal diameter. The indium thus sealed against the capillary tube, and no particular problem with leaking threads existed.

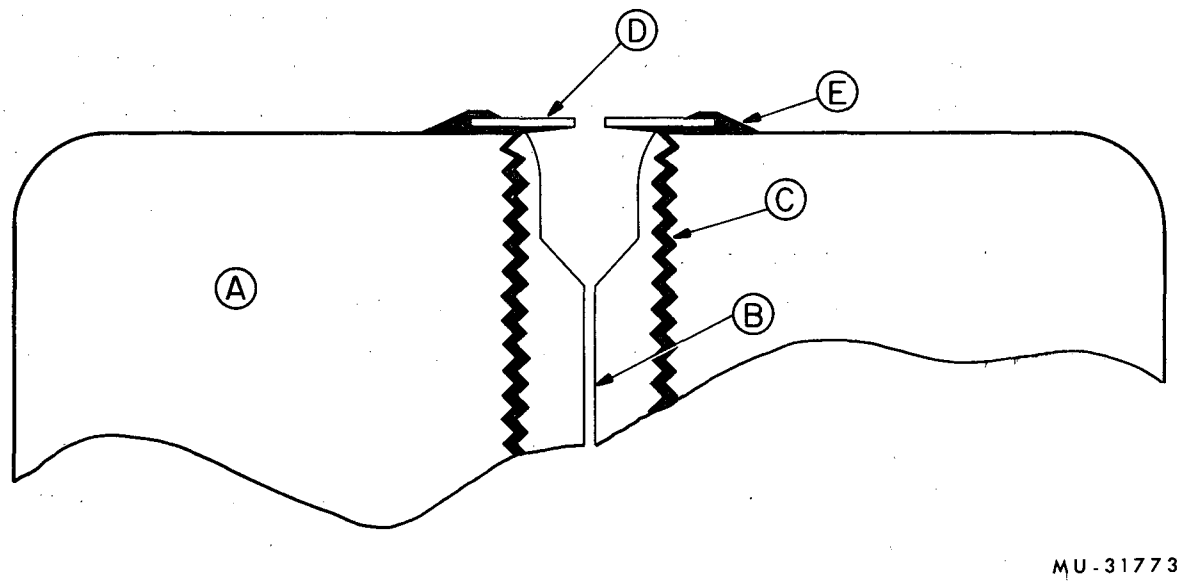


Fig. II-4. Capillary seal. A is the washer g of Fig. II-3. B is the capillary, C the soft-soldered threads. D is a thin copper plate, and E a fillet of soft solder.

4. Cryostat

Changes had to be made in the design of the cryostat and the associated electrical circuitry.

It was found that a single high-pressure capillary could be used to connect the cell to the pressure system. Orttung intended to use two, so that purging of the cell with the sample would be possible. Experience showed that the cell could be pumped out fairly well, and that filling with a sample to a few atmospheres, followed by reevacuation, was adequate to eliminate appreciable quantities of impurities. The stainless steel capillaries had a large electronic heat capacity, two capillaries caused severe difficulties in the heat-capacity measurements in the helium region. Using only one capillary also eliminated one high-pressure seal at the cell.

The vacuum seal at the flange where the capillary leaves the vacuum jacket was originally made of Armstrong Company's A-2 epoxy resin. We found that the cooling of the capillary that occurred when a sample was permitted to leave the cell caused cracking of this seal. The seal was thus made with soft solder.

The liquid nitrogen and outer liquid hydrogen baths functioned, in general, according to Orttung's calculations. Liquid helium was tried in the outer bath and was found to last 2 to 3 h with the nitrogen reservoir at the normal boiling point.

The heat leak to the inner liquid helium bath was measured by checking the rate at which helium gas escaped from it. It was found that the heat leak was higher by about a factor of 10 than the predicted 16 mW. The lowest temperature that could be reached was about 1.46 °K. The corresponding vapor pressure of 3 mm Hg agrees with the pumping speed of the Kinney KD-30 pump.

After considerable experimenting it was found that the excessive heat leak to the inner bath was caused by the vibrations of the gas column in the permanently mounted transfer tube. A removable transfer tube was built, and the original heat leak was reduced by a factor of three or four. After this change, 1.27 °K could be reached, corresponding to a vapor pressure of about 1 millimeter.

One filling of the inner bath with liquid helium lasted about 24 h. Four liters of liquid helium was required to cool the transfer tube and fill the bath. The lowest temperature attainable with solid hydrogen in this bath was 8.7 °K.

In a first attempt to measure the heat capacity of normal hydrogen at a molar volume of 18.8 cc, it was discovered that the 8 cc of solid contained in the low-pressure cell could not be cooled below 3 °K, with the inner bath at 1.5 °K, because of the large rate of heat generation due to the ortho-para conversion. Observation of the temperature of the vapor-pressure bulbs showed that most of the thermal gradient was across the contact surfaces of the thermal switch. The contact surfaces were therefore modified by covering them first with indium and later with gold. In the latter modification the contact area was also increased by a factor of 3.5. The change in area was made because the measurements with the indium surfaces seemed to indicate that the thermal conductivity of the switch was pressure-independent. The thermal conductivity of the switch was measured for the original design and for each modification by closing the switch, putting heat into the empty cell at a known rate, and measuring the corresponding temperature rise. The results are given in Table II-2. The improvement was not sufficient to cool normal hydrogen below the λ transition. It was therefore necessary to make measurements on normal hydrogen in the high-pressure cells, which had a smaller volume.

Table II-2. Thermal conductivity of the heat switch.

| Temp. (°K) | Thermal conductivity $\left(\frac{mW}{°K}\right)$ | | |
|---|---|---|---|
| | Orig. Design | 1st Modification | 2nd Modification |
| 1.6 | 0.8 | 2.5 | — |
| 4.3 | 3.1 | 7.0 | — |
| 10.5 | 9.5 | 17.0 | 21 |
| 20.0 | 21.0 | 39.0 | 44 |

The isothermal shield is essentially as described by Orttung. An additional semicircular disk of lead 1/2-in. thick and 1 3/8-in. in diameter was soldered into the bottom of the detachable half of the shield. The primary purpose of this was to dampen vibrations rather than to increase the heat capacity. The two parts of the shield were thermally connected by two heavy copper wires, one on each half, which were soft-soldered together. The thermal-switch contact surfaces on the shield were coated with indium.

Details of the cell design are given in Sec. B. 3. The thermometer and heater were changed from Orttung's design. The heater consisted of about 16 ft of Formvar-insulated manganin wire, 0.00175 in. in diameter (93.3 Ω/ft), that was bifilarly wound around the middle of the cell. The use of cigarette paper as insulating material, advocated by Orttung, was not found necessary. The heater was well covered with G. E. 7031 cement. The resistance of the current leads from the shield to the cell was measured with a Weston ohmmeter and found to be 1.2 Ω for each lead. One half of this was added to the measured heater resistance.

One germanium thermometer purchased from the Honeywell Company was mounted on the cell in a manner identical to that described by Orttung for the carbon thermometers. The thermometer was a Series II probe device.

Six solder lugs, each consisting of insulated copper wire, were glued to the cell with G. E. 7031 cement. Two were used for the heater and the other four for the thermometer.

One stainless steel capillary, 1/8 in. o. d. and 0.5 mm i. d., suspended the cell in the shield and connected it to the pressure system.

The approximate thermometer resistance R and its temperature coefficient $-\frac{dT}{dR}$ are given in Table II-3 as a function of the temperature (T).

Thermometer currents from 0.1 to 100 μA were required to obtain the necessary thermometer sensitivity over the entire range. A circuit similar to the one described by Orttung was used for the

Table II-3. Thermometer characteristics.

| T(°K) | R(Ω) | $-\frac{dT}{dR}$ (°K/Ω) |
|---|---|---|
| 1.5 | 13000 | 0.00004 |
| 2.0 | 6000 | 0.0001 |
| 4.0 | 1300 | 0.002 |
| 10.0 | 200 | 0.022 |
| 20.0 | 47 | 0.250 |

purpose. It differed only in that there was only one thermometer on the cell. The thermometer potential was read on a Rubicon 2773-S potentiometer.

The input impedance of the Beckman Instruments Model 14 dc breaking amplifier, which was used as a galvanometer, was 20 000 Ω. Below 4 °K, the high impedance of the thermometer caused a decrease in the amplification of the potentiometer unbalance. Frequent sensitivity readings were used to compensate for this.

A Leeds and Northrup K-3 potentiometer measured the potential across the 10 kΩ standard resistor in the thermometer circuit when the current was larger than 10 μA. This potentiometer was modified by disconnecting the internal ground to the chassis, which was then properly grounded. After this change was made, a potential from the same source gave the same reading on the K-3 and the Rubicon potentiometer, within the limits of the instruments. Currents smaller than 10 μA were measured on this potentiometer.

The heater circuit designed by Orttung was found to be unsuitable and had to be changed entirely. With the old circuit, the heater was not grounded when the current was switched to the dummy. Consequently the potential of the heater had to decay through the counter when the heater was turned off. The capacitance of the leads from the circuit to the heater were large enough to result in a time constant of about 1 sec with the 10 MΩ leak to ground through the counter. This caused the counter to turn off about 1 sec late. A new circuit was

built with the heater always close to ground potential. This made it necessary to operate the counter by a separate circuit, with a relay in series with the relay operating the heater. In the new circuit the counter operated within $2 \times 10^{-3}$ sec of the heater. The details of this circuit can be seen in Fig. II-5. The circuit components were those described by Orttung.

The electronic shield and bath-temperature regulator designed by Orttung was found to be rather unstable. They were used only to regulate the shield temperature for measurements above 4 °K. The shield temperature was monitored by means of a copper-iron vs copper difference thermocouple between the shield and the bath. The approximate sensitivity of the thermocouple is given in Table II-4. The copper-iron alloy contained 0.0111 wt% iron. For the shield regulation it is necessary only to maintain a constant temperature, and it is not necessary to know this temperature very accurately. A change of 0.5 μV in the thermocouple potential could be detected, corresponding to about 0.3° at 2°, 0.1° at 4° and 0.007° in the hydrogen region. Above 4 °K, the shield regulator was used during measurements, and it was adjusted when necessary as indicated by the thermocouple. In the helium region, the shield was left at the bath temperature, and the bath temperature was adjusted. This was possible because the shield was thermally coupled much better to the bath than the cell was to the shielf. Very accurate bath-temperature regulation was accomplished by means of a mechanical regulator similar to the one described by Walker.[8]

5. Sample-Analysis Units

The ortho-para analyzer described by Orttung was found to be somewhat unstable. It was believed that the instability arose primarily from convection along the wire. In Orttung's design, part of the sample was at room temperature, and convection can be expected to upset the otherwise stable thermal gradient in the sample. An analyzer was therefore designed in which all the sample was cold, except for that in the inlet tube. The inlet entered the analyzer at the bottom. A diagram of the analyzer is shown in Fig. II-6.

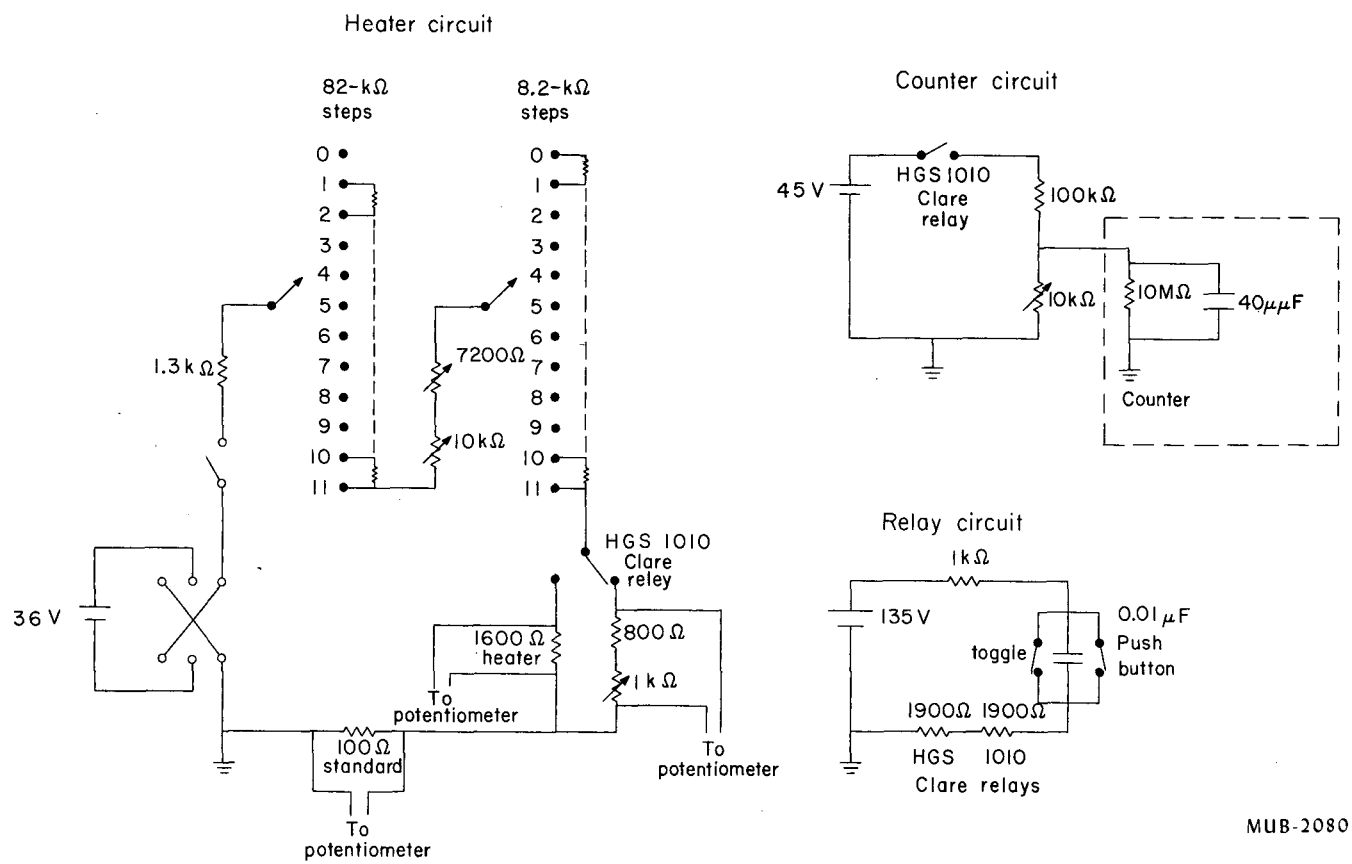


Fig. II-5. Heater and associated circuits.

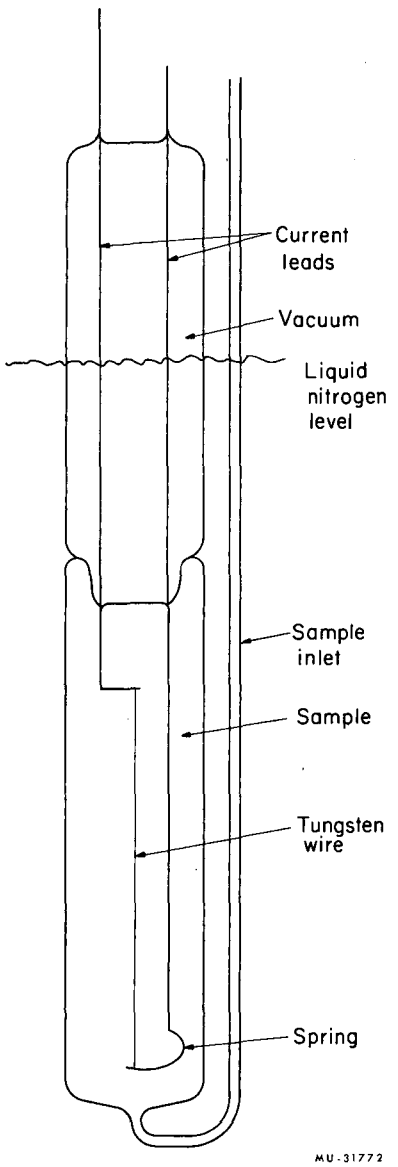


Fig. II-6. Ortho-para analyzer.

Table II-4. Approximate sensitivity of the copper-iron vs copper thermocouple.

| T (°K) | $\frac{dE}{dT}$ (μV/°K) |
|---|---|
| 20 | 7.4 |
| 18 | 7.4 |
| 16 | 7.3 |
| 14 | 7.2 |
| 12 | 7.0 |
| 10 | 6.7 |
| 9 | 6.4 |
| 8 | 6.0 |
| 7 | 5.5 |
| 6 | 5.0 |
| 5 | 4.3 |
| 4 | 3.6 |
| 3 | 2.7 |
| 2 | 1.8 |
| 1 | 0.7 |

The 6-V storage batteries were found to drift considerably at the high current needed. A Kepco Model SC-30-1 constant-current power supply was therefore used instead. A current of 0.8 A was used. Both the current and the potential were determined on the Rubicon potentiometer. Analysis were reproducible to ± 0.2% ortho hydrogen.

# III. EXPERIMENTAL ASPECTS

## A. Preparation for Experiments

Except when normal hydrogen was to be used, the sample on which measurements were to be made was generally prepared one day previous to the experiment. It was stored in the 5-liter bulbs in the sample-preparation section. Conversion from para to ortho hydrogen in these bulbs was measured by storing para hydrogen in them for over a year. The conversion rate was less than 1% per month.

On the same day the sample was prepared, the cell at room temperature was pumped out and flushed several times with hydrogen. Cooling of the cryostat was then started. All three baths were filled with liquid nitrogen and left over night. The cell was cooled by means of the mechanical "heat switch." Actually only a few hours were needed to cool to 78 °K.

On the day of the experiment, the cell was once more flushed a few times with a part of the sample. The rest of the sample was then put through the various compression stages and forced into the cell at 78 °K. In this way pressures of about 5000 atm could be reached without freezing the sample in the capillary. During experiments on para hydrogen it was observed that some conversion to ortho hydrogen occurred when the above procedure for pressurizing the sample was used. Thermal conductivity analyses of samples from various parts of the pressure system showed that this conversion occurred only in the medium- and high-pressure U-tubes.

For the compression of para hydrogen a different procedure was therefore adopted while still empty, the cell was first cooled to about 15 °K by removing the liquid $N_2$ from the upper and lower bath, then filling the lower bath with liquid $H_2$. The cell was then connected to the low-pressure system and storage bulbs. The sample was condensed in the condensing bomb, and put through the compression stages as usual. Thus the cell was filled with liquid without the use of high pressure. As the pressure was finally increased, the lower bath was emptied and bath and cell were rewarmed to some temperature above the freezing point of hydrogen by passing gaseous $N_2$ through

the bath. In this manner, only a small fraction of the sample was ever exposed to high pressure in the U-tubes. No conversion was observed on samples of para hydrogen treated in this manner.

After the sample was in the cell the thermal switch was opened, the liquid nitrogen was blown out of the two baths to be filled with liquid hydrogen, and liquid hydrogen was transferred. The thermal switch was closed soon after the hydrogen transfer.

After about 1 hour, the cell had reached a temperature of about 21 °K. The hydrogen was then blown out of the inner bath, and liquid helium was transferred if measurements in the helium temperature range were to be made. If the hydrogen range only was to be covered, the inner bath was pumped down. The outer bath was pumped down either after the helium transfer, or after pumping on the inner bath was started.

After both baths and the cell were at 10 °K or lower, the pressure in the room-temperature part of the system was released to somewhat less than 1 atm and monitored on a mercury manometer during experiments on para hydrogen. The room-temperature volume at this point was a few hundred ml, and the manometer pressure was very sensitive to any extrusion of hydrogen in the capillary. No movement of sample in the capillary was ever observed.

When experiments on normal hydrogen were done, it was never possible to reduce the external pressure to less than a few hundred psi without causing the capillary plug to break. The reasons for this are not fully understood.

After the above steps, the sample was ready for the thermal measurements.

## B. Thermometer Calibration

The thermometer was calibrated against the vapor pressures of para hydrogen and helium. Two vapor-pressure bulbs were located on the jaws of the heat switch, and the switch was kept closed during the calibration. The data of Wooley, et al.[30] were used for the hydrogen-vapor-pressure — temperature relation, and the 1958 $He^4$

scale of temperatures[31] was used in the helium region. The mechanical bath-temperature regulator was used to control temperatures that were stable to within $\pm 1 \times 10^{-3}$ °K for many minutes.

The calibration points were fitted on an IBM 7090 computer by the method of least squares to the relation

$$T_c = \frac{\log R}{[A + B \log R + C \log (1 + DR^E)]^2} \qquad \text{(III-1)}$$

where A, B, C, D, and E are adjustable parameters. This relation was suggested by the fact that a plot of $(\log R/T)^{1/2}$ vs log R seemed to asymptotically approach linear behavior at both the low and high ends of the temperature range of interest. This behavior can be represented by the relation

$$(\log R/T)^{1/2} = \log (a R^b + c R^d) , \qquad \text{(III-2)}$$

which when solved for T gives relation (III-1) except for the parameter C, which was arbitrarily added.

The equation fitted the data within 0.5% in T everywhere from 1.5 to 20 °K where calibration data were available. Temperatures were calculated from resistances by means of an IBM 650 data-processing machine. These temperatures are designated by $T_c$. The quantity

$$1 + \Delta = 1 + \frac{T - T_c}{T_c} = \frac{T}{T_c} \qquad \text{(III-3)}$$

was plotted on large-scale graph paper as a function of $T_c$, for all calibration points. In order to obtain true temperatures, one needs only to multiply $T_c$ by $1 + \Delta$:

$$T = (1 + \Delta)\, T_c . \qquad \text{(III-4)}$$

In the temperature range of interest one of the main problems in thermometry is the thermometer calibration between 4.2 and 10 °K. No vapor-pressure scale is available, and only gas thermometry can be used for direct calibration. An alternative indirect calibration can be obtained by the extrapolation of the difference plot $1 + \Delta$ vs $T_c$ from both the hydrogen and the helium regions into this range so as to

give a smooth relation. This procedure, in conjunction with suitable empirical equations, has frequently been used for the calibration of carbon thermometers.[9] Equation (III-1) represents the behavior of the germanium thermometer as well as any known relations represent the behavior of carbon thermometers in the regions where calibration data are available. The extrapolation of the difference (III-3) is thus equally justified. A comparison was also made of the direct extrapolation of the difference plot obtained from (III-1) with that obtained by calibrating the germanium thermometer against a carbon thermometer for which the difference plot had been extrapolated. No benefit could be derived from this procedure. Any extrapolation will of course introduce considerable errors in the temperature scale for any thermometer; but the effect on the heat capacity should be only a few percent.[9,10] For normal hydrogen the accuracy of the heat-capacity measurements was only of the order of several percent, so the above procedure is not unreasonable in this case. It was adopted in the present work.

The heat-capacity error introduced by the procedure adopted here was estimated from the measurements on copper reported below. The measurements on copper, when plotted as $C_L/T^3$ vs $T^2$ (where $C_L$ is the lattice heat capacity of copper), showed a definite dip in the region between 5 and 10 °K, and the maximum deviation from a well-behaved relation was 3.8 % of the total heat capacity. The same behavior was observed for the empty calorimeter and for para hydrogen. As a first approximation it can be assumed that errors in the heat capacity due to temperature-scale errors are proportional to the heat capacity.[17] Thus, all heat capacity measurements between 5 and 10°K were multiplied by an appropriate factor determined from the copper results. The effect is demonstrated in Figs. III-3, and III-5 for the copper data, and the results on empty calorimeter respectively. The factor derived from the copper data is given in Table III-1.

We hope that in the future we will be able to calibrate the thermometer used in these experiments by gas thermometry. Then all data can be recalculated.

Table III-1. Heat capacity correction factor derived from the copper results.

| T (°K) | Factor |
|---|---|
| 5.0 | 1.000 |
| 5.5 | 1.009 |
| 6.0 | 1.021 |
| 6.5 | 1.032 |
| 7.0 | 1.038 |
| 7.5 | 1.037 |
| 8.0 | 1.026 |
| 8.5 | 1.006 |
| 9.0 | 1.007 |
| 9.5 | 1.006 |
| 10.0 | 1.001 |

## C. Heat-Capacity Measurements

Heat-capacity measurements were made by passing a known current through the heater on the cell for a known time period, and measuring the corresponding temperature rise with the germanium thermometer. The heater current was measured by means of a standard 100 Ω series resistor to ± 0.05 % or better. The heater resistance was measured at several temperatures by passing a known current (usually 100 μA) through it and measuring the potential drop across it. Heater resistance was plotted as a function of temperature; for each heat-capacity point the appropriate value was read off this graph to ± 0.02 %. The heating time was measured with a Model 7250 CR time interval meter (Berkeley Division, Beckman Instruments, Inc.), to $\pm 2 \times 10^{-3}$ sec. The heat capacity is given by the relation

$$C = \frac{i^2 R \Delta t}{n \Delta T}, \qquad \text{(III-5)}$$

where n is the number of moles of sample, i is the heater current, R the heater resistance, Δt the heating time, and ΔT the temperature rise.

The determination of ΔT in some cases presented some special problems. In principle, the fore- and afterdrifts were extrapolated to the middle of the heating period. For a thermally well-isolated sample this is straightforward. For the bombs in which the present measurements were made, some complications existed because of the low thermal diffusivity and high heat capacity of the stainless steel capillary.

## D. The Effect of the Capillary on Afterdrifts

The treatment of foredrifts was in general quite straightforward. They could always be linearly extrapolated to the middle of the heating period. This extrapolation usually involved a time period of less than 30 sec, and introduced an error that was negligible compared with that due to the afterdrift extrapolation.

The treatment of afterdrifts was more complex. As Orttung[6] observed, after a heat input the sample cooled rapidly until a thermal

gradient dependent only on the sample and shield temperatures was established in the capillary. The time period within which this thermal gradient was established had to be reasonably small, both to make measurements possible in a reasonable length of time and to keep the length of afterdrift extrapolation to a minimum. Orttung's original length of capillary required about 2 h after a heat input for the establishment of a steady gradient. Therefore the capillary length had to be reduced considerably. This was accomplished by attaching a greater length of it to the shield. After this modification the afterdrifts for the empty calorimeter became well behaved after about 10 min. When measurements on para hydrogen were made, it was observed that the 0.5-mm-diam core of sample in the capillary had a considerable thermal conductivity, and with the full calorimeter the afterdrifts became well behaved within 3 or 4 min. We assumed that the thermal conductivity of the capillary was constant over the range between the sample temperature and shield temperature. This assumption implies that the thermal gradient established after the initial relaxation was linear. The drift observed after the initial relaxation had to be extrapolated to the middle of the heating period.

For measurements below 10 °K, the cell temperature had approached the shield temperature by an appreciable fraction of the original temperature difference by the time a linear gradient was established, and no truly linear afterdrift was ever observed. It was therefore necessary to make a more complicated drift extrapolation than is customarily done. The basic heat-flow equation for the problem is

$$\frac{dQ}{dt} = \frac{K}{L}(T - T_S) - H , \qquad \text{(III-6)}$$

where $Q$ is the energy leaving the cell, $t$ is the time elapsed since the middle of the heat input, $K$ is the thermal conductivity coefficient of the capillary, $L$ is the length of the capillary, $H$ is any shield-independent heat leak to the cell, and $T_S$ is the shield temperature. Now

$$\frac{dT}{dt} = -\frac{1}{C}\frac{dQ}{dt} , \qquad \text{(III-7)}$$

where T is the temperature and C the heat capacity of the cell. It was previously assumed that K was constant over the temperature range between the cell and the shield temperatures, and it is now further assumed that C was also constant over the narrower range of the afterdrift. Equations (III-6) and (III-7) then yield the solution

$$\log \frac{T_S' - T_0}{T_S' - T} = \frac{K}{CL} t , \qquad \text{(III-8)}$$

where

$$T_S' = T_S + LH/K . \qquad \text{(III-9)}$$

The presence of a shield-independent heat leak is equivalent to having an effective shield temperature $T_S' > T_S$.

If one has a means of determining $T_S'$, then it is easy to find $T_0$ from Eq. (III-8). From the fore- and afterdrifts and the differential equation

$$\frac{dT}{dt} = \frac{K}{CL} (T_S - T) + \frac{H}{C} , \qquad \text{(III-10)}$$

$T_S'$ was determined. Equation (III-10) readily follows from Eqs. (III-6) and (III-7). Simple manipulation yields

$$\frac{K}{CL} = \frac{1}{T_a - T_f} \left[ \left(\frac{dT}{dt}\right)_f - \left(\frac{dT}{dt}\right)_a \right] , \qquad \text{(III-11)}$$

where $T_a$ and $T_f$ are the temperatures at which the fore- and afterdrifts $(dT/dt)_f$ and $(dT/dt)_a$ were determined. Equations (III-9), (III-10), and (III-11) can now be used to find $T_S'$. One has

$$T_S' = \frac{(T_a - T_f)(dT/dt)_f}{(dT/dt)_f - (dT/dt)_a} + T_f . \qquad \text{(III-12)}$$

To find $T_0$, two points along the afterdrift are considered. Equation (III-8) gives

$$\frac{K}{CL} = \frac{1}{t_1 - t_2} \log \frac{T_2 - T_S'}{T_1 - T_S'} , \qquad \text{(III-13)}$$

where $T_1$ and $T_2$ are the temperatures at $t_1$ and $t_2$ minutes after the middle of the heat input. We preferred to use this value of K/CL rather than that of Eq. (III-11), for it is more representative of that experienced during the afterdrifts, and may differ slightly from that of Eq. (III-11), if K/CL is not truly temperature-independent. An error in $T_S'$ introduces a relatively smaller error in K/CL. $T_0$ can now be calculated from Eq. (III-8) and is given by

$$T_0 = T_S' \left(1 - e^{Kt_1/CL}\right) + T_1 e^{Kt_1/CL} . \qquad \text{(III-14)}$$

For the empty cell at 4 °K the effect of making the above drift extrapolation rather than a linear one is a decrease of about 2 % in the measured heat capacity. The temperature as a function of time along an afterdrift for the empty cell is plotted in Fig. III-1, together with the drift calculated according to the above theory. The theoretical points are based on Eq. (III-8), and the parameters were determined from the experimental points along the afterdrift at 10.1 and 20.1 min. After 80 min, the theoretical points are $4 \times 10^{-3}$ °K higher than the experimental points. This gives confidence to the use of the theory for extrapolation to zero time. The linear extrapolation through the points at 10.1 and 20.1 min is also shown.

In practice the evaluation of the parameters proved to be somewhat tedious and the problem was therefore programmed for an IBM 650 data processing machine.

## E. Measurement of Sample Volume and Density

For the measurements on para hydrogen, the number of moles of sample was determined after the thermal measurements were completed, by expanding the sample into large calibrated bulbs at room temperature. The bulb temperature was regulated and measured to ± 0.1 °C, and the pressure of the sample in the bulbs was determined on a mercury manometer to within ± 0.1 mm. Generally about 97 % of the sample was in the bulbs at constant temperature, and the rest was in the system at a less accurately known temperature. The total

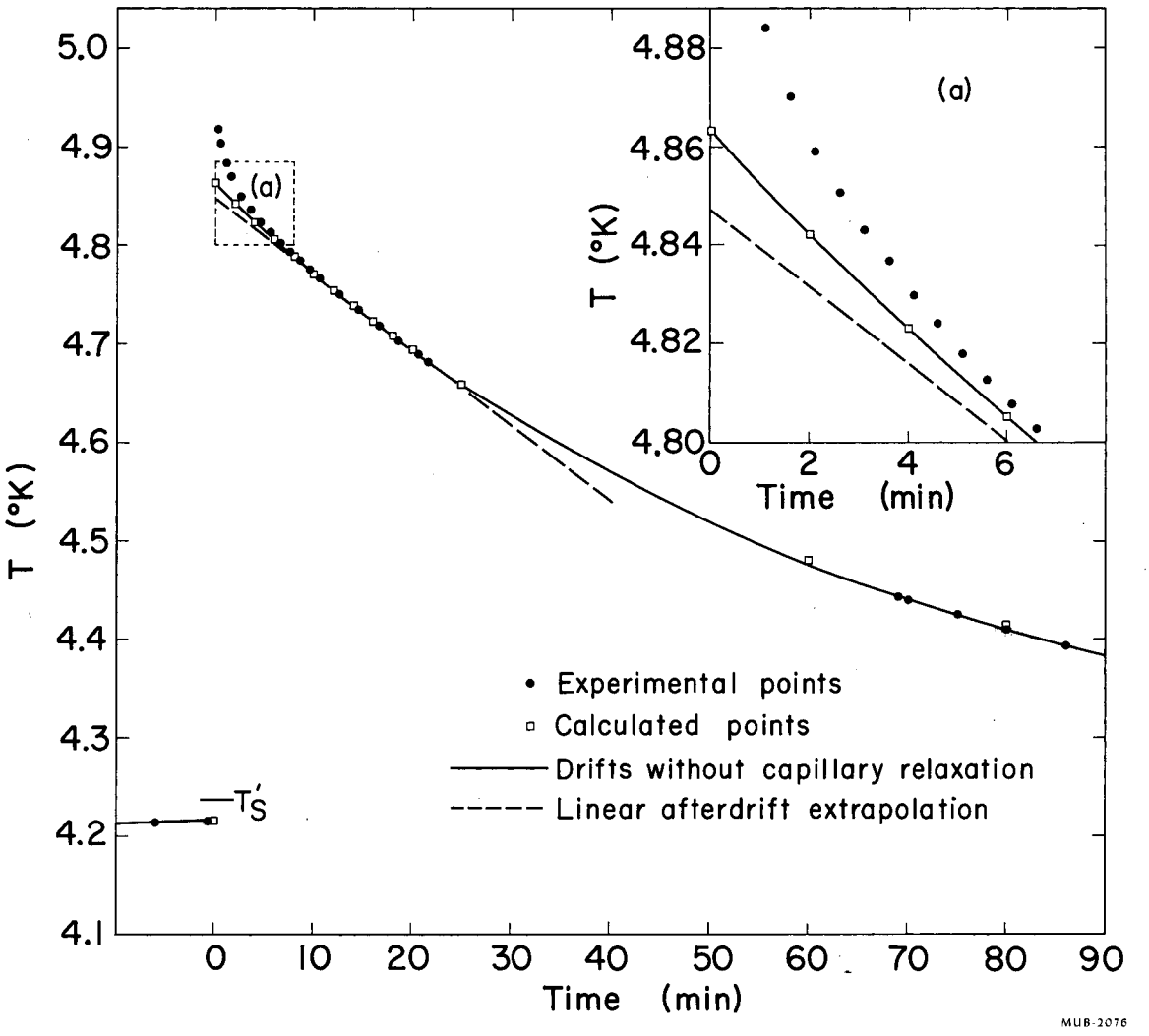


Fig. III-1. Capillary relaxation effect on afterdrifts.

number of moles could therefore have been determined to within ±0.1% if the volume of the bulbs had been known to this accuracy.

The bulbs were calibrated by expanding 2 liters of helium gas into them from a calibrated smaller bulb. The 2-liter bulb was calibrated to ± 0.05% by filling it with water and weighing it. The deviation of helium from the ideal gas law is small enough to be neglibible here, and the ideal gas law was used to calculate the volumes of the large bulbs. Successive measurements were reproducible to ± 0.3%, and it is believed that this is the probable error in the determination of the total number of moles of sample in the system.

Orttung discussed in considerable detail the problems involved in determining the fraction of the sample contained in the cell. Because of a number of uncertain quantities he estimated that the amount of sample in the cell can be determined with an accuracy of only a few percent. This problem was avoided in the case of para hydrogen by releasing the pressure in the room-temperature part of the system after a plug of solid hydrogen was formed in the capillary. This pressure was reduced to less than 1 atm and monitored on a mercury manometer during the thermal measurements to make sure that the solid hydrogen plug did not move. The room-temperature volume was a few hundred ml, and the pressure monitoring was thus very sensitive to shifts in the solid level in the capillary. With this method one needs to know the room-temperature volume of the pressure system to within only a few ml, and the PVT properties of the fluid need not be known to calculate the fraction of the sample in the cell. Only the lengths of the capillary at the various temperatures and the cell volume need be known. These are given in Table III-2.

Orttung showed that one-third of the sample in the capillary between the cell and the shield contributed to the heat capacity if the afterdrifts resulting from a linear thermal gradient in the capillary were extrapolated. This estimate was used in the measurements on para hydrogen and in this case the sample volume therefore was equal to the cell volume plus 0.022 cc.

It was necessary to know the length of capillary filled with solid and liquid, so that the proper correction could be made to the total

Table III-2. Capillary and cell volumes and lengths.

| Item | Length (cm) | Volume ($cm^3$) |
|---|---|---|
| Cell | — | 8.262 |
| Capillary at cell temperature | 3.5 | 0.010 |
| Capillary between cell and shield | 12.1 | 0.036 |
| Capillary at shield temperature | 30.3 | 0.090 |
| Capillary between shield and inner bath | 5.4 | 0.016 |
| Capillary at inner bath temperature | 4.8 | 0.014 |
| Capillary between inner and outer bath | 17.9 | 0.053 |
| Capillary at outer bath temperature | 3.8 | 0.011 |
| Capillary between outer and liquid $N_2$ bath | 43.3 | 0.129 |
| Capillary between liquid $N_2$ bath and room temperature | 21.3 | 0.063 |

amount of hydrogen in the system. This length was determined in each experiment from the vapor pressure in the capillary and the approximate thermal gradient along the capillary. An estimate of the thermal gradient was obtained from the temperatures of the outer and inner bath. The liquid ended anywhere between the inner bath and the liquid nitrogen baths. Depending on the location of this boundary, the amount of sample in the capillary could be estimated with an accuracy of 0.005 to 0.02 cc. The fraction in the cell could therefore always be determined to within ± 0.3% and usually was known more accurately.

The volume of the pressure system was always a part of the volume in which the total amount of hydrogen was measured after it was expanded. Since the medium- and high-pressure U-tubes contributed to this volume, and since the volume of these U-tubes depended on the mercury level in them, it was necessary to measure the volume of the pressure system after each experiment. The pressure system usually had a volume of about 140 cc. During the measurement of this volume, and of the total amount of sample, the cell temperature was determined and the amount of gas in the cell was estimated on the basis of the ideal gas law. The use of this law is justified in this case because of the small amount of sample involved in this correction.

The volume of the low-pressure cell at room temperature was determined by first weighing it empty and then filled with water. The thermal contraction between room temperature and the experimental temperature range was estimated, assuming the validity of the Grüeneisen relation

$$\beta = K \gamma C_V / 3V . \qquad \text{(III-15)}$$

$C_V$ was assumed to be given by the Debye theory, with $\theta$ equal to 340 °K. $\gamma$ was taken as 1.96, and a value of $1.67 \times 10^{-5}$ was used for $\beta$ at 60 °C. The calculated difference in cell volume between 300 °K and 0 °K was 1.02% for the low-pressure cell.

The volume of the low-pressure cell was also measured at liquid-hydrogen temperatures by filling the cell with liquid hydrogen at a pressure of less than 1 atm and measuring the amount of hydrogen

in the calibrated bulbs at room temperature. During these measurements the cell was first filled at 78 °K to a pressure of about 10 atm, and then cooled at constant pressure to approximately 18 °K. The cell temperature was then kept constant to ± 0.002 °K, when the pressure was slowly reduced to less than 1 atm but more than the vapor pressure at the cell temperature. After thermal equilibrium had been reached both in the cell and in the capillary, the vapor pressure in the capillary and the cell temperature were measured. From these data the length of capillary filled with liquid could be estimated. The amount of hydrogen in the cell was determined as described above, and the molar volume of hydrogen under the particular conditions was taken from the measurements of Scott and Brickwedde;[11] they represented their measurements by the equations

LIQUID

$$\left.\begin{aligned} V(n-H_2) &= 24.747 - 0.08005\ T + 0.012716\ T^2 \\ V(p-H_2) &= 24.902 - 0.0888\ T + 0.011104\ T^2 \end{aligned}\right\} \qquad \text{(III-16)}$$

with V in cc/mole. These equations are claimed to represent the molar volume of hydrogen to an accuracy of 0.03%. In this calibration normal hydrogen was used, and the ortho-para conversion was calculated on the basis of a second-order rate law with a rate constant of $12 \times 10^{-5}$ (% h)$^{-1}$. A linear interpolation between the volumes for para and normal hydrogen was made. The effect of the conversion on the volumes was about 0.05%.

The error due to the uncertainty in the liquid level in the capillary was estimated to be 0.005 cc or 0.1%. Thus the largest source of error in the determination of the density of samples rested in the determination of the amount of sample in the capillary, and this varied somewhat between different experiments and was discussed above.

The volume determination by the liquid-hydrogen method differed by about 1% from the room-temperature determination and the thermal-contraction calculation. This is attributed to permanent stretch of the cell after pressurization. The volume determined by the liquid-hydrogen method was used in the evaluation of the data.

The volume change of the cell with pressure was discussed extensively by Orttung.[6] The cell was pressurized to the maximum

pressure at which it was to be used, and in subsequent experiments was assumed to behave elastically up to this pressure. For the low-pressure cell, the ratio of outside-to-inside diameter was 1.83, and Orttung's estimate of the stretch should apply. Thus

$$\frac{\Delta V}{V} = 2.2 \times 10^{-7} P \qquad \text{(III-17)}$$

where P is the pressure in psi. The pressures at the temperature of the thermal measurements were all below 25 000 psi, and thus the correction was at most 0.5%.

## F. Measurements at High Ortho-Hydrogen Concentrations

Heat-capacity measurements at high ortho-hydrogen concentrations presented difficulties not encountered in other samples, due to the heat generated by the ortho-para conversion in the sample. Hill and Ricketson[4] and also Orttung[6] discussed this problem. The rate of heat generation due to the conversion is given by

$$\frac{dH}{dt} = - \frac{n\ \Delta H}{360\,000} \frac{dq}{dt} \qquad \text{(III-20)}$$

where (dH/dt) is in milliwatts if n is the number of moles of sample, $\Delta H$ is the heat of conversion in millijoules (mJ) per mole, and (dq/dt) is the rate of conversion in % ortho hydrogen per hour. It is assumed here that the perturbation of the $J = 0$ and $J = 1$ levels is small compared with the energy difference between these levels, and that therefore the value $\Delta H = 1430$ J per mole ortho hydrogen for the gas phase can be used. If the conversion follows a second-order rate law, then

$$\begin{aligned} \frac{dH}{dt} &= \frac{1}{360\,000} \Delta H\, n\, k\, q^2 \\ &= 3.98\, k\, q^2\, n\,, \end{aligned} \qquad \text{(III-21)}$$

where k is in $(\%\ h)^{-1}$ and q is in % ortho hydrogen. At the normal molar volume of 22.6 cc the rate constant is $18 \times 10^{-5}\ (\%\ h)^{-1}$. This corresponds to a rate of heat generation of 4 mW per mole of sample. At the highest densities studied this rate increased by a factor of about four. Even though the samples had a rather large heat capacity

in the anomalous region, this heat generation caused rapid warming, and heat-capacity measurements were necessarily rather crude. The situation did not improve much as the ortho-hydrogen concentration decreased, for the anomalous heat capacity also decreased with concentration. The temperature of the $\lambda$ anomaly could of course be easily observed when the sample was allowed to warm of its own accord. Estimates of the heat capacity in the region of the $\lambda$ anomaly were possible from the rate of temperature change, if one assumed that the rate of conversion was constant in the region of the anomaly, and if reasonable thermal equilibrium existed throughout the sample. Direct measurement of the heat capacity was possible only above the $\lambda$ point, and in this region the rate of conversion could be determined by comparing the drifts with the measured heat capacity. Even above the $\lambda$ point, heat capacity measurements were rather poor and generally showed a scatter of several percent. An additional difficulty arose from the fact that the sample composition changed with time. The composition at any given time could of course be calculated from the conversion rate and the thermal history of the sample.

The primary interest in this work on samples of high ortho-hydrogen concentrations was in the $\lambda$ anomaly, and little work was done on the total much broader anomaly in the heat capacity. For this reason most of the measurements consisted of determining heating curves rather than of measuring heat capacities directly by the conventional method outlined in Sec. III.C. In general the heating curves are related to the heat capacity and to the rate of heat generation by the relation

$$\frac{dt}{dT} = \frac{C}{(dH/dt)} . \qquad \text{(III-22)}$$

With the aid of Eq. (III-21) this becomes

$$\frac{dt}{dT} = \frac{C}{3.98\ kq^2 n} , \qquad \text{(III-23)}$$

and thus for the heat capacity per mole

$$C = 3.98\ k\ q^2\ \frac{dt}{dT} , \qquad \text{(III-24)}$$

provided that the heat capacity of the empty cell is negligible. In the region of the $\lambda$ anomaly this is certainly the case.

In order to reduce the effort of numerical computations, heat capacities, temperatures, and entropy changes were calculated from thermometer resistances and heating times by means of an IBM 650 data processing machine.

The problem of thermal equilibrium during the measurement of heating curves is more extensively discussed in Sec. V.

## G. Preliminary Measurements

### 1. The Heat Capacity of Copper

In order to determine the reliability of the thermal measurements, the heat capacity of copper was measured. The heat capacity of copper was determined below 4 °K, by a number of investigators, and a recent compilation of results was given by O'Neal[17] in the form of $\gamma$ and $\alpha$, where $\gamma$ and $\alpha$ are the coefficients in the equation

$$C = \gamma T + \alpha T^3 . \qquad \text{(III-25)}$$

This summary is reproduced in Table III-3. Franck et al.[13] recently made measurements on copper up to 30 °K, and comparison with literature data over the entire temperature range of interest here is therefore possible.

The sample used here consisted of 6.902 moles of 99.999% pure copper obtained from the American Smelting and Refining Company, and 0.035 mole of copper of unknown purity in the form of the thermometer capsule, soldering lugs, etc. A correction to the heat capacity for the manganin heater and the G.E. 7031 cement was made, and amounted to

$$\Delta C = 0.002\ T + 0.0094\ T^3 . \qquad \text{(III-26)}$$

The heat capacity of the G.E. cement was taken as $0.041\ T^3$ mJ/g °K. At high temperatures this correction is undoubtedly only approximately correct and may well introduce a systematic error of 1 or 2 %.

The experimental results are given in Table III-4. A plot of $C_L/T^3$ vs $T^2$, where $C_L$ is the lattice heat capacity $C - \gamma T$ is given

Table III-3. Recent heat-capacity results in copper.

| Investigator | $\gamma\left(\frac{mJ}{mole\ (°K)^2}\right)$ | $a\left(\frac{mJ}{mole\ (°K)^4}\right)$ | Purity (%) |
|---|---|---|---|
| Phillips, N. E.[14] | 0.694 | 0.0482 | 98.999 |
| Kneip, G.[15] | 0.698 | 0.0482 | 99.999 |
| Rayne, J.[16] | 0.686 | 0.0473 | 99.999 |
| Corak, et.al.[17] | 0.688 | 0.0478 | 99.999 |
| du Chaterier and de Nobel[18] | 0.721 | 0.0500 | 99.999 |
| Giffel, et al.[19] | 0.691 | 0.0486 | 99.99 |
| Manchester, F. D.[20] | 0.696 | 0.0478 | 99.999 |
| Ramanathan and Srinivasan[21] | 0.720 | 0.0523 | — |
| Franck et al.[13] | 0.690 | 0.0478 | 99.999 |
| O'Neal, H. R.[12] | 0.702 | — | 99.999 |
| Ahlers, Guenter, this work | 0.704 | 0.0478 | 99.999 |

Table III-4. The heat capacity of copper.

| T (°K) | C (mJ mole$^{-1}$°K$^{-1}$) |
|---|---|
| Data of 8-5-62 | |
| 9.534 | 48.24 |
| 10.100 | 56.92 |
| 9.062 | 41.92 |
| 9.588 | 49.02 |
| 10.206 | 58.64 |
| 10.815 | 69.20 |
| 11.464 | 81.90 |
| 12.146 | 96.93 |
| 12.665 | 109.66 |
| 13.013 | 118.78 |
| 8.993 | 41.01 |
| 9.438 | 46.89 |
| 10.735 | 67.65 |
| 11.369 | 79.85 |
| 12.588 | 107.74 |
| 13.298 | 126.15 |
| 13.989 | 148.03 |
| 15.290 | 194.24 |
| 16.202 | 233.06 |
| 17.026 | 272.60 |
| 17.823 | 315.0 |
| 18.510 | 354.9 |
| 19.086 | 391.1 |
| 19.725 | 431.4 |
| 4.408 | 7.073 |
| 4.688 | 8.184 |
| 5.139 | 10.081 |
| 5.618 | 12.254 |
| 6.073 | 14.65 |
| 6.417 | 16.67 |
| 7.779 | 18.99 |
| 7.184 | 21.97 |
| 7.624 | 25.68 |
| 8.086 | 30.34 |
| 8.556 | 36.01 |
| 9.037 | 41.57 |
| 9.572 | 48.76 |
| 10.252 | 59.45 |
| 10.969 | 72.03 |
| 11.669 | 86.15 |
| 12.693 | 110.51 |
| 13.862 | 143.84 |
| 15.128 | 188.02 |
| 16.434 | 244.41 |
| Data of 8-31-62 | |
| 2.340 | 2.261 |
| 2.857 | 3.130 |
| 2.279 | 2.180 |
| 2.715 | 2.869 |
| 2.284 | 2.178 |
| 2.694 | 2.850 |
| 3.159 | 3.731 |
| 3.017 | 3.437 |
| 3.656 | 4.921 |
| 4.325 | 6.925 |
| 2.255 | 2.136 |
| 2.602 | 2.665 |
| 2.970 | 3.335 |
| 3.406 | 4.292 |

Table III-4 (Continued)

| T (°K) | C (mJ mole$^{-1}$°K$^{-1}$) | T (°K) | C (mJ mole$^{-1}$°K$^{-1}$) |
|---|---|---|---|
| Data of 8-31-62 (Contd.) | | 5.886 | 13.688 |
| 3.945 | 5.722 | 6.340 | 16.250 |
| 4.456 | 7.372 | 6.831 | 19.435 |
| 4.922 | 9.179 | 7.437 | 24.119 |
| 4.409 | 7.214 | 8.053 | 30.02 |
| 4.846 | 8.853 | 8.592 | 36.39 |
| 5.335 | 10.987 | 9.175 | 43.41 |
| 4.469 | 7.413 | 9.663 | 50.10 |
| 4.984 | 9.421 | 10.037 | 55.91 |
| 5.497 | 11.723 | 10.530 | 64.10 |
| 6.050 | 14.590 | 11.130 | 75.10 |
| 6.669 | 18.346 | 11.749 | 87.98 |
| 7.222 | 22.339 | 12.417 | 103.40 |
| 7.679 | 26.270 | 13.076 | 120.50 |
| 8.249 | 32.29 | 13.703 | 138.93 |
| 8.938 | 40.48 | 14.393 | 160.94 |
| 4.421 | 7.262 | 15.178 | 189.75 |
| 4.887 | 9.036 | 16.128 | 229.36 |
| 5.393 | 11.253 | 17.223 | 282.74 |

in Fig. III-2 for values of $\gamma$ of 0.700, 0.704, and 0.707, and for temperatures below 5 °K. The value

$$\gamma = 0.704 \text{ mJ/(°K)}^2 \text{ mole} \qquad \text{(III-27)}$$

clearly gives the most reasonable behavior of the lattice heat capacity.

A plot of the Debye $\theta$ vs T is given in Fig. III-3. The $\theta$ values were calculated from each experimental point after the electronic term 0.704 T was subtracted. The smoothed values of Franck et al. are also plotted, together with an approximate indication of their scatter. The effect of systematic errors in the temperature scale between 5 and 10 °K can clearly be seen. The values of $\theta$ after correction according to the method discussed in Sec. III. B are also shown.

The general agreement with literature data is very satisfactory. This is a strong indication that the various circuits and experimental procedures that enter into the measurements are reliable.

## 2. Heat Capacity of the Empty Calorimeter

The heat capacity of the low-pressure cell was measured when the cell was empty so that it could be subtracted from the heat capacity of the full cell. The low-pressure cell consisted of 279.8 g berryllium-copper, 2.4 g copper, 3.8 g gold, 0.5 g indium, 2.9 g stainless steel, approximately 0.3 g G.E. 7034 varnish, and a negligible amount of manganin wire. The weight of the stainless steel was based on the assumption that 1/3 of the length of capillary between the cell and shield is measured with the cell. The method of afterdrift extrapolation described above was employed. The heat capacity was measured between 2 and 20 °K, and can be represented analytically by the equation

$$C = 6.54\ T + 0.2168\ T^3 + 2.70 \times 10^{-4}\ T^5 - 2.8 \times 10^{-7}\ T^7 . \qquad \text{(III-28)}$$

The units of the heat capacity are millijoules per °K. The individual measurements are reported in Table III-5. Figure III-4 shows a plot of C/T vs $T^2$ for the helium region, and Fig. III-5 shows $C_L/T^3$ vs $T^2$

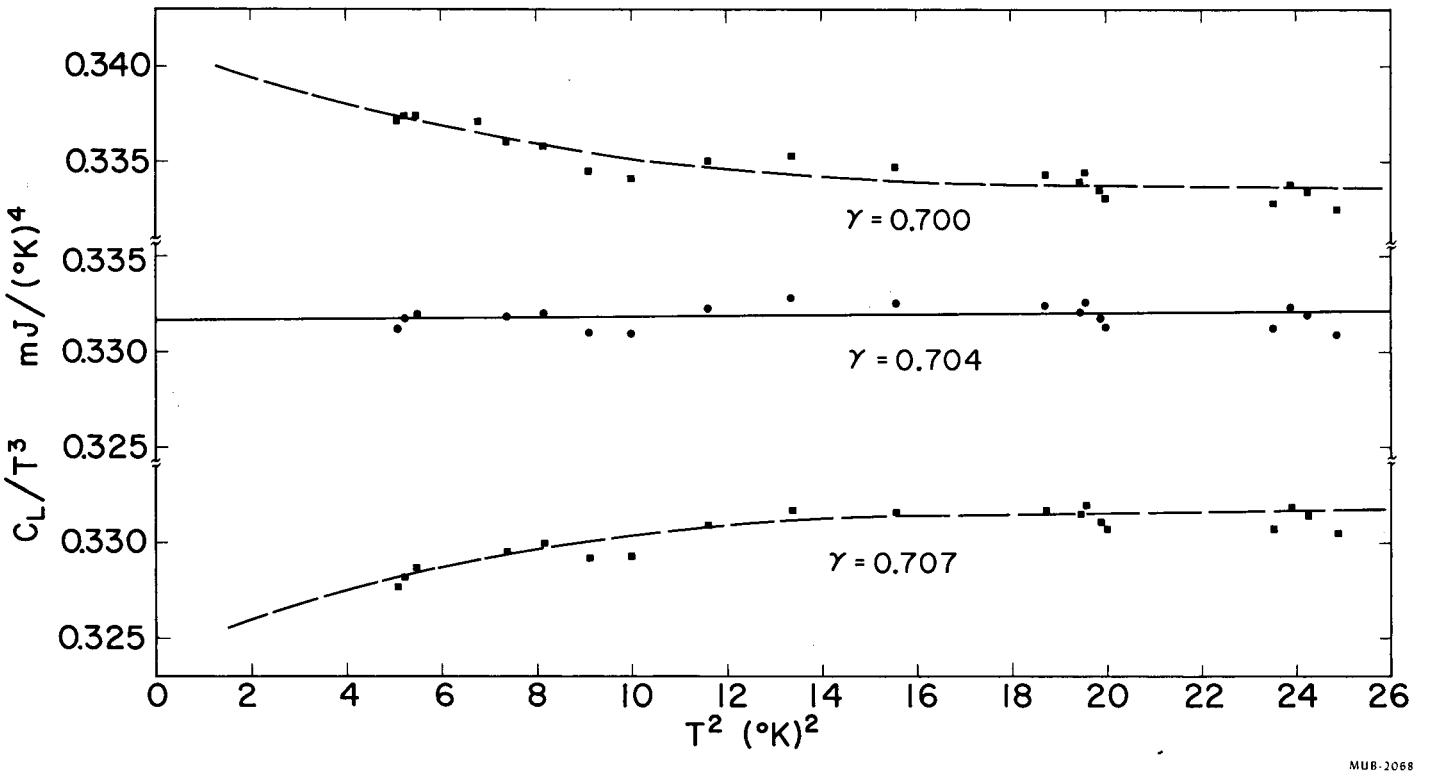


Fig. III-2. The lattice heat capacity of copper below 5 °K.

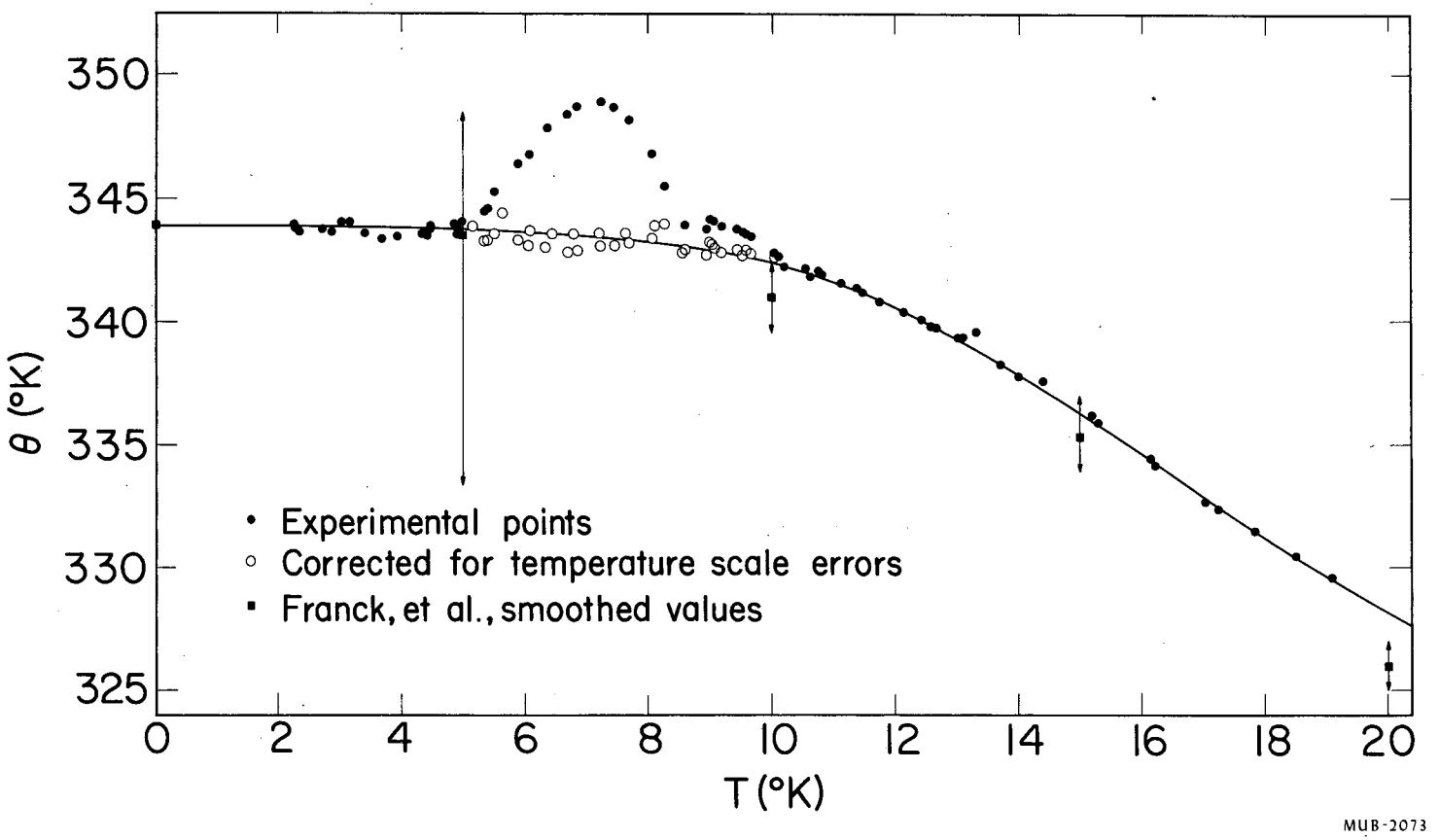


Fig. III-3. The Debye theta of copper. The arrows attached to the points by Franck et. al.[13] approximately indicate the scatter in the experimental points.

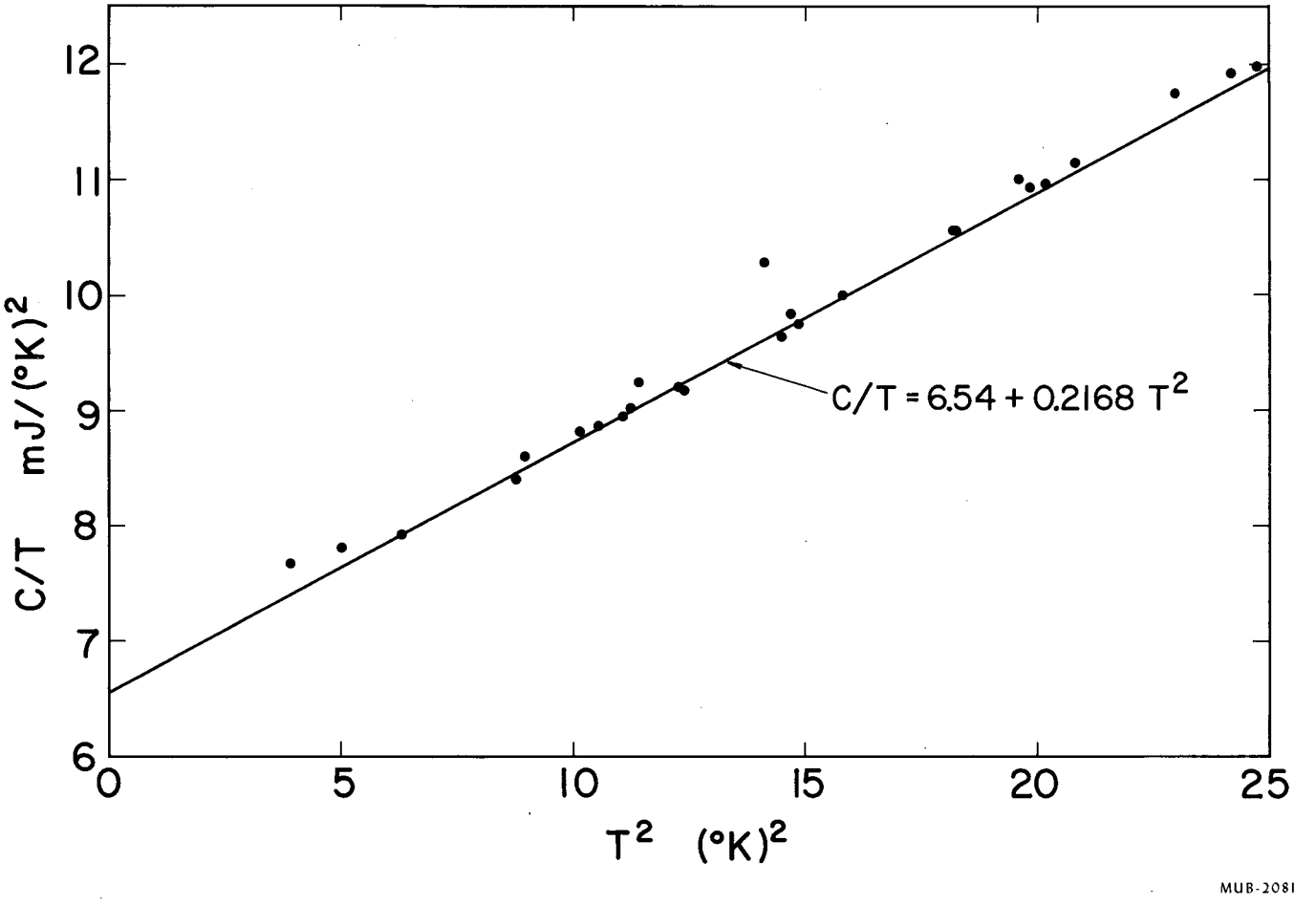


Fig. III-4. The heat capacity of the low-pressure cell below 5 °K.

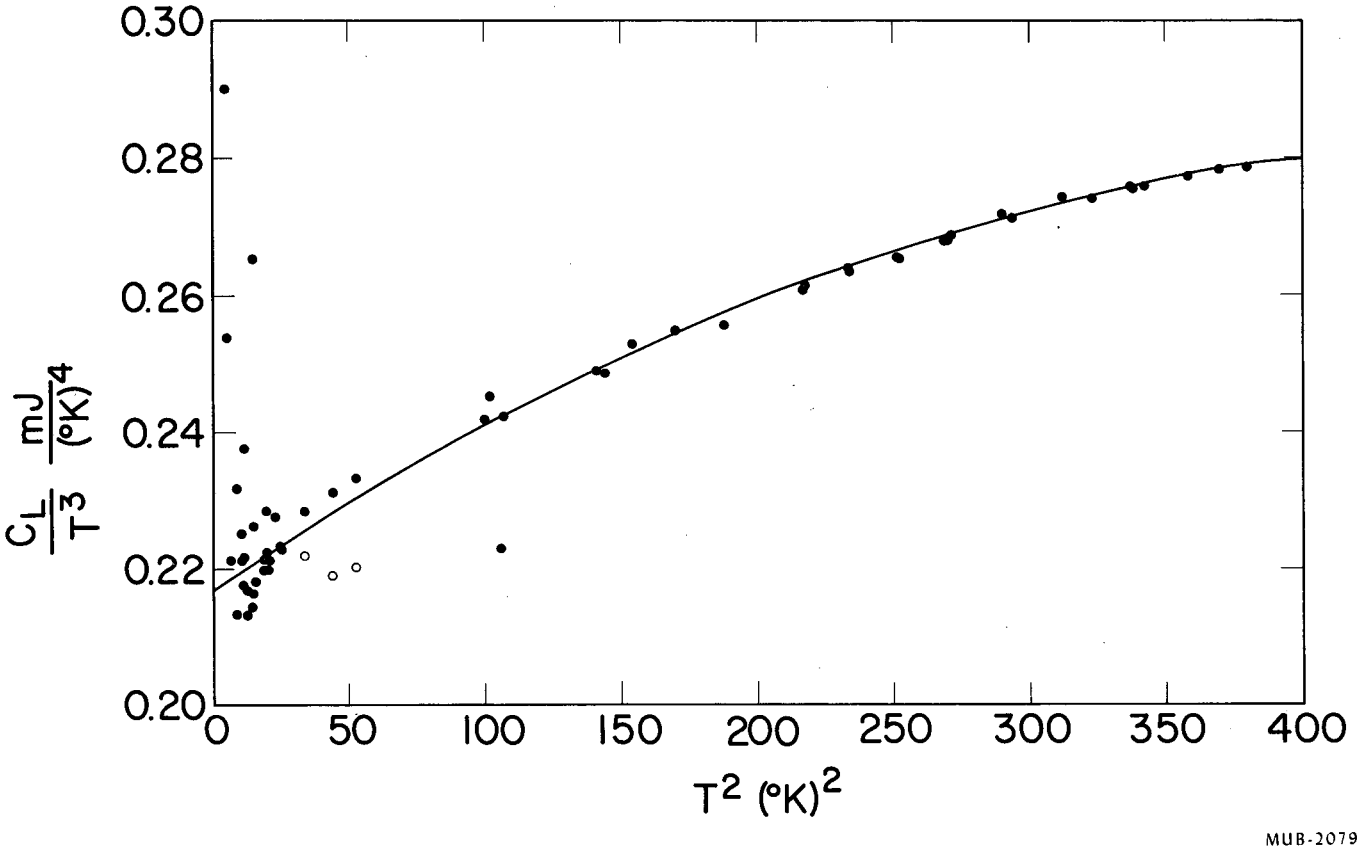


Fig. III-5. The lattice heat capacity of the empty low-pressure cell. Full circles are points corrected with the aid of the copper heat capacity. Open circles are based on the extrapolation difference plot.

Table III-5. Heat capacity of empty low-pressure cell.

| T (°K) | C (mJ °K$^{-1}$) | T (°K) | C (mJ °K$^{-1}$) |
|---|---|---|---|
| Data of 9-21-62 | | 4.561 | 50.80 |
| 10.067 | 315.8 | 4.915 | 58.65 |
| 10.288 | 310.3 | 5.817 | 81.73 |
| 9.9991 | 306.3 | 6.595 | 105.8 |
| 10.331 | 334.8 | 7.218 | 130.0 |
| 18.493 | 1866.0 | 4.487 | 49.20 |
| 19.221 | 2103.0 | 4.986 | 60.23 |
| 18.375 | 1830.0 | 3.348 | 30.21 |
| 18.910 | 2000.0 | 3.805 | 36.68 |
| 19.484 | 2189.0 | 4.273 | 45.08 |
| 16.380 | 1285.0 | 4.791 | 56.36 |
| 17.000 | 1447.0 | 3.246 | 28.78 |
| 17.648 | 1623.0 | 3.518 | 32.28 |
| 18.338 | 1821.0 | 3.852 | 37.54 |
| 16.403 | 1290.0 | 4.261 | 44.98 |
| 17.119 | 1473.0 | 1.976 | 15.16 |
| 17.956 | 1704.0 | 2.235 | 17.45 |
| 14.732 | 932.4 | 2.507 | 19.88 |
| 15.260 | 1038.0 | Data of 10-9-62 | |
| 15.836 | 1158.0 | | |
| 16.444 | 1302.0 | 4.424 | 48.70 |
| 14.701 | 924.8 | 3.751 | 38.54 |
| 15.270 | 1038.0 | 3.831 | 37.71 |
| 15.856 | 1162.0 | 3.971 | 39.69 |
| 11.851 | 491.9 | 3.323 | 29.72 |
| 12.407 | 564.4 | 3.376 | 31.22 |
| 13.013 | 647.1 | 3.501 | 32.19 |
| 13.686 | 754.4 | 2.958 | 24.85 |
| 11.990 | 507.1 | 2.990 | 25.75 |
| 4.453 | 48.75 | 3.182 | 28.05 |

for the entire temperature range. The line in Fig. III-5 is that corresponding to the analytical expression.

Also given in Fig. III-5 are the points between 5 and 10 °K corrected according to the method outlined in Sec. III.B.

After a part of the measurements in the low-pressure cell had been completed, it became necessary to replace the seal. The change in the material of the seal was carefully measured, and the change in the heat capacity was calculated from the known heat capacity of the components. This calculation resulted in the equation

$$C = 6.50\ T + 0.2205\ T^3 + 2.70 \times 10^{-4}\ T^5 + 2.8 \times 10^{-7}\ T^7 \quad \text{(III-29)}$$

for the heat capacity of the low-pressure cell after the seal replacement.

The scatter in the data for the empty calorimeter was almost entirely due to the effect of the stainless steel capillary. This effect was worse for the empty cell than it was for the cell filled with a sample, because the thermal conductivity of the capillary is of the same order of magnitude as that of the 0.5 mm core of solid hydrogen. Consequently the relaxation time for the empty cell was two to three times as long as it was for the filled cell. The accuracy to which the heat capacity of the empty cell was known is a major factor in the accuracy to which the heat capacity of para hydrogen could be determined.

# IV. THE LATTICE HEAT CAPACITY OF HYDROGEN

## A. General Comments

The lattice heat capacities of the solidified gases are of considerable interest in relation to the theory of lattice dynamics. From the theoretical point of view the quantity of interest is the heat capacity at constant volume $C_v$. Aside from fairly extensive measurements on solid helium[22 to 27] and rather limited measurements on hydrogen,[28] all data available so far refer to the heat capacity at the saturation vapor pressure, or essentially constant and zero pressure $C_p$. Whereas the correction of constant-pressure data to constant-volume conditions is small at low temperatures for the heavier solidified gases, it can be expected to become very appreciable for the lighter elements He, $H_2$, $D_2$, and Ne. Even for argon above 40 °K this correction is large enough to cause considerable uncertainty in $C_v$.[2] The difference between $C_p$ and $C_v$ is given by

$$C_p - C_v = \frac{\alpha^2 VT}{K}, \qquad \text{(IV-1)}$$

where $\alpha$ is the thermal expansion and K is the isothermal compressibility. Thus, if $\alpha$ and K are known with sufficient accuracy and if $C_p - C_v$ is small, then reasonable estimates of $C_v$ can be made from the $C_p$ data. These conditions seem to be met in the case of argon and krypton.[2] One realizes that $C_v$ obtained from $C_p$ by means of Eq. (IV-1) refers to the volume of the substance at the pressure and temperatures of the $C_p$ measurements. This $C_v$ will be designated as $C_v(V_T)$. The quantity desirable to obtain from a theoretical point of view is $C_v(V_0)$, i. e., $C_v$ at the molar volume at 0 °K. Thus, a further correction to $C_v(V_T)$ is necessary, and is given by

$$\theta(V_0) = \theta(V_T)\,(V_T/V_0)^{\gamma} \qquad \text{(IV-2)}$$

in terms of the Debye $\theta$. Here $\gamma$ is the Grüneisen constant

$$\gamma = -\left(\frac{\partial \ln \theta}{\partial \ln V}\right)_T . \qquad \text{(IV-3)}$$

The Grüneisen constant is generally of the same magnitude for all substances, and usually has a value between 2 and 4. However, its exact value is usually not known and there is no guarantee that $\gamma$ is indeed a constant.

In view of the need for $C_v$ data on simple crystals and the difficulties involved in deducing these data from $C_p$, it is most desirable to obtain direct measurements at constant volume. From the theoretical point of view, the most urgent need is for data on the heavier rare gases. Accurate theoretical treatment of lattice dynamics is now limited to substances with negligible zero-point energy and anharmonicity.[1] Even for argon the zero-point energy amounts to 8% of the cohesion energy at 0 °K.[2] For hydrogen this figure is approximately 47%,[29] and any harmonic theory that neglects the effect of zero-point energy cannot be expected to yield reasonable results. On the other hand, comparison of data on the lighter elements with theory may be expected to yield some information on the manner in which zero-point energy manifests itself. From the experimental point of view, the heavier rare gases present more severe difficulties because the relative magnitudes of the thermal expansion of the solid, the compressibility of the fluid, and the melting temperature are such that rather high pressures would be required to reach molar volumes in the fluid smaller than $V_0$ for the solid. Hydrogen, however, does not present any unreasonable problems. The lattice heat capacity of hydrogen was thus measured at three molar volumes, and at constant pressure. The temperature range of the measurements extends from liquid-helium temperatures either to the melting point, or to 20 °K. The four sets of measurements together with their implications will be discussed in the following sections.

## B. Experimental Measurements

### 1. The Heat Capacity of Para Hydrogen at Constant Pressure

The sample was prepared electrolytically, passed over silica gel at 78 °K, and stored in a steel cylinder at 2000 psi. One day previous to the thermal measurements, the sample was passed over copper

at 600 °C, through a liquid nitrogen cold trap, through the ortho-para converter at 20 °K, and into four 5-liter bulbs. The performance of the ortho-para converter was checked by varying the flow rate of the exit gas both above and below the rate at which the actual sample was withdrawn. No change in the ortho hydrogen concentration due to flow rate was observed by the thermal conductivity method. The method of analysis is sensitive to about ± 0.2% ortho hydrogen. It thus seems reasonable to assume that the sample contained 0.2% ortho hydrogen, which is the equilibrium concentration at 20 °K. The rate of conversion in the 5-liter bulbs was checked on a sample that had been stored for over 1 year, and was found to be less than 1% per month. The conversion to ortho hydrogen during the 1-day storage may thus be assumed to be negligible.

The sample was condensed into the same beryllium-copper cell later used for $C_v$ measurements by cooling this bomb to a temperature just above the triple point. When the bomb was full, the bath was further cooled to about 9 °K. This caused the sample in the capillary to freeze. After the capillary was blocked, the liquid in the cell was frozen by closing the mechanical heat switch and the solid was cooled to about 9 °K. Heat-capacity measurements were then made up to the triple point. Liquid helium was then transferred to the bath, and the heat capacity was measured from 2.5 °K to the triple point. The scatter in the data is less than ± 1% over most of the temperature range. At the very lowest temperatures it becomes slightly larger because the electronic heat capacity of the cell becomes very appreciable, and above 11 °K the scatter becomes as large as ± 1.4% because of a decrease in the thermometer sensitivity. In subsequent measurements this effect was eliminated by taking larger temperature increments. The temperature increments were, however, always kept at less than 10% of the absolute temperature.

The amount of sample, determined after the thermal measurements by expansion into calibrated bulbs at room temperature, was found to be 0.303 mole.

Because of the electronic heat capacity of the cell, the heat capacity of the sample became a smaller fraction of the total heat capacity as the temperature decreased. Table IV-1 gives the fraction of the heat capacity attributable to the sample at several temperatures.

It was unnecessary to make corrections for the vaporization of solid because the volume available to the vapor was very small, and was essentially equal only to the volume change due to solidification.

The heat capacity measurements are given in Table IV-2. The function $C_p/T^3$ is plotted against $T^2$ in Fig. IV-1.

The results of Hill and Lounasmaa (Fig. IV-1)[32] are in general somewhat higher than those reported here. The difference is as large as 14% at 3 °K, and at low temperatures decreases with increasing temperature. At 7 °K the difference has vanished. At 9 °K Hill and Lounasmaa's data are again slightly higher. The scatter in their data is approximately ± 6%.[32] At the higher temperatures the scatter of the two measurements overlaps. Below 4 °K, however, there seems to be a real discrepancy that cannot be easily explained.

Comparison with other measurements on solid para hydrogen was made by Hill and Lounasmaa, and will not be repeated here because of the relatively large scatter exhibited by all other data.

The heat of melting at the triple point was also determined on this sample and found to be (118 ±1) J/M. The uncertainty in this value is rather large because upon heating above the triple point some of the solid in the capillary also melted. Melting occurred over a temperature range of $1 \times 10^{-3}$ °K. The value obtained here compares well with that found by others[30] (117.3 J/M).

## 2. The Heat Capacity of 2% Ortho Hydrogen at 22.56 cc/M

The sample preparation as far as the storage in the 5-liter bulbs was identical to that used for the $C_p$ measurements. The sample was forced into the cell at 78 °K and about 1000 atm. This procedure resulted in slight conversion to ortho hydrogen in the room-temperature part of the system. The final concentration of ortho hydrogen was measured after the experiment and found to be (2 ± 1)%.

Table IV-1. The fraction of the heat capacity attributable to the sample.

| T (°K) | $\frac{C_{H_2}}{C_{Total}} \times 100$ |
|---|---|
| 2.5 | 25 |
| 4.0 | 42 |
| 9.0 | 70 |
| 13.0 | 75 |

Table IV-2. $C_p$ of para hydrogen.

| T (°K) | $C_p\left(\frac{mJ}{M°K}\right)$ | T (°K) | $C_p\left(\frac{mJ}{M°K}\right)$ | T (°K) | $C_p\left(\frac{mJ}{M°K}\right)$ |
|---|---|---|---|---|---|
| 9.061 | 1366 | 11.857 | 3398.0 | 4.135 | 87.7 |
| 9.532 | 1623 | 12.450 | 4070.0 | 3.625 | 56.8 |
| 10.079 | 1979 | 4.403 | 106.7 | 3.778 | 64.9 |
| 10.742 | 2489 | 4.689 | 135.5 | 3.291 | 42.0 |
| 11.387 | 2961 | 4.924 | 159.7 | 3.489 | 50.1 |
| 11.964 | 3496 | 5.115 | 181.1 | 2.736 | 22.85 |
| 12.477 | 4028 | 5.424 | 244.5 | 2.935 | 28.46 |
| 12.857 | 4418 | 5.878 | 298.0 | 2.461 | 16.73 |
| 13.115 | 4848 | 6.330 | 386.7 | 2.565 | 19.21 |
| 13.390 | 5082 | 6.720 | 481.1 | | |
| 9.090 | 1383 | 7.063 | 571.4 | | |
| 9.595 | 1671 | 7.369 | 661.9 | | |
| 10.523 | 2272 | 7.719 | 780.9 | | |
| 10.931 | 2581 | 3.895 | 71.2 | | |
| 11.402 | 2992 | 3.987 | 77.7 | | |

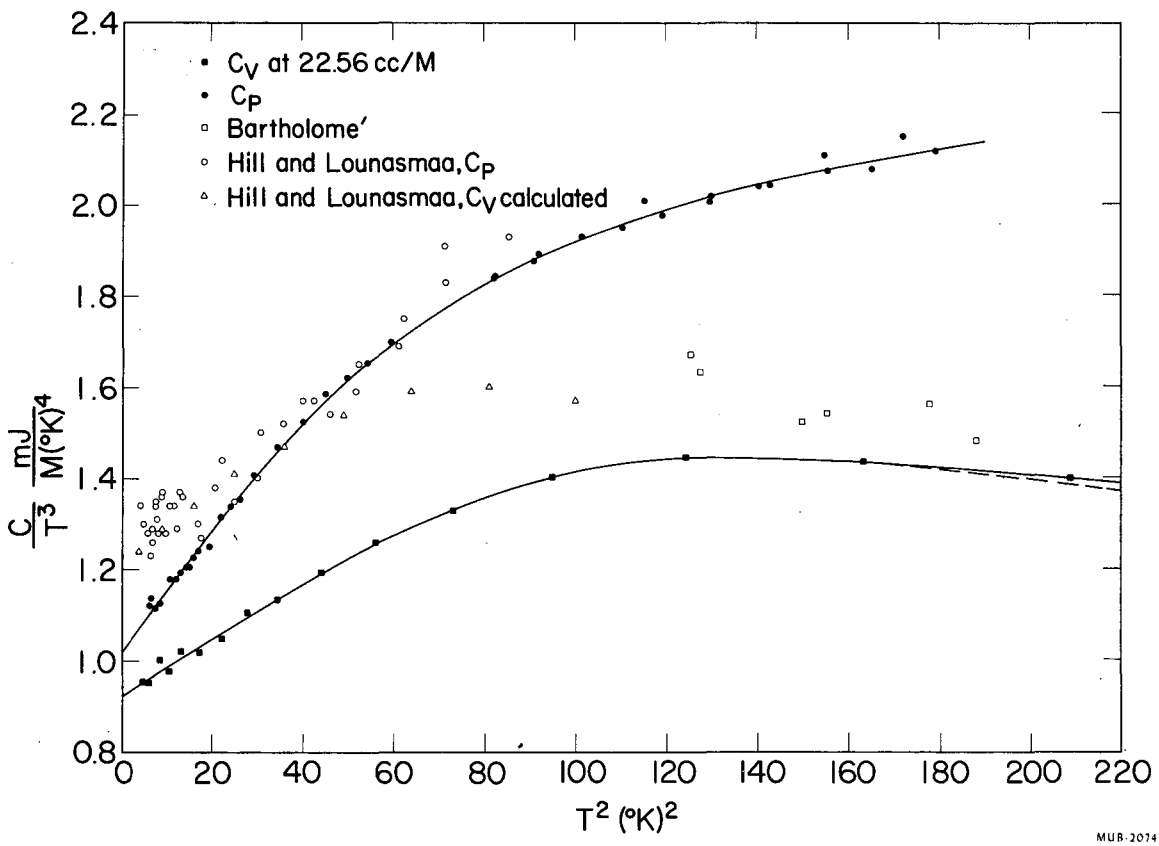


Fig. IV-1. The lattice heat capacity of solid hydrogen at constant pressure and at 22.56 cc/M.

After the thermal measurements, the amount of sample was determined as described previously. The cell contained 0.364 mole of sample, and the molar volume was found to be (22.60 ± 0.10) cc/M. At high temperatures the heat capacity measurements extend into the two-phase region, and melting was found to start at 16.35 °K. Bartholomé[33] determined the volume change on melting for normal hydrogen, and recently Goodwin and Roder[34] determined the molar volume of fluid para hydrogen in equilibrium with solid. Assuming that Bartholomé's data can be applied to para hydrogen, the molar volume corresponding to 16.35 °K along the melting line should be 22.52 cc/M. The largest uncertainty in this value is the one due to the uncertainty in the volume change on melting, and this was estimated by Bartholomé to be 4% or 0.1 cc/M. The molar volume of the sample, therefore, was 22.56 ± 0.06 cc/M.

The heat capacity of this sample was measured from 1.5 to 17.3 °K. The fraction of the heat capacity attributable to the sample is given in Table IV-3 for several temperatures. The heat capacity results are listed in Table IV-4.

Because this sample contained about 2% ortho hydrogen, there was a contribution to the heat capacity from the anomaly characteristic of ortho hydrogen at low temperatures. The relative contribution of this anomaly is indicated in Table IV-3. An attempt was made to subtract this anomalous contribution from the lattice heat capacity. At temperatures much larger than the difference between the energy levels responsible for the anomaly, one can expand the heat-capacity contribution into the form

$$C_A = aT^{-2} + bT^{-3} + \cdots . \qquad \text{(IV-4)}$$

At temperatures at which the anomalous contribution is appreciable, the lattice heat capacity could be written in the form

$$C_L = AT^3 + BT^5 . \qquad \text{(IV-5)}$$

B could be estimated for temperatures at which the anomalous contribution was negligible. Several values of A were used with the same

Table IV-3. The fraction of the heat capacity attributable to the sample for $C_v$ at 22.6 cc/M.

$C_A$ = anomalous heat capacity
$C_L$ = lattice heat capacity

| T | $\frac{C_{H_2}}{C_{Total}} \times 100$ | $\frac{C_A}{C_L} \times 100$ |
|---|---|---|
| 2.5 | 42 | 140.0 |
| 4.0 | 41 | 12.0 |
| 9.0 | 59 | 0.23 |
| 13.0 | 63 | 0.03 |

Table IV-4. The heat capacity of para hydrogen at 22.56 cc/M. C indicates the measured molar heat capacity of the sample, and $C_L$ indicates the lattice contribution.

| T (°K) | C $\left(\frac{mJ}{M°K}\right)$ | $C_L$ $\left(\frac{mJ}{M°K}\right)$ | T (°K) | C $\left(\frac{mJ}{M°K}\right)$ | $C_L$ $\left(\frac{mJ}{M°K}\right)$ |
|---|---|---|---|---|---|
| 1.528 | 42.42 | — | 5.863 | 233.2 | 228.5 |
| 1.821 | 37.03 | — | 6.633 | 351.7 | 348.1 |
| 2.048 | 41.77 | — | 7.491 | 532.7 | 529.8 |
| 2.196 | 43.27 | 10.1 | 8.553 | 833.5 | 831.3 |
| 2.404 | 40.88 | 13.2 | 9.745 | 1299.0 | 1297.0 |
| 2.581 | 42.62 | 18.6 | 11.153 | 2004.0 | 2003.0 |
| 2.879 | 43.20 | 23.9 | 12.779 | 2991.0 | 2990.0 |
| 3.230 | 48.25 | 32.9 | 14.446 | 4210.0 | 4209.0 |
| 3.631 | 61.11 | 49.0 | 15.892 | 8485.0 | 8484.0 |
| 4.146 | 81.96 | 72.6 | 16.822 | 23360.0 | 23360.0 |
| 4.708 | 116.7 | 109.5 | 17.326 | 24460.0 | 24460.0 |
| 5.262 | 166.9 | 161.1 | 17.807 | 25600.0 | 25600.0 |

value of B to calculate trial values of $C_A$ from

$$C_A = C - AT^3 - BT^5 . \qquad \text{(IV-6)}$$

These values of $C_A$ were then plotted in the form of $C_A T^2$ vs $T^{-1}$. Figure IV-2 shows this plot for three values of A that differ by only about 2%. At high temperatures $C_A$ is extremely sensitive to the choice of A, and A can be estimated to within ± 0.5%. Within experimental error, b is negligibly small, and the anomalous heat capacity can be subtracted from the total heat capacity in the form of a $T^{-2}$ correction with a = 160 mJ °K/M. On the basis of the behavior of $C_A T^2$ vs $T^{-1}$, it is estimated that this is a reasonable correction at temperatures above 2.2 °K.

Table IV-4 lists both the total-heat capacity and the estimated lattice heat capacity. The lattice heat capacity is also plotted in Fig. IV-1 in the form of $C/T^3$ vs $T^2$. Above 5 °K, the precision is somewhat better than 1%. A 1% systematic error due to the uncertainty in the heat capacity of the empty calorimeter is possible.

The only previous measurements of $C_v$ of para hydrogen with which the present measurements can be compared are those by Bartholomé and Eucken.[28] Considerable confusion exists in the literature about the molar volume at which Bartholomé's measurements were made. Megaw[35] believed that it was the molar volume at zero pressure and 11 °K, which would be 23.0 cc/M. Megaw assumed that Bartholomé and Eucken had filled their calorimeter at this temperature. This idea was taken over by Hill and Lounasmaa.[32] Actually Bartholomé and Eucken's calorimeter was filled with solid at a temperature somewhere in the liquid hydrogen region, the exact temperature not being specified; their molar volume thus is not known at all. However, their heat capacity measurements extended at least as high as 17.9 °K, giving an upper limit of 22.1 cc/M to the molar volume on the basis of the molar volume of solid in equilibrium with liquid. Their molar volume thus was at least 2% less than the one in this experiment. Nonetheless, his heat capacity is 7% larger than the one found here. There is, therefore, a considerable discrepancy between

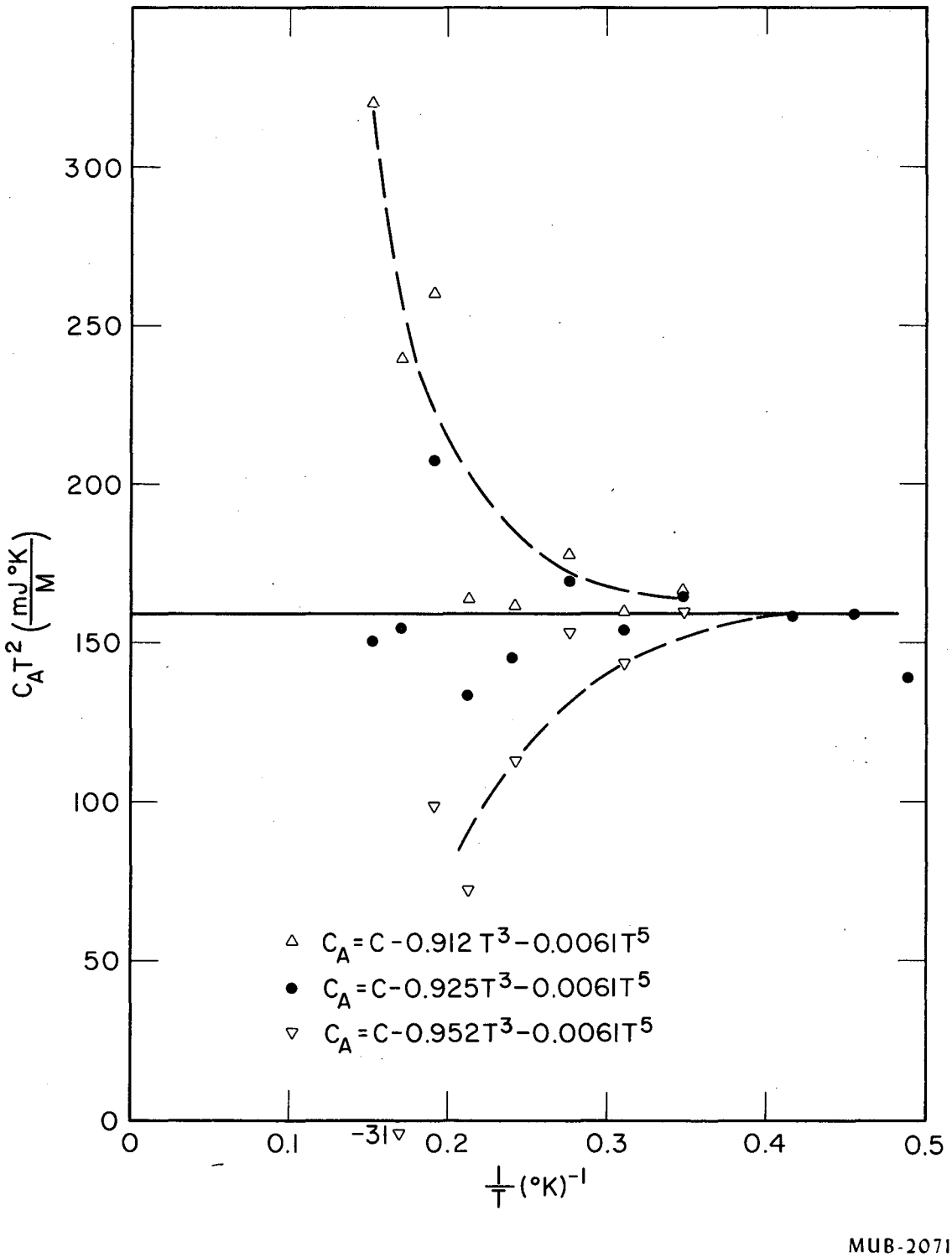


Fig. IV-2. The anomalous heat capacity of 2% ortho hydrogen at 22.56 cc/M.

the old data and the ones reported on here. Bartholomé and Eucken's data are also shown in Fig. IV-1.

Hill and Lounasmaa attempted to estimate $C_v$ from their $C_p$ measurements. The basic relation, of course, is Eq. (IV-1). In view of the fact that $\alpha$ and K are not known, they assumed the validity of the Grüneisen relation (IV-13), which yields

$$C_p - C_v = ATC_v^2 \qquad \text{(IV-7)}$$

with

$$A = \frac{\gamma^2 K}{V}. \qquad \text{(IV-8)}$$

They determined A at high temperatures from their data for $C_p$ and Bartholomé and Eucken's data for $C_v$. Once A is known, Eq. (IV-4) can be solved for $C_v$ if $C_p$ is known. This method has several faults. Equation (IV-1) involves $C_v(V_T)$, as pointed out previously. In the case of hydrogen, V varies considerably with T. Bartholomé's data were, however, determined at constant volume. Furthermore, Bartholomé's volume was considerably smaller than even the 0 °K and zero-pressure volume. And lastly, the Grüneisen relation leading to Eq. (IV-7) is not likely to hold in the case of hydrogen, as pointed out by Megaw.[35] Hill and Lounasmaa's values for $C_v$ are thus likely to be in error by a considerable amount. They are also shown in Fig. IV-1 and they do not agree with the measurements reported here.

### 3. The Heat Capacity of Para Hydrogen at 19.83 cc/M

The sample preparation up to the storage in the 5-liter bulbs was identical to that used for the $C_p$ measurements. In view of the experience with ortho-para conversion in the room-temperature part of the system, the cell was filled with liquid in a manner similar to that used for the $C_p$ measurements. The remainder of the sample was then compressed to about 1000 atm and the calorimeter was warmed to about 40 °K. By this procedure only a small fraction of the sample was exposed to the room-temperature part of the system at densities at which conversion might occur. Analysis of the sample after the experiment revealed no measureable amount of ortho hydrogen.

The sample was found to consist of 0.417 mole and the molar volume was (19.83 ± 0.1) cc/M. At this molar volume, hydrogen starts to melt at too high a temperature to permit an independent check on the molar volume.

The heat capacity was measured from 4.4 to 20 °K. Below 4.4 °K the relative contribution of the empty calorimeter became too large to make measurements worthwhile. The fraction of the heat capacity attributable to the sample is given in Table IV-5. There was no observable anomalous contribution to the heat capacity due to ortho hydrogen. The heat capacity results are listed in Table IV-6.

Some difficulties were encountered in the extrapolation of afterdrifts below 10 °K. The method outlined in Sec. III.D failed because of the very high thermal conductivity of the hydrogen core in the capillary and the resulting very steep and nonlinear afterdrifts. The high thermal conductivity of the core did, however, cause the initial relaxation to occur very rapidly. Below 7 °K a linear extrapolation of the temperature along the afterdrift immediately after the initial relaxation was used to establish the temperature after the heat input. Whereas it was felt that the error due to this procedure would be of the order of 1%, this error is severely magnified due to the relatively small contribution of the sample to the total heat capacity. Above 7 °K, a linear extrapolation was made of the thermometer resistance after the initial relaxation. Use of these two procedures resulted in a discontinuity of 2.2% in the total heat capacity, or 6.3% in the sample heat capacity. It is felt that above 9 °K no severe error is introduced by the method of afterdrift extrapolation. A plot of $C/T^3$ vs $T^2$ is given in Fig. IV-3. From this plot it becomes clear that the data between 7 and 9 °K are somewhat high, and those between 4.4 and 7 °K are somewhat low. The accuracy of the extrapolation of $C/T^3$ vs $T^2$ to $T^2 = 0$ is, of course, affected by this difficulty. The error in $C/T^3$ at 0 degrees is estimated to be ± 5%. Above 9 °K, the scatter in the data is of the order of 1%. A systematic error of 1.5% of the sample heat capacity at the high temperatures and 3% of the sample heat capacity at the lowest temperatures is possible due to the 1% uncertainty in the heat capacity of the empty calorimeter.

Table IV-5. The fraction of the heat capacity attributable to the sample for $C_v$ at 19.8 cc/M.

| T (°K) | $\frac{C_{H_2}}{C_{Total}} \times 100$ |
|---|---|
| 4.5 | 24 |
| 9.0 | 40 |
| 13.0 | 45 |
| 20.0 | 45 |

Table IV-6. The heat capacity of para hydrogen at 19.8 cc/M.

| T (°K) | C $\left(\frac{mJ}{M°K}\right)$ | T (°K) | C $\left(\frac{mJ}{M°K}\right)$ |
|---|---|---|---|
| 4.413 | 37.1 | 12.974 | 1251.0 |
| 4.527 | 37.6 | 14.229 | 1667.0 |
| 4.359 | 34.3 | 16.344 | 2554.0 |
| 4.550 | 39.7 | 17.285 | 3036.0 |
| 4.745 | 44.2 | 18.200 | 3444.0 |
| 5.004 | 51.2 | 19.154 | 3935.0 |
| 5.345 | 63.2 | 8.725 | 334.2 |
| 5.729 | 78.3 | 9.239 | 399.9 |
| 6.273 | 107.6 | 9.665 | 471.2 |
| 6.956 | 163.9 | 10.250 | 575.6 |
| 7.783 | 233.4 | 10.956 | 718.1 |
| 8.495 | 311.4 | 11.804 | 919.2 |
| 9.305 | 411.4 | 12.809 | 1209.0 |
| 10.192 | 558.5 | 13.875 | 1534.0 |
| 11.137 | 752.6 | 15.086 | 2029.0 |
| 11.958 | 964.6 | | |

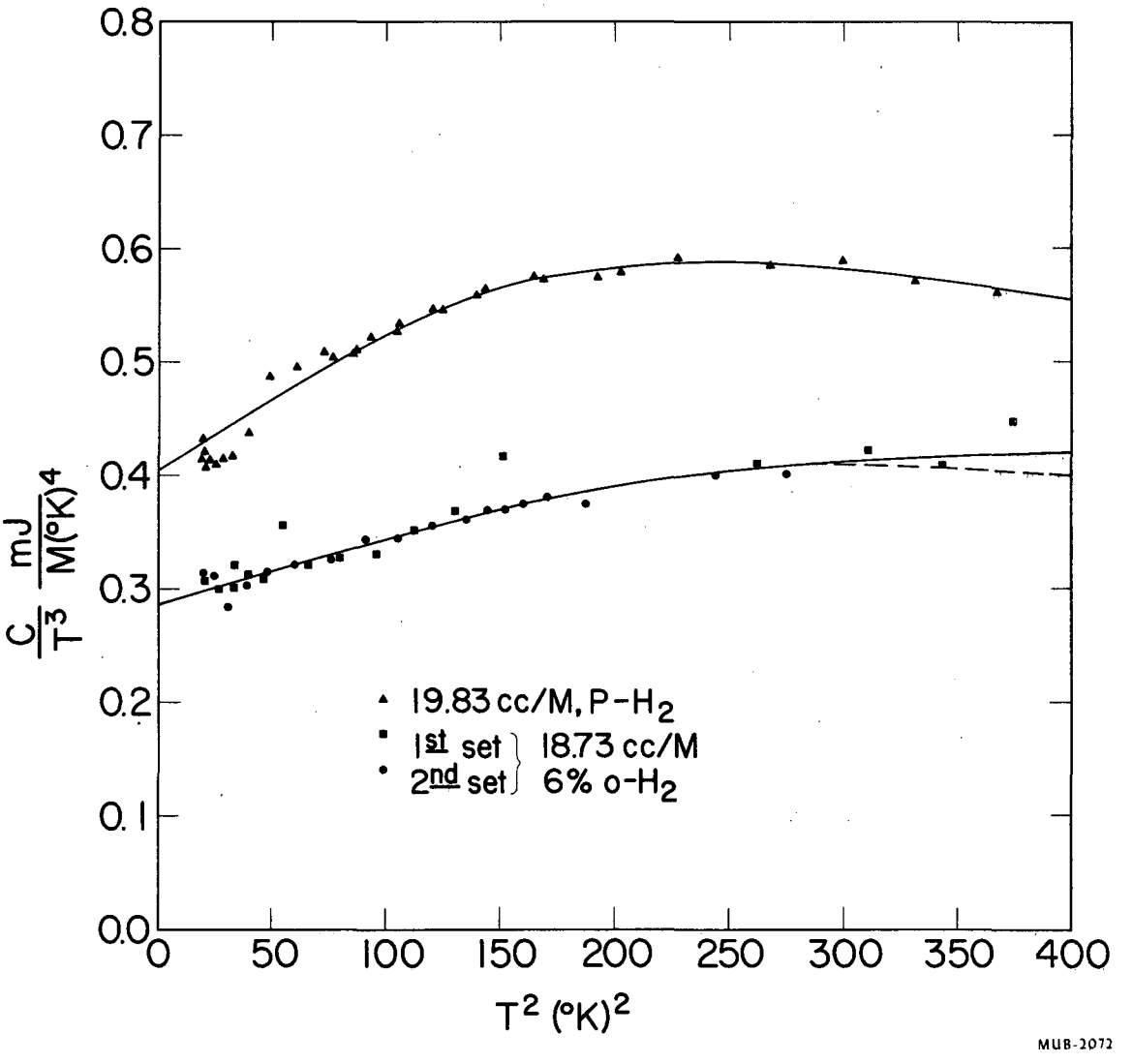


Fig. IV-3. The lattice heat capacity of hydrogen at 19.83 cc/M and at 18.73 cc/M.

There are no previous data on the heat capacity of para hydrogen at a similar molar volume with which the present results could be compared.

4. Heat Capacity of 6% Ortho Hydrogen at 18.73 cc/M.

Sample preparation up to storage in the 5-liter bulbs was identical to that used for the $C_p$ measurements. The sample was forced into the cell at 78 °K and about 2000 atm. This procedure resulted in partial conversion of the sample to ortho hydrogen. The final concentration of the ortho hydrogen was measured after the experiment and found to be (6.3 ± 0.5)%. The amount of sample was determined as usual and found to be 0.441 mole. The molar volume was (18.73 ± 0.1) cc/M.

Heat capacity of this sample was measured from 4.5 °K to 20 °K, and then again from 1.5 °K to 17 °K. A considerable anomalous contribution to the heat capacity at low temperatures was calculated by subtracting the lattice heat capacity in the form of Eq. (IV-5) in the same way as that for the measurements at 22.56 cc/M. The anomalous contribution in the first set of measurements is plotted in Fig. IV-4(a) in the form $C_A T^2$ vs $T^{-1}$, for three values of the $T^3$ coefficient of the lattice heat capacity. Again $C_A T^2$ is very sensitive to changes in the estimate of the lattice contributions. Figure IV-4(b) shows the data from the second set of measurements, calculated with the lattice $T^3$ coefficient that gave the best linear relation in Fig. IV-4(a). Both sets of data yield a straight line for $C_A T^2$ vs $T^{-1}$ with the same values for the lattice heat capacity. However, the two lines are not identical because of changes in ortho-hydrogen concentration between the two sets of measurements. The anomalous contributions can be expressed as

$$C_A^{(1)} = 4400\ T^{-2} - 10250\ T^{-3}$$

and

$$C_A^{(2)} = 3200\ T^{-2} - 6400\ T^{-3}$$

for the first and second set of data respectively at temperatures above 4 °K. These contributions were subtracted from the total heat

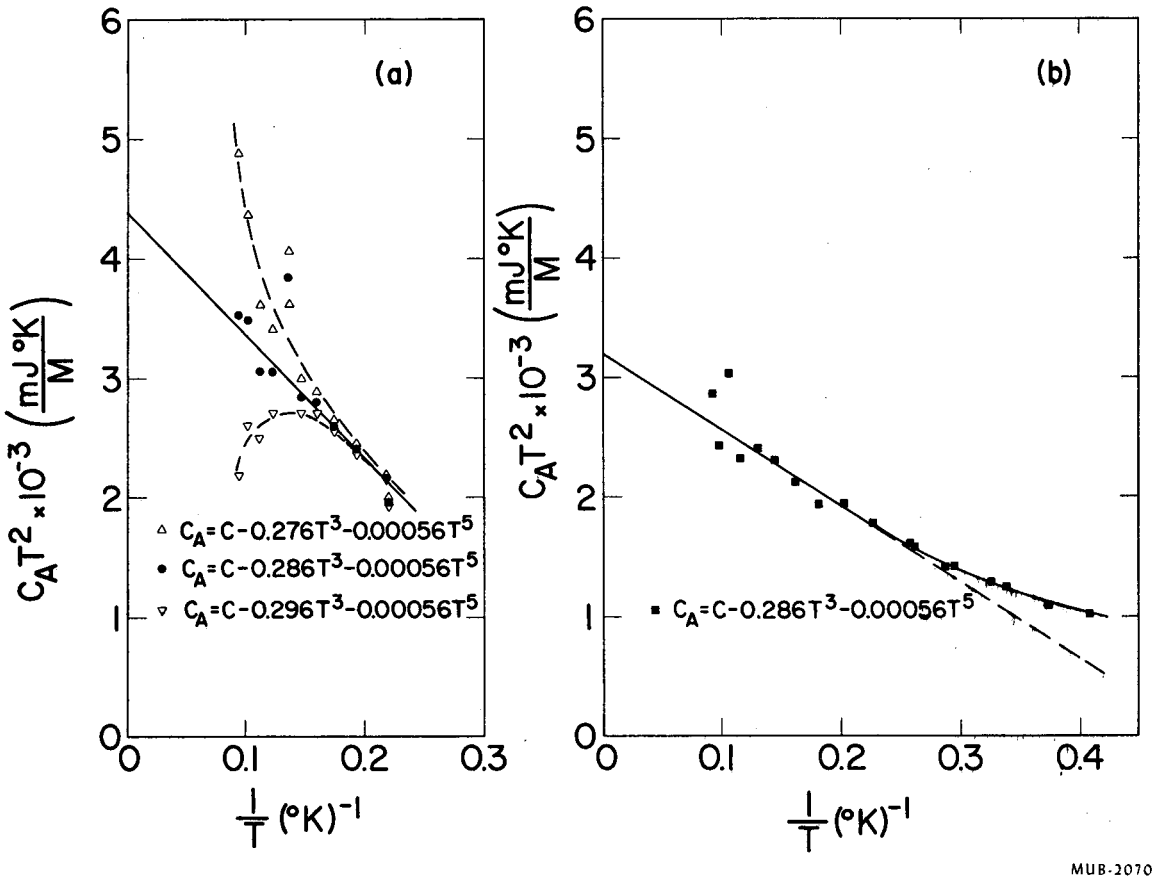


Fig. IV-4. The anomalous heat capacity of 6.3% ortho hydrogen at 18.7 cc/M.

A. First set of measurements
B. Second set of measurements.

capacity to yield the lattice contribution. The results are listed in Table IV-7. The lattice heat capacity is also plotted in Fig. IV-3 in the form of $C/T^3$ vs $T^2$.

During the first set of measurements a strong heat evolution, beyond the rate of heating due to the ortho-para conversion, was observed above 12 °K. This made it impossible to measure heat capacities between 13 and 15 °K, and made fore- and afterdrift extrapolations difficult for all temperatures above 12 °K. Consequently the scatter in the data is of the order of ±5%. When the second set of data was taken, this phenomenon was not observed. The second set shows a scatter of ±2%. A systematic error of 2% due to the 1% uncertainty in the empty calorimeter heat capacity is also possible.

## C. The Debye Characteristic Temperature and the Grüneisen Gamma of Hydrogen

Smoothed values of the heat capacities were obtained from large-scale graphs of $C/T^3$ vs $T^2$ at integral values of T. The Debye temperatures were calculated from these data for the $C_v$ measurements. These smoothed values are presented in Table IV-8. The experimental data on $C_v$ extend down to $T/\theta \approx 0.025$, and the accuracy is smallest at the low temperatures. This makes extrapolation to $T = 0$ somewhat difficult. This problem has been discussed by others, and particularly by Beaumont et al.[2] for argon and krypton. For the data presented here it was preferred to extrapolate $C/T^3$ vs $T^2$ rather than $\theta$ vs T. The Debye temperatures at 0 degrees are estimated to be (128.1 ± 2)°K at 22.56 cc/M, (169.0 ± 4)°K at 19.83 cc/M, and (189.4 ± 5)°K at 18.73 cc/M.

The temperature dependence of $\theta$ is conveniently displayed in the form of a graph of $\theta/\theta_0$ vs $T/\theta_0$, where $\theta_0$ is the Debye temperature at 0 degrees. Values of $\theta/\theta_0$ and $T/\theta_0$ are given in Table IV-9 and are presented graphically in Fig. IV-5. Also shown for comparison in Fig. IV-5 are the curves for argon[3] and krypton.[2]

It is clear that the general behavior of $\theta/\theta_0$ is very similar to that observed for more classical solids such as argon and krypton. However, there appears to be a small systematic change in $\theta/\theta_0$ at a

Table IV-7. Heat capacity of 6% ortho hydrogen at 18.73 cc/M. C is the total and $C_i$ the lattice heat capacity.

| First set of measurements | | | Second set of measurements | | |
|---|---|---|---|---|---|
| T (°K) | $C\left(\frac{mJ}{M°K}\right)$ | $C_L\left(\frac{mJ}{M°K}\right)$ | T (°K) | $C\left(\frac{mJ}{M°K}\right)$ | $C_L\left(\frac{mJ}{M°K}\right)$ |
| 4.560 | 132.6 | 29.1 | 4.428 | 116.7 | 27.2 |
| 4.542 | 123.1 | 19.2 | 4.955 | 115.6 | 37.9 |
| 5.170 | 131.9 | 41.1 | 5.512 | 114.6 | 47.5 |
| 5.745 | 136.2 | 57.0 | 6.206 | 128.5 | 72.2 |
| 6.255 | 146.9 | 76.3 | 6.921 | 151.8 | 104.3 |
| 6.780 | 149.2 | 96.3 | 7.706 | 186.6 | 146.6 |
| 7.370 | 197.4 | 142.0 | 8.677 | 245.3 | 212.6 |
| 8.113 | 218.8 | 171.2 | 9.539 | 325.8 | 298.0 |
| 8.918 | 272.8 | 232.0 | 10.294 | 399.8 | 375.5 |
| 9.759 | 352.0 | 316.8 | 10.998 | 494.4 | 472.7 |
| 10.628 | 450.8 | 420.3 | 11.632 | 585.0 | 566.0 |
| 11.442 | 579.0 | 552.0 | 12.037 | 663.0 | 644.0 |
| 12.299 | 797.0 | 773.0 | 12.355 | 713.0 | 696.0 |
| 14.182 | 1746.0 | 1731.0 | 12.666 | 777.0 | 760.0 |
| 17.621 | 2312.0 | 2299.0 | 13.071 | 864.0 | 848.0 |
| 18.528 | 2598.0 | 2586.0 | 13.693 | 974.0 | 960.0 |
| 19.331 | 3226.0 | 3215.0 | 15.616 | 1526.0 | 1515.0 |
| | | | 16.577 | 1826.0 | 1816.0 |

Table IV-8. Smoothed values for the lattice heat capacities and Debye thetas for hydrogen.

| T (°K) | $C_p\left(\frac{mJ}{M°K}\right)$ | $C_v\left(\frac{mJ}{M°K}\right)$ at | | | $\theta_D$ (°K) at | | |
|---|---|---|---|---|---|---|---|
| | | 22.56 cc/M | 19.83 cc/M | 18.73 cc/M | 22.56 cc/M | 19.83 cc/M | 18.73 cc/M |
| 0 | 0.00 | 0.00 | 0.00 | 0.00 | 128.1 | 169.0 | 189.4 |
| 1 | 1.03 | 0.93 | 0.40 | 0.29 | 127.8 | 168.8 | 189.2 |
| 2 | 8.57 | 7.58 | 3.26 | 2.31 | 127.0 | 168.3 | 188.8 |
| 3 | 30.7 | 26.4 | 11.28 | 7.88 | 125.7 | 167.4 | 188.1 |
| 4 | 78.7 | 65.3 | 27.1 | 18.94 | 123.9 | 166.2 | 187.3 |
| 5 | 168.5 | 134.6 | 54.2 | 37.5 | 121.8 | 164.9 | 186.4 |
| 6 | 318.8 | 247 | 96.8 | 66.3 | 119.3 | 163.1 | 185.0 |
| 7 | 551 | 418 | 159.1 | 107.7 | 116.9 | 161.2 | 183.6 |
| 8 | 882 | 662 | 247 | 164.9 | 114.5 | 159.1 | 182.1 |
| 9 | 1333 | 990 | 367 | 242 | 112.5 | 156.9 | 180.0 |
| 10 | 1917 | 1413 | 523 | 343 | 110.7 | 154.9 | 178.3 |
| 11 | 2651 | 1919 | 723 | 471 | 109.4 | 152.8 | 176.4 |
| 12 | 3548 | 2499 | 968 | 632 | 108.5 | 151.2 | 174.4 |
| 13 | 4618 | 3142 | 1259 | 830 | 107.8 | 149.8 | 172.4 |
| 14 | 5910 | 3866 | 1597 | 1067 | 107.0 | 148.6 | 170.7 |
| 15 | — | 4678 | 1978 | 1340 | 105.8 | 147.6 | 169.2 |
| 16 | — | — | 2405 | 1655 | — | 146.7 | 167.7 |
| 17 | — | — | 2869 | 2009 | — | 146.0 | 166.4 |
| 18 | — | — | 3359 | 2409 | — | 145.5 | 165.1 |
| 19 | — | — | 3882 | 2860 | — | 144.9 | 163.4 |
| 20 | — | — | 4432 | 3360 | — | 144.4 | 161.6 |

Table IV-9. Reduced Debye temperatures for solid hydrogen.

| T (°K) | 22.56 | | 19.83 | | 18.73 | |
|---|---|---|---|---|---|---|
| | $\theta/\theta_0$ | $T/\theta_0$ | $\theta/\theta_0$ | $T/\theta_0$ | $\theta/\theta_0$ | $T/\theta_0$ |
| 1 | 0.998 | 0.0078 | 0.999 | 0.0059 | 0.999 | 0.0053 |
| 2 | 0.991 | 0.0156 | 0.996 | 0.0118 | 0.997 | 0.0106 |
| 3 | 0.981 | 0.0234 | 0.990 | 0.0178 | 0.993 | 0.0158 |
| 4 | 0.967 | 0.0312 | 0.983 | 0.0237 | 0.989 | 0.0211 |
| 5 | 0.951 | 0.0390 | 0.976 | 0.0296 | 0.984 | 0.0264 |
| 6 | 0.931 | 0.0468 | 0.965 | 0.0355 | 0.977 | 0.0317 |
| 7 | 0.912 | 0.0546 | 0.954 | 0.0414 | 0.969 | 0.0370 |
| 8 | 0.894 | 0.0624 | 0.941 | 0.0473 | 0.961 | 0.0422 |
| 9 | 0.878 | 0.0702 | 0.928 | 0.0532 | 0.951 | 0.0475 |
| 10 | 0.864 | 0.0781 | 0.916 | 0.0592 | 0.941 | 0.0528 |
| 11 | 0.854 | 0.0859 | 0.904 | 0.0651 | 0.931 | 0.0581 |
| 12 | 0.847 | 0.0937 | 0.895 | 0.0710 | 0.921 | 0.0633 |
| 13 | 0.841 | 0.1015 | 0.886 | 0.0769 | 0.911 | 0.0686 |
| 14 | 0.835 | 0.1093 | 0.879 | 0.0828 | 0.901 | 0.0739 |
| 15 | 0.826 | 0.1171 | 0.873 | 0.0888 | 0.893 | 0.0792 |
| 16 | — | — | 0.868 | 0.0946 | 0.885 | 0.0845 |
| 17 | — | — | 0.864 | 0.1006 | 0.879 | 0.0898 |
| 18 | — | — | 0.861 | 0.1065 | 0.872 | 0.0950 |
| 19 | — | — | 0.857 | 0.1124 | 0.863 | 0.1003 |
| 20 | — | — | 0.854 | 0.1183 | 0.853 | 0.1056 |

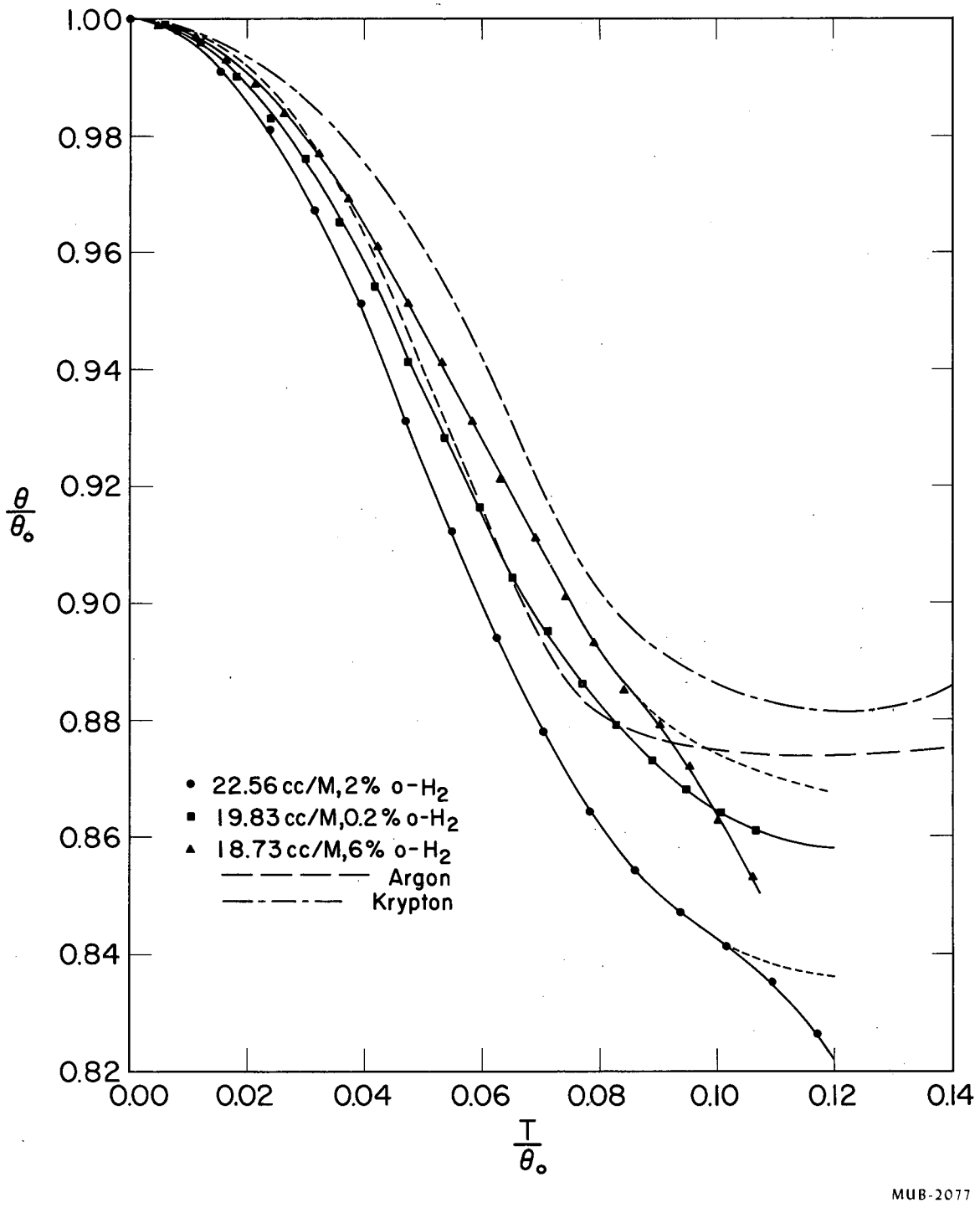


Fig. IV-5. The reduced Debye temperature as a function of the reduced temperature for hydrogen, argon, and krypton.

given value of $T/\theta_0$ with molar volume. Whereas changes in $\theta_0$ within the stated limits of error can be made in such a fashion that the $\theta/\theta_0$ curves for the three molar volumes coincide, it must be considered that 35 to 50% of the errors in $\theta_0$ are systematic errors due to the uncertainty in the heat capacity of the empty calorimeter. The remaining random errors due to the extrapolation of $C/T^3$ to $T^2 = 0$ are not large enough to permit adjustments in the $\theta_0$ values that would cause the $\theta/\theta_0$ curves to coincide. It thus appears that there is a real increase in $\theta/\theta_0$ with decreasing molar volume. The fact that anharmonicity effects become smaller at smaller molar volumes tends to suggest that anharmonicity causes a decrease in $\theta$ at relative temperatures below $T/\theta_0 \approx 0.1$. Beaumont, et al.[2] suggested an effect in the opposite direction at much higher temperatures.

The samples for the measurements at 22.56 cc/M and 18.73 cc/M contained 2% and 6% ortho hydrogen respectively. Possible effects of the ortho hydrogen on the lattice heat capacity cannot be ruled out completely. Such effects are, however, believed to be negligible because the reduced Debye thetas are in accord with those for the measurements on 0.2% ortho hydrogen at 19.83 cc/M.

Above $T/\theta_0 \approx 0.10$, the Debye thetas at 22.56 cc/M and 18.73 cc/M appear to suddenly decrease excessively fast. Such an effect can be due to several phenomena, and particularly could be an indication of vacancy formation. However, the effect observed here is so small that it may well be due to a slight error in the estimates of $C/T^3$ from which the $\theta$ values were derived. The dotted extensions in Fig. IV-5 of $\theta/\theta_0$ below $T/\theta_0 = 0.10$ correspond to the dotted high-temperature ends of the lines through $C/T^3$ vs $T^2$ in Figs. IV-1 and IV-3.

Although it appears that anharmonic effects on $\theta/\theta_0$ are small in hydrogen, the effect of anharmonicity on $\theta_0$ may well be quite large. It would be interesting to compare the Debye thetas with those predicted by the harmonic approximation, but these calculations are beyond the scope of this work. In the case of argon and krypton such a comparison has been made,[1] and although it appears that anharmonic effects are present, these effects are relatively small. In hydrogen

with a relative 0-point energy about five times that of argon, these effects should show up more clearly.

Two sets of values of Grüneisen gammas, Eq.(IV-3), were calculated from the measurements at the three molar volumes and are given in Table IV-10. Gamma calculated from the heat capacities at 18.73 cc/M and 19.83 cc/M appears to be about 8% smaller than $\gamma$ calculated from the measurements at 19.83 cc/M and 22.56 cc/M; however the difference is well within the possible error due to the errors in the molar volumes. The temperature dependence of $\gamma$ is shown in Fig. IV-6.

## D. The Thermodynamic Properties of Solid Para Hydrogen

Very limited thermodynamic data are now available on solid hydrogen, and except for the $C_p$ measurements by Hill and Lounasmaa,[32] there were no reliable data on solid para hydrogen previous to this work. Fluid para hydrogen was recently studied extensively at pressures as high as 300 atm,[34,36 to 39] and its properties are now well defined over perhaps a larger volume and temperature range than that of any other substance. The PVT properties of solid para hydrogen can be expected to differ only slightly from those of solid normal hydrogen. In the liquid state at 14 °K, for example, the molar volumes at the vapor pressure differ by only 0.4%.[37] This figure gives a rough indication of what can be expected when available information on solid hydrogen of a variety of ortho-para compositions is pooled in an attempt to arrive at some conclusions about the PVT properties. A brief review of the available information is now given.

The molar volume of solid hydrogen was measured by Megaw[35] at 4.2 °K from 0 to 100 kg/cm$^2$. Megaw purified her samples at liquid-air temperatures and thus probably had about 50% para hydrogen. Her measurements were later extended to 20 000 kg/cm$^2$ by Stewart, whose samples originally contained 25% para hydrogen.[40,41,42] But no doubt the composition changed during the course of the measurements, particularly at the higher pressures, due to the ortho-para conversion.

Table IV-10. Grüneisen gammas for hydrogen as a function of temperature.

| T(°K) | Values of $\gamma$ from $\theta$ at 19.83 and 22.56 cc/M | Values of $\gamma$ from $\theta$ at 18.73 and 19.83 cc/M |
|---|---|---|
| 0 | 2.14 | 2.00 |
| 1 | 2.15 | 2.00 |
| 2 | 2.18 | 2.02 |
| 3 | 2.22 | 2.05 |
| 4 | 2.27 | 2.10 |
| 5 | 2.34 | 2.14 |
| 6 | 2.42 | 2.20 |
| 7 | 2.49 | 2.28 |
| 8 | 2.54 | 2.37 |
| 9 | 2.57 | 2.40 |
| 10 | 2.60 | 2.46 |
| 11 | 2.58 | 2.51 |
| 12 | 2.57 | 2.50 |
| 13 | 2.55 | 2.46 |
| 14 | 2.54 | 2.43 |
| 15 | 2.57 | 2.39 |
| 16 | — | 2.34 |
| 17 | — | 2.30 |
| 18 | — | 2.22 |
| 19 | — | 2.11 |

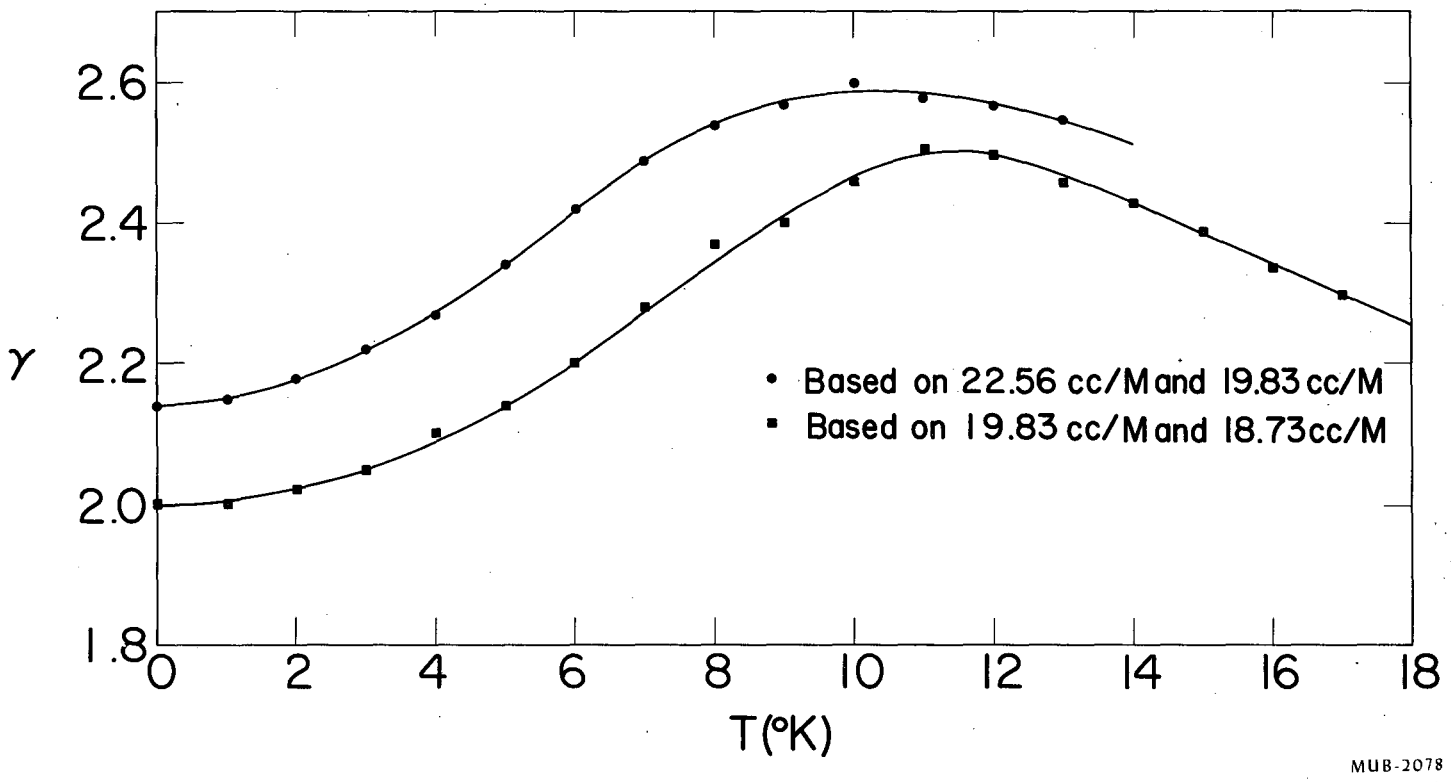


Fig. IV-6. The Grüneisen gamma as a function of temperature.

The molar volume of para hydrogen at the triple point can be estimated with considerable accuracy from other thermodynamic data. The properties of the liquid are now very well known; the heat of melting was measured by Clusius and Hiller,[43] and again during the course of this work. With the help of the Clapeyron equation these data yield a triple-point volume of (23.32 ± 0.01) cc/M and a volume change on melting of (2.86 ± 0.01) cc/M.

The volume change on melting of normal hydrogen was measured by Bartholomé at two temperatures.[33] This volume change would be expected to be affected little by the para concentration, and Bartholomé's data in conjunction with those by Goodwin and Roder on the liquid[34] can be expected to give the volume of solid para hydrogen at the melting line to ± 0.10 cc/M.

The melting pressure as a function of temperature of normal hydrogen was determined by Mills and Grilly up to 3500 kg/cm$^2$,[44] and recently the melting pressure of para hydrogen was evaluated by Goodwin and Roder up to 5500 kg/cm$^2$.[34]

The average compressibility of normal hydrogen between 0 and 230 atm and 6 to 9 °K was determined very approximately by Smith and Squire by means of nuclear magnetic resonance (NMR) measurements.[45]

Bartholomé and Euken[28] measured the heat capacity at constant volumes of para hydrogen; but as discussed earlier, the volume for these measurements is unknown. Hill and Lounasmaa's $C_p$ measurements[32] have already been mentioned. There appears to be no further information on the PVT properties of solid hydrogen.

In spite of this scarcity of data, it already was apparent to Megaw[35] that solid hydrogen does not behave like a classical solid. Her PV measurements at 4.2 °K showed that the compressibility decreased exceptionally rapidly with increasing pressure. Megaw also considered the fact that both $C_p$[46] and $C_v$[28] varied as $T^3$. The thermodynamic relation (IV-1) then implies that $\alpha$ varies as T if K is independent of T. On the other hand, Grüneisen's law implies that $\alpha$ varies approximately as $T^3$, for according to the Grüneisen

equation of state

$$\alpha = \frac{\gamma C_v K}{V} . \qquad \text{(IV-13)}$$

It was thus apparent that the Grüneisen equation of state was not valid for solid hydrogen. Megaw's arguments can now be repeated and extended on the basis of the more extensive and accurate data presented in this work.

As was shown in the previous section, the Grüneisen relation

$$\frac{d \ln \theta}{d \ln V} = - \gamma , \qquad \text{(IV-14)}$$

with constant $\gamma$ is not strictly valid in the case of hydrogen. But the temperature dependence of $\gamma$ is no more severe than that expected for other more classical solids,[1, 2] and the volume dependence of $\gamma$ is smaller than the experimental error. If $\gamma$ were constant, then according to Grüneisen, Eq. (IV-13) would also be valid. But comparison of the thermodynamic properties predicted by Eq. (IV-13) with known properties of solid hydrogen will show some severe discrepancies.

If it is assumed that Eq. (IV-13) is valid, then

$$\left(\frac{\partial P}{\partial T}\right)_V = \alpha/K = \frac{\gamma C_v}{V} . \qquad \text{(IV-15)}$$

It is thus possible to integrate relation (IV-15) from $T = 0$ to the temperature at which melting starts and thereby to determine the pressure change in the solid at constant volume between 0 °K and the melting point. At 22.56 cc/M and 4 °K, the data due to Megaw[35] indicate that the pressure is 8 kg/cm$^2$. The integration outlined above yields a pressure change of 30 kg/cm$^2$ up to the melting point, yielding a pressure of 38 kg/cm$^2$ at 16.35 °K for solid in equilibrium with liquid. The actual melting pressure determined by Goodwin and Roder[34] is 82.5 atm, showing a disagreement well outside that of experimental error. It must therefore be concluded that Eq. (IV-13) is not valid at 22.56 cc/M.

A similar calculation can be carried out at 19.83 cc/M. The pressure at 4 °K is 426 atm. Melting should start at about 27 °K, at a pressure of about 560 atm. The pressure change predicted by

(IV-13) and the heat capacity measurements (extrapolated with a Debye $\theta$ of 145 °K above 20 °K) is about 80 atm. Unfortunately the uncertainties in both the sample volume and the temperature at which melting starts are too large to permit any conclusions. But again the predicted pressure change appears low.

Comparison of $C_p$ and $C_v$ leads to the same contradiction between Eqs. (IV-13) and (IV-1) as that discussed by Megaw.

In view of the failure of Grüneisen's law, we attempted to obtain information about the PVT properties of solid para hydrogen by purely thermodynamic means. First we discuss the discontinuity in the heat capacity at the beginning of melting at 22.56 cc/M, and then we compare the $C_p$ and $C_v$ measurements.

Lounasmaa[47] showed that the discontinuity in the heat capacity at constant volume at the boundary between a single-phase and a two-phase region is given by

$$\Delta C_v = T \frac{dV}{dT} \left[ \left(\frac{\partial P}{\partial T}\right)_V - \frac{dP}{dT} \right] \tag{IV-16}$$

where $\Delta C_v$ is always taken to be positive. The partial derivatives refer to the single phase, dV/dT is the volume change of the single phase along the boundary, and dP/dT is the pressure change along the transition. Furthermore the equation

$$\left(\frac{\partial P}{\partial T}\right)_V - \frac{dP}{dT} = - \frac{dV}{dT} \left(\frac{\partial P}{\partial V}\right)_T \tag{IV-17}$$

is also valid. Equations (IV-16) and (IV-17) lead to

$$\left(\frac{\partial P}{\partial T}\right)_V = \frac{\Delta C_v}{T\,(dV/dT)} + \frac{dP}{dT} \tag{IV-18}$$

$$\left(\frac{\partial P}{\partial V}\right)_T = - \frac{\Delta C_v}{T\,(dV/dT)^2} \tag{IV-19}$$

$$\begin{aligned} \left(\frac{\partial V}{\partial T}\right)_P &= \frac{dV}{dT} + \frac{T}{\Delta C_v} \left(\frac{dV}{dT}\right)^2 \frac{dP}{dT} \\ &= \frac{dV}{dT} - \left(\frac{\partial V}{\partial P}\right)_T \frac{dP}{dT} \end{aligned} \tag{IV-20}$$

for the partial derivatives in terms of the properties along the boundary. Equation (IV-20) was used by Grilly and Mills to derive some properties of α- and γ-$He^4$.[48] As they pointed out, Eq. (IV-20) can be combined for the solid and liquid to give

$$\left(\frac{\partial V}{\partial T}\right)_{P,s} = \left(\frac{\partial V}{\partial T}\right)_{P,\ell} - \frac{d\,\Delta V}{dT} + \left[\left(\frac{\partial V}{\partial P}\right)_{T,\ell} - \left(\frac{\partial V}{\partial P}\right)_{T,s}\right]\frac{dP}{dT}, \quad \text{(IV-21)}$$

where the subscripts s and $\ell$ indicate that the derivative refers to the solid or liquid phase, respectively. It is thus possible to obtain the three derivatives for solid hydrogen at the onset of melting. The numerical values used in and derived from the equations are given in Table IV-11.

The term $(\partial V/\partial T)_P$ is obtained as a small difference between two large quantities in either Eq.(IV-20) or (IV-21). It therefore has a rather large error associated with it. Only $(\partial P/\partial V)_T$ can be determined with reasonable accuracy. Nonetheless, comparison with the properties at 4.2 °K yields some interesting results.

The compressibility changed little if at all between 4.2 and 16.35 °K. Megaw at 100 kg/cm$^2$ obtained $3.2 \times 10^{-4}$ cm$^2$/kg.[35] The value at 16.35 °K and 82.5 atm is $3.8 \times 10^{-4}$ atm$^{-1}$. Thus, it appears that at constant pressure K is reasonably temperature independent. This is also in agreement with the approximate value of $2 \times 10^{-4}$ between 0 and 230 atm at 6 to 9 °K found by Smith and Squire.[45]

The thermal expansion at 16.35 °K and 82.5 atm is essentially zero, with rather wide limits of uncertainty. The largest possible value for $(\partial V/\partial T)_P$ is 0.06 cc/°K. The total thermal expansion between 4.2 °K and 16.35 °K is 0.80 cc. Thus even for the largest possible value of $(\partial V/\partial T)_P$ the 82.5 atm isobar must have a point of inflection, and this implies that α must have a maximum between 4.2 and 16.35 °K, and probably between 10 °K and 15 °K. We now proceed to the comparison of the $C_p$ and $C_v$ measurements.

In principle it is possible to calculate $\alpha^2/K$ from $C_p$ and $C_v$ by means of Eq. (IV-1). But as was already pointed out, both $C_p$ and $C_v$ must be measured at the same volume. If Eq. (IV-2) is obeyed, it is possible to calculate $C_v$ at the volumes $V_T$ of the $C_p$ measurements

Table IV-11. Properties of solid para hydrogen at the melting line.

| Variable | Value | Source |
|---|---|---|
| T | (16.35 ± 0.02) °K | This work |
| $\Delta C$ | (16.4 + 0.4) J/M °K | This work |
| P | 82.5 atm | Goodwin and Roder [34] |
| dP/dT | 35.2 atm/°K | Goodwin and Roder [34] |
| dV/dT | -(0.290 ± 0.03) cc/°K | Goodwin and Roder [34]<br>Bartholomé [33] |
| $d\Delta V/dT$ | -(0.18 ± 0.03) cc/°K | Bartholomé [33] |
| $\left(\frac{\partial V}{\partial P}\right)_{T,\ell}$ | -(0.0188 ± 0.0001) cc/°K | Goodwin et al. [36] |
| $\left(\frac{\partial V}{\partial T}\right)_{P,\ell}$ | (0.180 ± 0.005) cc/°K | Goodwin et al. [36] |
| $\left(\frac{\partial P}{\partial V}\right)_{T,s}$ | -(118 ± 13) atm/cc | Eq. (IV-19) |
| $\left(\frac{\partial P}{\partial T}\right)_{V,s}$ | (1 ± 5) atm/°K | Eq. (IV-18) |
| $\left(\frac{\partial V}{\partial T}\right)_{P}$ | (0.008 ± 0.1) cc/°K | Eq. (IV-20) |
| $\left(\frac{\partial V}{\partial T}\right)_{P}$ | (0.00 ± 0.06) cc/°K | Eq. (IV-21) |

from $C_v$ at 22.56 cc/M, provided the volumes of the $C_p$ measurements are known. It was shown in Sec. IV.C that for molar volumes between 18.73 cc and 22.56 cc, Eq. (IV-2) is obeyed within experimental error. In view of the fact that the calculation of $C_v(V_T)$ involves an extrapolation over a maximum of 0.7 cc/M, one would expect that reasonable values of $C_v(V_T)$ can be calculated. Of course the possibility of strong deviations from Eq. (IV-2) near the solid-vapor equilibrium line cannot be entirely ruled out. In order to calculate $C_v(V_T)$, $V_T$ must be known. $V_T$ can be calculated only if $\alpha$ is known. Thus a method of successive approximations was used to calculate $\alpha$ from Eq. (IV-1), assuming first that $C_v$ at 22.65 cc/M is equal to $C_v(V_T)$. The resulting values of $\alpha$ were used to calculate $V_T$, and a new set of values for $\alpha$ was obtained. The calculation had converged sufficiently after the fourth approximation. The values of $\gamma$ used were the ones calculated from $C_v$ at 19.83 cc/M and 22.56 cc/M, and the value for K was the one obtained by Megaw at zero pressure ($7.0 \times 10^{-4}$ atm$^{-1}$).[35] The final values for $\alpha$ and $V_T$ are given in Table IV-7. The term $V_T$ is based on Megaw's value for the volume at 4.2 °K. The predicted triple-point volume is 23.27 cc/M, compared with the experimental value of 23.32 cc/M.

It is difficult to estimate the accuracy of the values for $\alpha$ obtained by the above calculation because it is not known how reliable the calculation of $C_v(V_T)$ is. It thus seemed desirable to calculate $\alpha$ by an independent method that involves different approximations. The basic relation between the PVT and the thermal properties is

$$\left(\frac{\partial S}{\partial V}\right)_T = \frac{\alpha}{K} . \qquad \text{(IV-22)}$$

If $\alpha/K$ is independent of V between the volumes of the $C_p$ and $C_v$ measurements, then one can evaluate $\alpha/K$ from

$$\left(\frac{\alpha}{K}\right) = \frac{\Delta S}{\Delta V} , \qquad \text{(IV-23)}$$

where $\Delta V = V_T - V(C_v)$.

Equation (IV-23) is not usable as it stands for the calculation of $\alpha$, because again $\Delta V$ is not known. But

$$\Delta V = \Delta V_0 + V_0 \int_0^T \alpha \, dT \, , \qquad \text{(IV-24)}$$

where $\Delta V_0$ is the volume difference between the $C_p$ and $C_v$ measurements at 0 °K. Now

$$\Delta V_0 \, \alpha + V_0 \, \alpha \int_0^T \alpha \, dT = K \, \Delta S \, . \qquad \text{(IV-25)}$$

This equation has the solution

$$\alpha = \frac{K \, \Delta S}{V_0 \left[ (\Delta V_0 / V_0)^2 + (2K/V_0) \int_0^T \Delta S \, dT \right]^{1/2}} \, . \qquad \text{(IV-26)}$$

In obtaining Eq. (IV-26) it was assumed that K is independent of T. The terms $\Delta S$ and $\int \Delta S \, dT$ can be obtained from the heat-capacity measurements. The value used for K was again the one measured by Megaw[35] at 4.2 °K and zero pressure. The calculations of $\alpha$ with $\Delta V_0 = 0.00$, 0.06, and 0.12 cc/M, are given in Table IV-12. The most probable value of $\Delta V_0$ is 0.08 cc/M, based on the experimental volume of 22.56 cc/M, Megaw's estimate of the volume at 4.2 °K, and the calculated thermal expansion between 0 and 4.2 °K. The volume as a function of T was calculated with $\alpha$ from $\Delta V_0 = 0.06$ cc/M and Megaw's volume at 4.2 °K. The values of $V_T$ are also listed in Table IV-12. The predicted triple-point volume is 23.21 cc/M. The experimental value is 23.32 cc/M. The two methods of calculating $\alpha$ involve partially different assumptions. They both assume that K is independent of T. This assumption is supported by the values of K at 82.5 atm at 4.2 °K and 16.35 °K. The method employing Eqs. (IV-1) and (IV-2) assumes further only the validity of Eq. (IV-2). The method employing Eq. (IV-26) assumes that $\alpha/K$ is independent of V over the small volume range in question. In view of the rapid change of K with V observed by Megaw, this may well be the least-reliable assumption. Qualitatively both methods yield the same results for $\alpha$ at high temperatures. At low temperatures, Eq. (IV-26) is very

Table IV-12. Thermal expansion coefficient and molar volume of solid hydrogen at zero pressure.

| T (°K) | $\alpha \times 10^4$ (°K)$^{-1}$ | | | | V (cc/M) | |
|---|---|---|---|---|---|---|
| | Eq. (IV-1) | Eq. (IV-26) | | | Eq. (IV-1) | Eq. (IV-26) $\Delta V_0 = 0.06$ |
| | | $\Delta V_0 = 0.00$ | $\Delta V_0 = 0.06$ | $\Delta V_0 = 0.12$ | | |
| 1 | 1.6 | 1.1 | 0.022 | 0.015 | 22.614 | 22.645 |
| 2 | 3.4 | 2.6 | 0.22 | 0.16 | 22.619 | 22.645 |
| 3 | 6.0 | 4.6 | 1.0 | 0.7 | 22.629 | 22.646 |
| 4 | 9.4 | 7.3 | 3.0 | 2.2 | 22.646 | 22.650 |
| 5 | 13.6 | 10.6 | 6.5 | 5.1 | 22.672 | 22.660 |
| 6 | 17.8 | 14.5 | 11.3 | 9.6 | 22.708 | 22.678 |
| 7 | 22.0 | 18.7 | 16.5 | 14.9 | 22.753 | 22.711 |
| 8 | 25.5 | 23.2 | 21.7 | 20.5 | 22.806 | 22.754 |
| 9 | 28.9 | 27.7 | 26.7 | 25.8 | 22.868 | 22.809 |
| 10 | 33.4 | 31.0 | 30.4 | 29.8 | 22.937 | 22.873 |
| 11 | 35.1 | 35.0 | 34.6 | 34.2 | 23.013 | 22.947 |
| 12 | 38.9 | 39.8 | 39.4 | 39.1 | 23.097 | 23.031 |
| 13 | 43.4 | 45.1 | 44.7 | 44.5 | 23.190 | 23.125 |
| 13.80 | 48.0 | 49.5 | 49.1 | 48.8 | 23.273 | 23.211 |

sensitive to errors in $\Delta V_0$, and of course $\Delta V_0$ is not known very accurately. On the other hand, $\alpha$ calculated from Eqs. (IV-1) and (IV-2) is not sensitive to small changes in $\Delta V_0$, and at low temperatures these values for $\alpha$ are perhaps more reliable.

The differences between the predicted triple-point volumes and the actual triple-point volume are smaller than the possible error in Megaw's volume at 4.2 °K for both approximations.

The estimates of $\alpha$ are presented graphically in Fig. IV-7. Above 4 °K, $\alpha$ approaches almost linear behavior. Above 10 °K the possibility exists of a considerable contribution to $\alpha$ from vacancy formation. It is thus conceivable that in the absence of vacancies, $\alpha$ would rise less rapidly than T, and possibly would even go through a maximum similar to that deduced for the 82 atm isobar. In fact, there is an indication between 9 °K and 11 °K that $\alpha$ is beginning to rise less rapidly than at lower temperatures. For comparison the qualitative features of $\alpha$ at 82.5 atm are also shown in Fig. IV-7.

Whereas at this time the volume of solid hydrogen is not known with an accuracy greater than 0.5% under any conditions except at the triple point, the best estimates of the PVT properties have been compiled in Fig. IV-8 in the form of a V-T diagram.

Dugdale and Simon used Eq. (IV-15) to calculate the PVT properties of solid $He^4$.[24] They determined their integration constant from the melting pressure, and calculated P and $(\partial P/\partial V)_T$ as a function of T down to 0 °K.

There are no direct low-temperature measurements of the volume of solid helium, and the validity of Eq. (IV-15) thus cannot be checked. The results reported here for hydrogen would make such a check extremely desirable, especially since the high-pressure work by Stewart[49,63] on the molar volume of $He^4$ at 4.2 °K is based on the data by Dugdale and Simon.

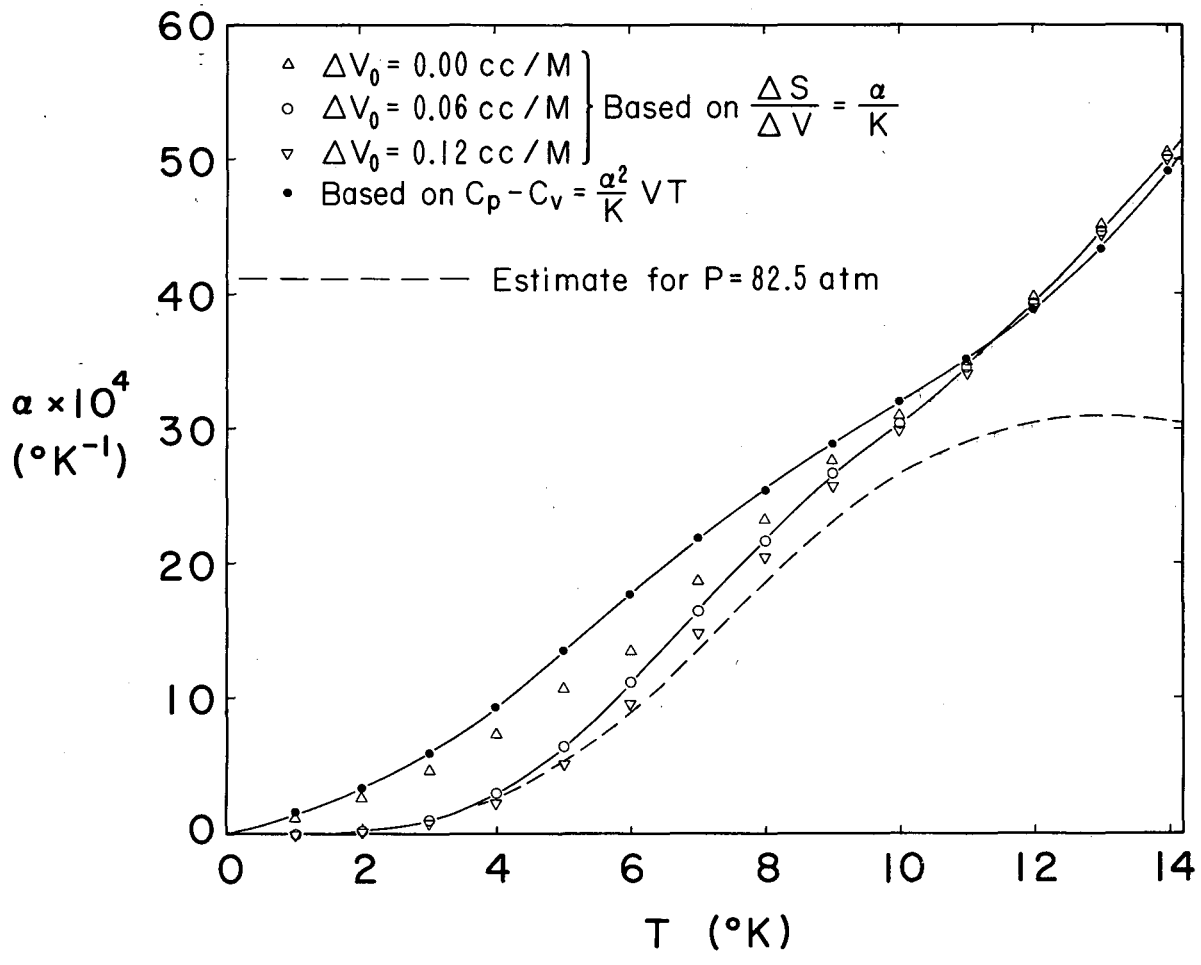


Fig. IV-7. The thermal-expansion coefficient of solid hydrogen. The points represent the calculated values at zero pressure, and the dashed line represents the qualitative features of the coefficient at 82.5 atmospheres.

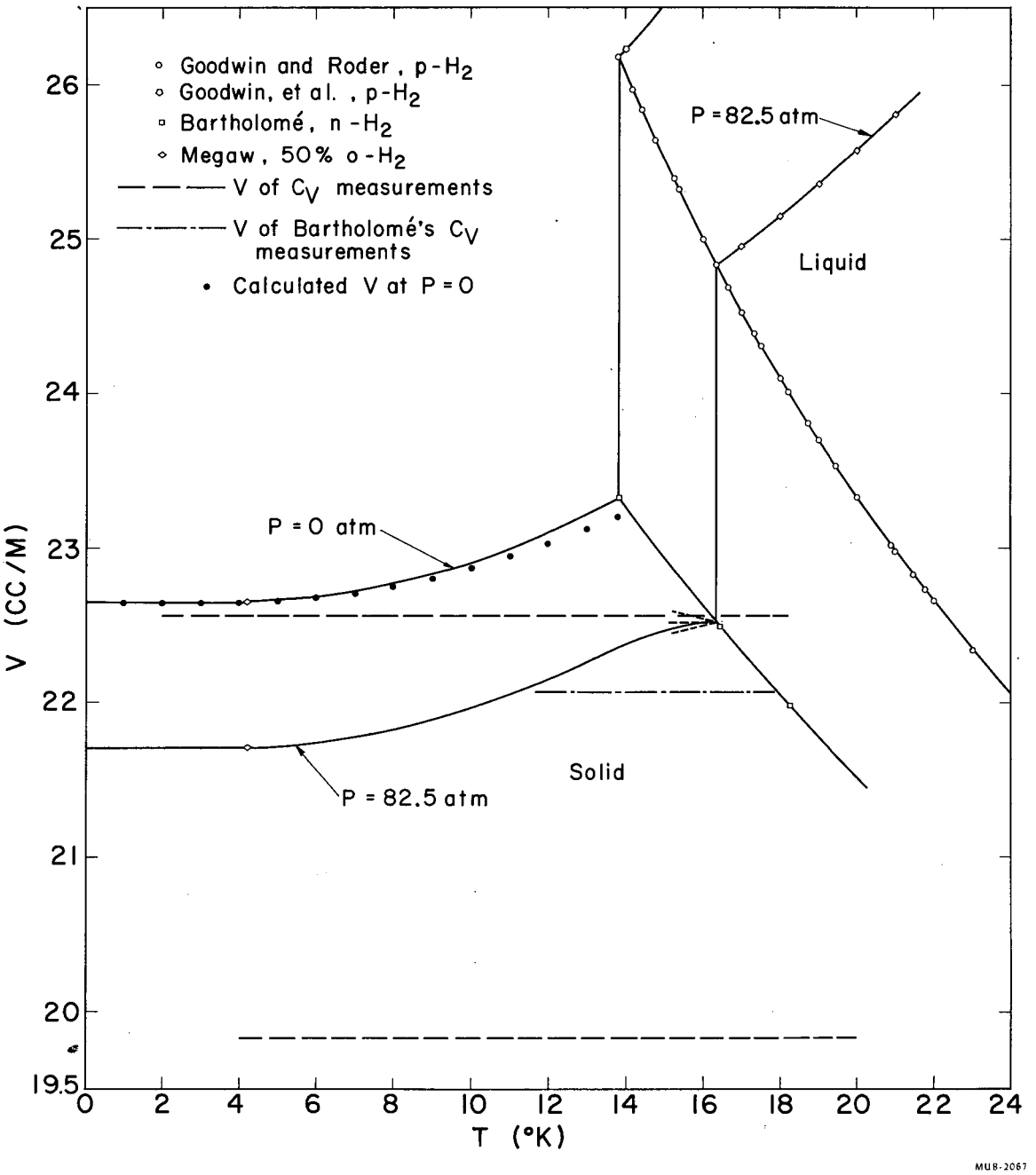


Fig. IV-8. The PVT properties of solid hydrogen.

## V. THE ANOMALOUS HEAT CAPACITY OF ORTHO HYDROGEN

The problem of the anomalous heat capacity of ortho hydrogen due to the molecular rotation was discussed by Orttung[6] in some detail, and is outlined briefly here. The lowest rotational state of ortho hydrogen is the one identified by $J = 1$, and in the ideal gas is threefold degenerate. In the solid state the degenerate levels are perturbed by the interaction between the molecules, and the degeneracy is removed. This perturbation results in a contribution to the heat capacity at low temperatures. At high concentrations of ortho hydrogen it was observed experimentally[4,5] that the heat-capacity contribution is not entirely of the Schottky type, but that there is a $\lambda$-type transition in the vicinity of 1.5 °K. Such a transition is indicative of a cooperative phenomenon. Although the theoretical treatment of the problem presents severe difficulties, it is clear that the entropy contribution from the rotational states should be $q\,R\ln 3$, where $q$ is the concentration of ortho hydrogen in mole fraction.

### A. The Anomalous Heat Capacity at Low Ortho-Hydrogen Concentrations

The anomalous heat capacity was measured at $(2 \pm 1)\%$ and at $(6.3 \pm 0.5)\%$ ortho hydrogen at 22.56 and 18.73 cc/M, respectively at temperatures above 1.6 °K. The experimental measurements are described in Sec. IV. The lattice heat capacity was estimated at higher temperatures and subtracted from the total heat capacity. The anomalous heat capacity is given in Tables V-1 and V-2 and Figs. V-1 and V-2. It was pointed out in Sec. IV that at high temperatures the heat capacity could be expressed by the equation

$$C_A = 160\ T^{-2} \tag{V-1}$$

for 2% ortho hydrogen at 22.56 cc/M, and by

$$C_A^{(1)} = 4400\ T^{-2} - 10250\ T^{-3} \tag{V-2}$$

$$C_A^{(2)} = 3200\ T^{-2} - 6400\ T^{-3} \tag{V-3}$$

Table V-1. The anomalous heat capacity of 2% ortho hydrogen at 22.56 cc/M.

| T (°K) | $C\left(\frac{mJ}{M°K}\right)$ |
|---|---|
| 1.528 | 39.1 |
| 1.821 | 31.3 |
| 2.048 | 33.6 |
| 2.196 | 33.2 |
| 2.404 | 27.5 |
| 2.581 | 26.0 |
| 2.879 | 19.9 |
| 3.230 | 14.9 |
| 3.631 | 13.0 |
| 4.146 | 8.6 |
| 4.708 | 6.1 |
| 5.262 | 7.5 |
| 5.863 | 4.5 |
| 6.633 | 3.4 |

Table V-2. The anomalous heat capacity of 6.3% ortho hydrogen at 18.73 cc/M.

| 1st Set of Measurements | | 2nd Set of Measurements | |
|---|---|---|---|
| T (°K) | $C_A\left(\frac{mJ}{M°K}\right)$ | T (°K) | $C_A\left(\frac{mJ}{M°K}\right)$ |
| 4.560 | 104.4 | 1.597 | 174.5 |
| 4.542 | 95.2 | 2.077 | 171.0 |
| 5.170 | 90.3 | 1.686 | 181.4 |
| 5.745 | 78.5 | 2.206 | 172.9 |
| 6.255 | 71.5 | 2.683 | 151.4 |
| 6.780 | 61.9 | 3.079 | 134.9 |
| 7.370 | 70.7 | 3.488 | 116.5 |
| 8.113 | 46.4 | 3.824 | 108.2 |
| 8.918 | 38.4 | 1.618 | 169.8 |
| 9.759 | 36.6 | 1.990 | 176.9 |
| 10.628 | 31.5 | 2.452 | 170.4 |
| 11.442 | 40.6 | 2.955 | 141.5 |
| 12.299 | 10.7 | 3.387 | 123.7 |
| | | 3.887 | 105.8 |
| | | 4.428 | 90.9 |
| | | 4.955 | 79.1 |
| | | 5.512 | 63.8 |
| | | 6.206 | 55.0 |
| | | 6.921 | 48.1 |
| | | 7.706 | 40.5 |
| | | 8.677 | 30.9 |
| | | 9.539 | 33.3 |
| | | 10.294 | 23.1 |
| | | 10.998 | 23.8 |
| | | 11.632 | 16.0 |
| | | 12.037 | 22.4 |
| | | 12.355 | 12.9 |
| | | 12.666 | 13.4 |
| | | 13.071 | 11.5 |

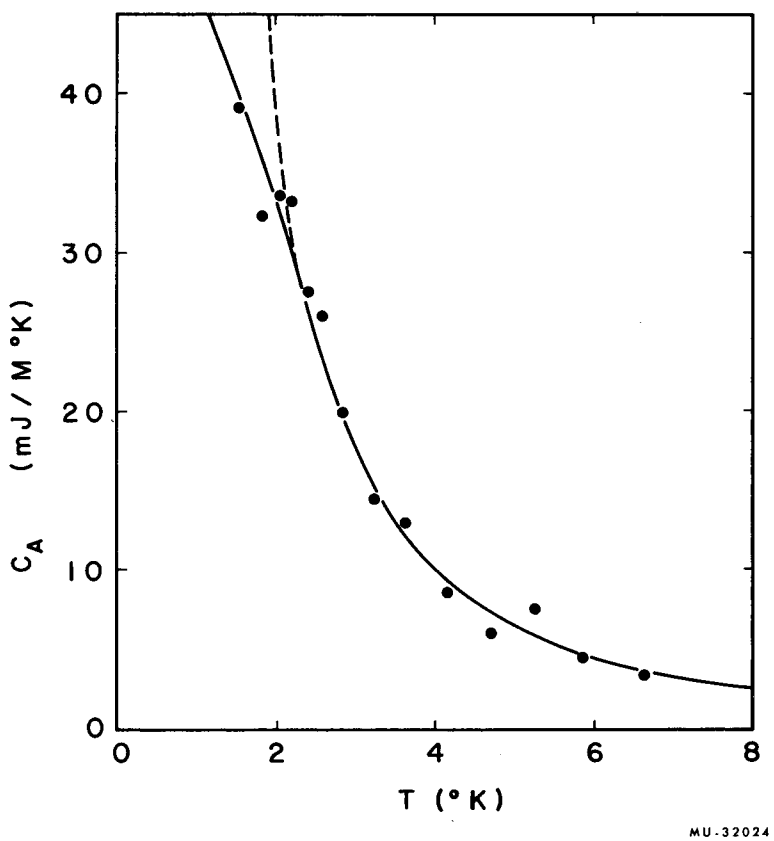


Fig. V-1. The anomalous heat capacity of 2% ortho hydrogen at 22.56 cc/M. The dotted extension corresponds to Eq. (V-1), and show the deviation from the experimental points at low temperatures.

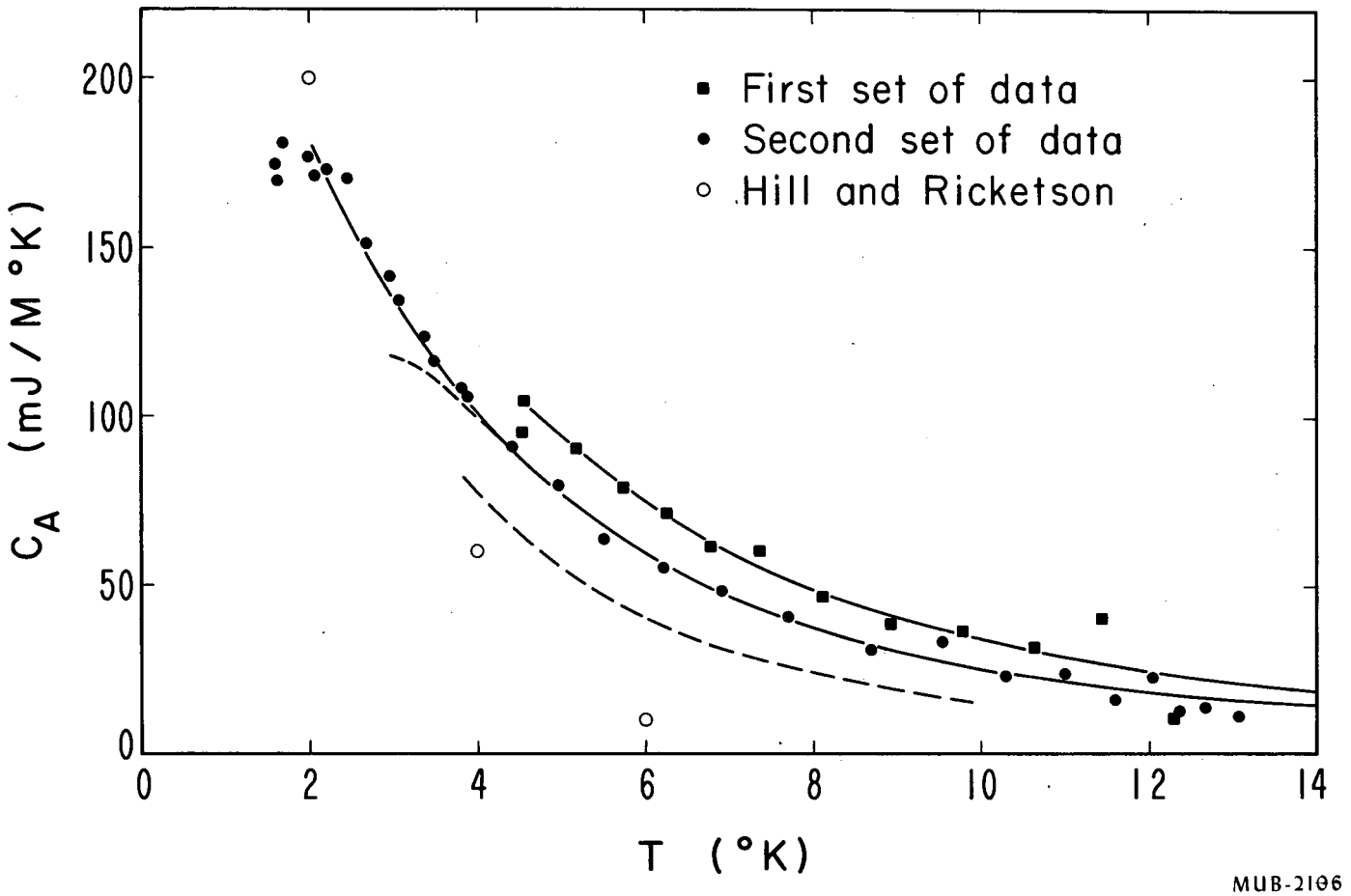


Fig. V-2. The anomalous heat capacity of 6.3% ortho hydrogen at 18.73 cc/M. The dotted extension of the solid line corresponds to Eq. (V-3) and shows the deviation of this equation from the experimental points at low temperatures. The lower dashed line represents Eq. (V-3) after a volume correction to 22.56 cc/M.

for 6.3% ortho hydrogen at 18.73 cc/M for the first and second set of data, respectively. The lines corresponding to these equations deviate from the experimental points at the lowest temperatures, and at these temperatures are shown as dashed extensions of the solid lines through the experimental points in Figs. V-1 and V-2. Equation (V-1) fits the data at temperatures above 2 °K, and Eqs. (V-2) and (V-3) fit the data above 4 °K.

Aside from the data by Hill and Ricketson[4] on 7% ortho hydrogen and zero pressure, there are no data on low concentrations of ortho hydrogen with which the results reported here could be compared. Hill and Ricketson's data are shown in Fig. V-2. Little can be expected from making a detailed comparison, because none of the measurements were made on sufficiently well-defined samples. At the smaller molar volume the anomaly is shifted to higher temperatures. From the high temperature expansion given by Eq. (IV-4), one would expect the coefficients of the $T^{-2}$ and $T^{-3}$ terms to vary as some linear combinations of the second and third powers of the energy levels respectively. If the interaction responsible for the anomaly is primarily the electric-quadrupole interaction between adjacent ortho molecules, then the energy levels will vary as $R^{-5}$, where R is the intermolecular distance. The coefficients in Eq. (V-3), when changed to correspond to a molar volume of 22.65 cc/M in accordance with the above scheme, yield the lower dashed line in Fig. V-2. This line indicates a heat capacity considerably larger than that measured by Hill and Ricketson.

The two sets of measurements at 18.73 cc/M show a considerable difference in the anomalous heat capacity. This difference is too large to be due only to the change in ortho hydrogen concentration due to the ortho-para conversion. Between the two sets of measurements the sample was warmed to 19.7 °K. During this warming a considerable heat evolution was observed, starting at about 13 °K. These observations are consistent with a change in the arrangement of the ortho-hydrogen molecules due to self diffusion. Originally the sample had been cooled from 22 °K below 13 °K in about two minutes, and it

very possibly did not contain an equilibrium distribution of the ortho molecules. It is, however, somewhat surprising that a rearrangement of the molecules could occur at temperatures as low as 13 °K. Self diffusion at the pressure in this sample (about 800 atm) should not start below about 21 °K according to an extrapolation of the data by Smith and Squire.[45]

The second set of measurements is believed to represent an equilibrium distribution of ortho hydrogen because no further heat effects were observed when the sample was heated above 13 °K after these measurements. The possibility of different distributions of ortho molecules at the same average concentration makes comparison of experimental data with theoretical calculations such as those by Orttung[50] extremely difficult, for even an equilibrium distribution is not necessarily a random one.

One of the important questions about the anomalous heat capacity at low ortho hydrogen concentrations is whether the isolated ortho molecules contribute to it. Theoretically, in a hexagonal close-packed lattice there is no splitting of the rotational states due to para neighbors.[50] In order to achieve agreement between theory and experiment, Orttung had to postulate a contribution from isolated ortho molecules in the case of hydrogen, and perhaps a considerably smaller contribution in the case of deuterium. Various excuses such as translational effects,[51] and next-nearest-neighbor interactions[50] can be made for allowing a contribution to the heat capacity from isolated ortho molecules. But there is no real experimental evidence for such a contribution. A knowledge of the total entropy involved in the anomaly would decide this question. Unfortunately none of the available data, including the ones reported on here, extend to sufficiently low temperatures to permit definite conclusions. The measurements at 2% ortho hydrogen yield about 30 mJ/M °K for the entropy above 1.5 °K. The total entropy due to the rotational levels for 2% ortho hydrogen should be 183 mJ/M °K. A random distribution of the ortho molecules would contain 78% of the ortho molecules isolated and surrounded completely by para molecules. If the isolated molecules do not contribute, then

the total entropy in the anomaly should only be 40 mJ/M °K. It does not seem likely that the entropy below 1.5 °K is only 10 mJ/M °K. Unfurtunately the uncertainties in the over-all concentration and in the actual distribution do not permit definite conclusions. The situation is similar for the measurements at 6.3% ortho hydrogen.

## B. The λ Anomaly

### 1. Thermal Equilibrium

It was mentioned in Sec. III that the λ anomaly in solid hydrogen could be studied only by measuring the temperature as a function of time as the sample warmed up due to the ortho-para conversion. Each sample was permitted to warm repeatedly through the region of the λ anomaly. Each of these heating curves corresponded to a different ortho-hydrogen concentration because of the time which necessarily elapsed between successive heatings. The concentration corresponding to any particular heating curve was calculated from the initial and final concentrations, assuming a second-order rate law.

Any errors in the heat capacities and entropy changes calculated from the heating curves depend on the extent to which thermal equilibrium existed in the sample during the heating. Although a quantitative calculation of thermal gradients in the sample does not seem feasible, certain qualitative considerations may be worthwhile.

The most severe thermal gradients existed in the cell when the heat switch was closed. In this situation all the heat generated had to be conducted to the outside of the cell and to the heat switch. Schematically this situation is represented in Fig. V-3, by line 1. There is some thermal gradient in the sample itself, a discontinuity at the cell wall, and another gradient in the cell wall.

Upon opening of the switch, only enough heat has to be conducted across the sample to heat the cell walls. The rest is used to heat the sample itself. For the cell used in this work at temperatures removed from the λ anomaly, the heat flow to the outside will be about one order of magnitude less than it is with the switch closed. Consequently the thermal gradients will relax to those indicated by line 2. If the

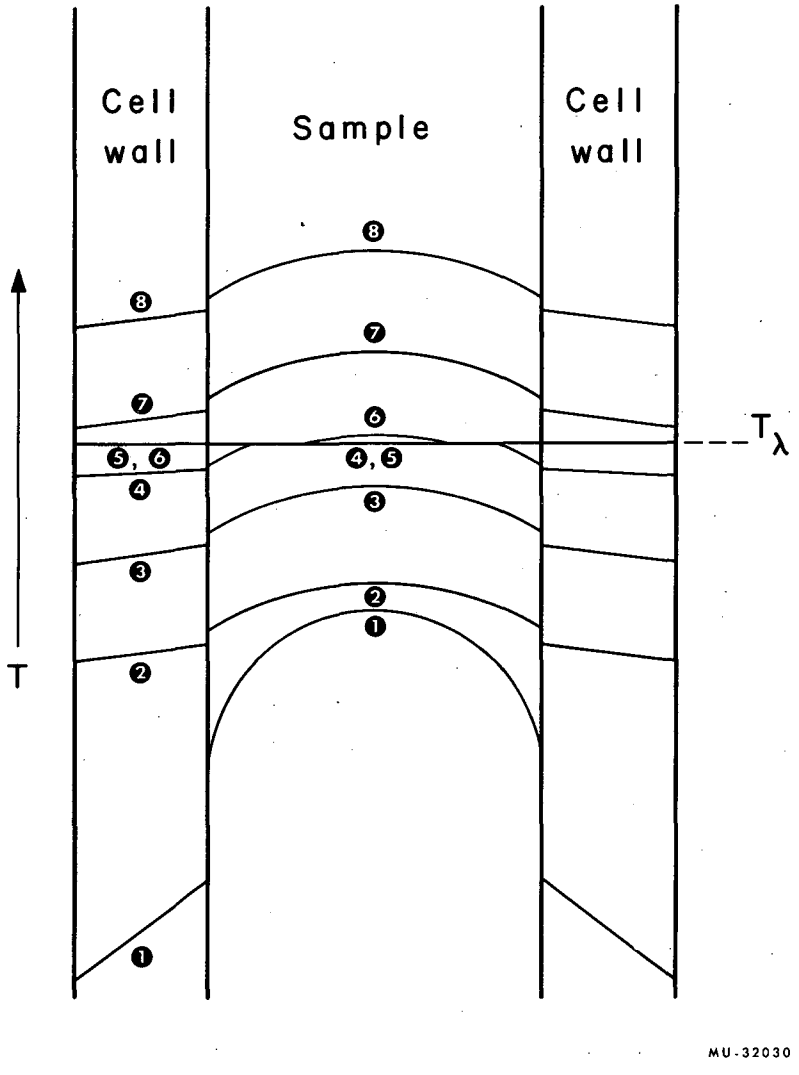


Fig. V-3. The thermal gradients in the cell when cooling well below $T_\lambda$ is possible.

sample temperature at this point is still below the λ anomaly, then from here on up to line 3 the heating curve will reasonably represent the heat capacity of the sample. The fact that the measured temperature is somewhat below the sample temperature is unimportant because the heat capacity varies very slowly with temperature.

When the sample approaches the λ temperature it will cease warming up, and the heat flow to the outside will become smaller. This will result in a measured λ anomaly that rises somewhat more gradually and at a lower temperature than the actual anomaly (line 4).

As the maximum in the λ anomaly is approached, it can be expected that the outside temperature of the cell catches up with the sample temperature (line 5). Thus the temperature of the maximum in the anomaly should be correct reflected in the heating curves.

The cental part of the sample reached the λ temperature first, and thus can be expected to warm up beyond it first (line 6). The outside of the cell should not start warming until all the sample has passed through the λ anomaly. When the sample is warming again at its usual rate, the outside should first lag behind until the proper gradient has been established again, resulting again in an apparent heat capacity that is too high. From this point on (lines 7, 8) the proper heat capacity will again be recorded. Thus the presence of thermal gradients primarily results in a broadening of the transition. The enthalpy involved in the λ anomaly can be expected to be properly reflected in the heating curves, because what is added to the heat capacity at the sides of the anomaly will be subtracted from the peak. In view of the small temperature range over which the λ transition occurs, the entropy calculated from the heating curves will also be correct. The width and height of the anomaly will be meaningful only on a relative basis.

A less-favorable situation exists when it is not possible to cool the entire sample below the λ temperature. This condition is presented in Fig. V-4, line 1. The outside of the cell may be well below the λ temperature but the thermal gradient in the sample with the heat switch closed extends well above it. In this situation the thermal gradient in the cell walls will rapidly relax, indicating a low heat

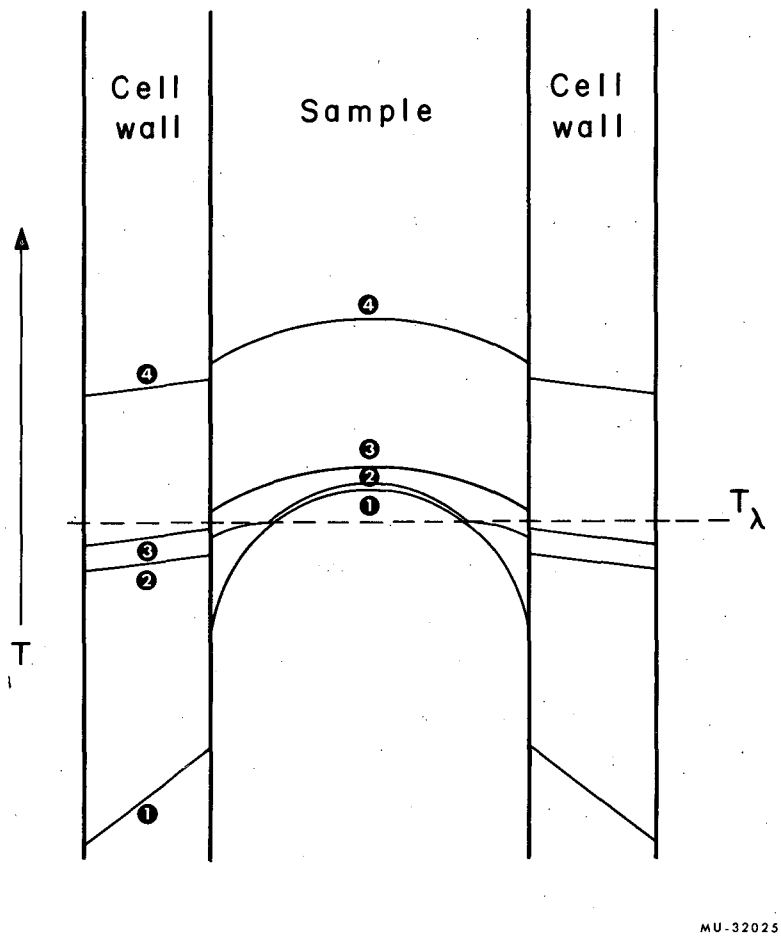


Fig. V-4. The thermal gradients in the cell when cooling well below $T_\lambda$ is not possible.

capacity (line 2). Depending on how much of the sample was cooled below the λ point, the maximum in the heat capacity will come just below or at the λ temperature (line 3). The heat capacity above the λ point can be expected to be correct (line 4). In this last situation, the measured enthalpy and entropy can be regarded only as a lower limit.

The above considerations yield a necessary condition for the reliability of measured entropies. The measured heat capacity must assume a constant or very slowly varying value below the λ anomaly. In practice it was found that the λ anomaly had to be 0.1 to 0.2 °K above the minimum accessible temperature before this condition was reached.

The criterion established here for the reliability of entropy measurements is sufficient only if the relaxation time between the rotational system and the lattice vibrations is small. If it is large, then the entire broad anomalous heat capacity can be expected to be unusually low if the sample was not kept at a low enough temperature for sufficient time.

In order to estimate the effect of the thermal gradients in the sample on the measured heat capacity, two experimental approaches were used. One of them consisted of determining heating curves after the disappearance of the λ anomaly with various external heat inputs, and the other consisted of studying the effect of cell geometry on the λ anomaly. In the first approach the external heat input varied from 0 to 0.2 mW. The internal rate of heat generation was about 0.15 mW and the ortho concentration was between 60 and 65%. Alternate heating curves were measured without external heat input, and the internal rate of heat generation during the heating curves with external-heat input was estimated by interpolation. For the heating rate with external-heat input, one has from Eq. (III-22)

$$\left(\frac{dt}{dT}\right)_i = \frac{C}{3.98\ k\ q^2 n + P_i} \qquad \text{(V-4)}$$

where $P_i$ is the heater power. One can now form the ratio

$$\frac{(dt/dT)}{(dt/dT)_i} = D_i = 1 + \frac{P_i}{3.98\ k\ q^2 n} \qquad \text{(V-5)}$$

where (dt/dT) is the quantity obtained with the heater off. It is seen that D is independent of C, and at constant T should be proportional to $P/q^2$, even if the rate constant k were temperature dependent. D was found to vary according to Eq. (V-5) for $1.7\ °K \leq T \leq 2.7\ °K$. The scatter in D was about 6%. At 1.6 °K, the lowest temperature at which these measurements could be made, D increased more rapidly than $P/q^2$, and at a heater power of 0.1 mW was 18% too large. These measurements show that reasonable thermal equilibrium existed in the sample after the initial relaxation. The slight deviation from thermal equilibrium at 1.6 °K is due to this initial thermal gradient that must be expected with the heat switch closed. With the switch closed and no external heat input, it was possible to cool the sample to 1.46 °K. Inspection of dt/dT vs T curves indicated that the initial gradient completely relaxed in less than one minute just above 1.6 °K. Thus with this particular rate of heat generation, it was necessary to cool about 0.15 °K below the λ anomaly in order for the initial thermal gradient to relax before the λ anomaly was reached. Values of D as a function of T and $P/q^2$ are given in Table V-3.

The other approach to estimating the effects of thermal gradients consisted of varying the cell geometry. Measurements were made in the cells II and III described in Chapter II. In cell II the sample was 3/4 inch long and 1/4 inch thick, and in cell III the sample was 3-5/8 inches long and 0.094 inch thick. Measurements of the entropy involved in the λ anomaly yielded the same results in the two cells. However, the anomaly at constant volume was much broader in cell III than in cell II. From the consideration of thermal gradients the opposite effect might be expected. It is believed that the broadening in cell III was due to pressure gradients in the cell. The broadening is consistent with the extrusion data on solid hydrogen by Stewart.[41]

Table V-3. Values of D as a function of T and $P/q^2$.

| T (°K) | D at | | | | |
|---|---|---|---|---|---|
| | $\frac{P}{q^2}$ = 0.480 mW | $\frac{P}{q^2}$ = 0.219 mW | $\frac{P}{q^2}$ = 0.126 mW | $\frac{P}{q^2}$ = 0.0575 mW | $\frac{P}{q^2}$ = 0.531 mW |
| 1.6 | — | 2.07 | 1.49 | 1.21 | — |
| 1.7 | 2.50 | 1.75 | 1.42 | 1.21 | 2.99 |
| 1.8 | 2.50 | 1.76 | 1.44 | 1.20 | 2.86 |
| 1.9 | 2.57 | 1.76 | 1.45 | 1.19 | 2.87 |
| 2.0 | 2.65 | 1.79 | 1.45 | 1.20 | 2.86 |
| 2.1 | 2.68 | 1.81 | 1.46 | 1.20 | 2.88 |
| 2.2 | 2.73 | 1.81 | 1.46 | 1.21 | 2.95 |
| 2.3 | 2.77 | 1.80 | 1.47 | 1.21 | 3.01 |
| 2.4 | 2.79 | 1.81 | 1.48 | 1.22 | 3.05 |
| 2.5 | 2.78 | 1.81 | 1.47 | 1.22 | 3.02 |
| 2.6 | 2.78 | 1.80 | 1.47 | 1.22 | 3.02 |
| 2.7 | 2.79 | 1.80 | 1.47 | 1.21 | 3.02 |

## 2. The λ Anomaly at Zero Pressure

Hill and Ricketson first observed the existence of a λ anomaly in the heat capacity of solid hydrogen at high ortho concentrations, and they determined the effect of concentration on the λ temperature.[4] Essentially their work indicates that the λ anomaly exists only at concentrations greater than 62% ortho hydrogen.[5] The λ temperature changed from 1.1 °K to 1.6 °K as the concentration changed from 62 to 74% ortho hydrogen. The maximum heat capacity was 63 J/M °K at 74% and 22 J/M °K at 66% ortho hydrogen. Unfortunately no information was given about the entropy involved in the λ anomaly. Only the entropy of the total anomaly was reported to be slightly less than R ln 3, where R is the gas constant.

The interaction between ortho molecules has also been studied by nuclear-magnetic-resonance experiments.[45,52 to 56] Hatton and Rollin observed the appearance of side peaks in the NMR line at low temperatures, and attributed this phenomenon to changes in the rotational states of the ortho molecules.[52] Most recently this NMR transition was studied by Smith and Housley for ortho hydrogen concentrations between 67% and 86%.[56] The concentration dependence of the transition temperature is very similar to the dependence of the λ temperature in the heat capacity measurements on concentration.

It seemed desirable to repeat at least some of the work on the heat capacity at zero pressure, both to look for any possible systematic differences due to experimental procedures and geometries, and to obtain more detailed information about the λ anomaly.

With the apparatus used here, only concentrations greater than about 70% ortho hydrogen could be studied. At lower concentrations the λ temperature is too low, and is not experimentally accessible. Whereas the bath can be cooled to 1.28 °K, the thermal gradient across the heat switch is about 0.1 °K. The discussion in Sec. V.B.1 shows that an additional thermal gradient of about the same magnitude exists in the cell with the thermal switch closed. Thus the minimum temperature at which the λ anomaly can be observed is about 1.48 °K.

Two experiments were carried out at zero pressure. In Experiment I the cell was precooled to 14.5 °K. The sample was purified in

a manner identical to that described for the para hydrogen measurements, passed over the ortho-para catalyst at room temperature, and condensed into the bomb. In Experiment II the cell was precooled to 20 °K, and the sample was admitted directly from the hydrogen cylinder at a delivery pressure of 300 psi. The gas in the cylinder had been prepared electrolytically, purified over silica gel at 78 °K, and stored at 2000 psi for over 1 year in the cylinder before use. This same cylinder was used for all constant-volume measurements on the λ anomaly as well. In both experiments liquid helium was transferred as soon as the sample had been introduced, and cooling below the λ anomaly was carried out as rapidly as possible. The results of the two experiments were essentially identical.

One of the most interesting features of the λ anomaly is the existence of structure. The anomaly does not appear to be a single λ-shaped transition such as is found in liquid helium, but rather seems to have three distinguishable maxima. This is illustrated in Figs. V-5, V-6, and V-7. The maximum at the lowest temperature invariably was the largest of the three. It frequently, but not always, showed a side peak at a temperature about 0.015 °K to 0.025 °K higher than the main peak. This side peak was not always observable, possibly because of its proximity to the larger main peak. In addition there invariably appeared a third much smaller maximum at a temperature about 0.1 °K higher than the main peak.

In Fig. V-8 the λ temperatures are plotted against concentration of ortho hydrogen. All maxima that appeared in the heating curves are shown, and those belonging to the same heating are connected by a solid line. The data of Hill et al. are also shown.[4,5] The agreement of the temperature for the main peak with the λ temperature observed by Hill et al. is very satisfactory.

In these measurements the various concentrations were obtained by waiting for the ortho-para conversion to proceed below the minimum temperature for self diffusion. Under these conditions the λ transition disappeared at a concentration of 71.5% ortho hydrogen. In Experiment I the sample was melted at a concentration of 71.4%, then

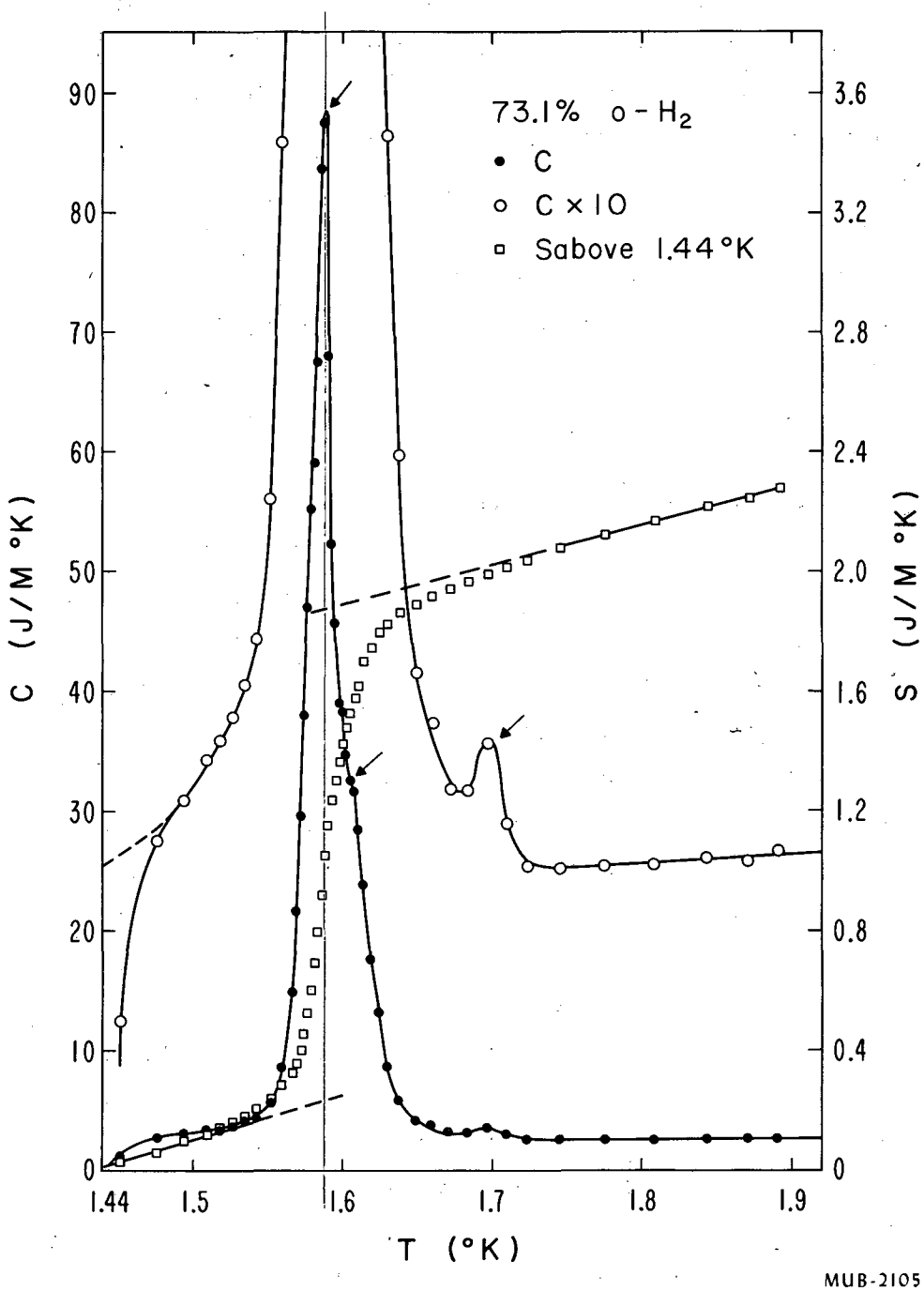


Fig. V-5. The shape of the λ anomaly at zero pressure. The arrows indicate distinguishable peaks. Also shown is the entropy above 1.44 °K as a function of T.

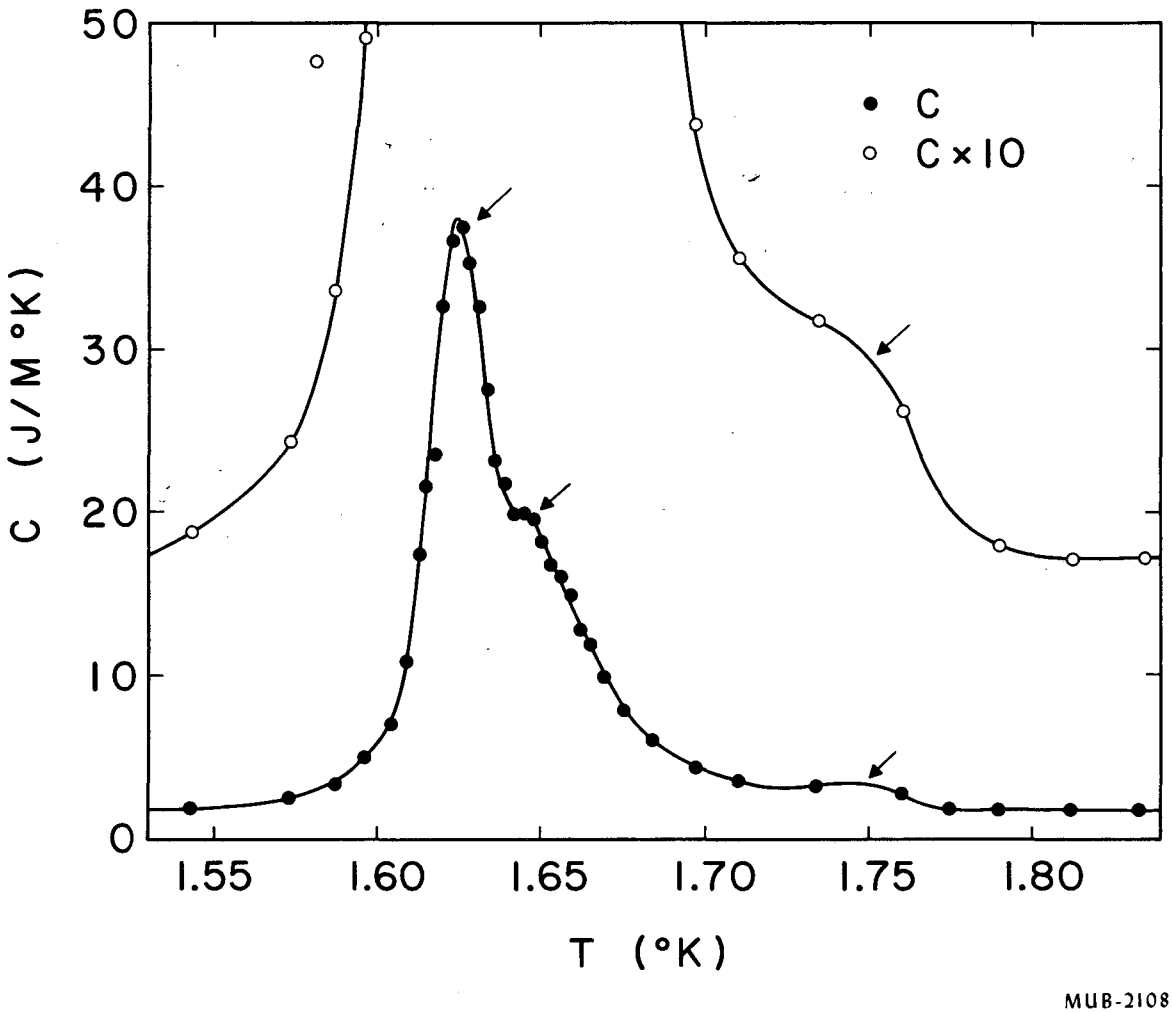


Fig. V-6. The shape of the λ anomaly at zero pressure. The arrows indicate distinguishable peaks.

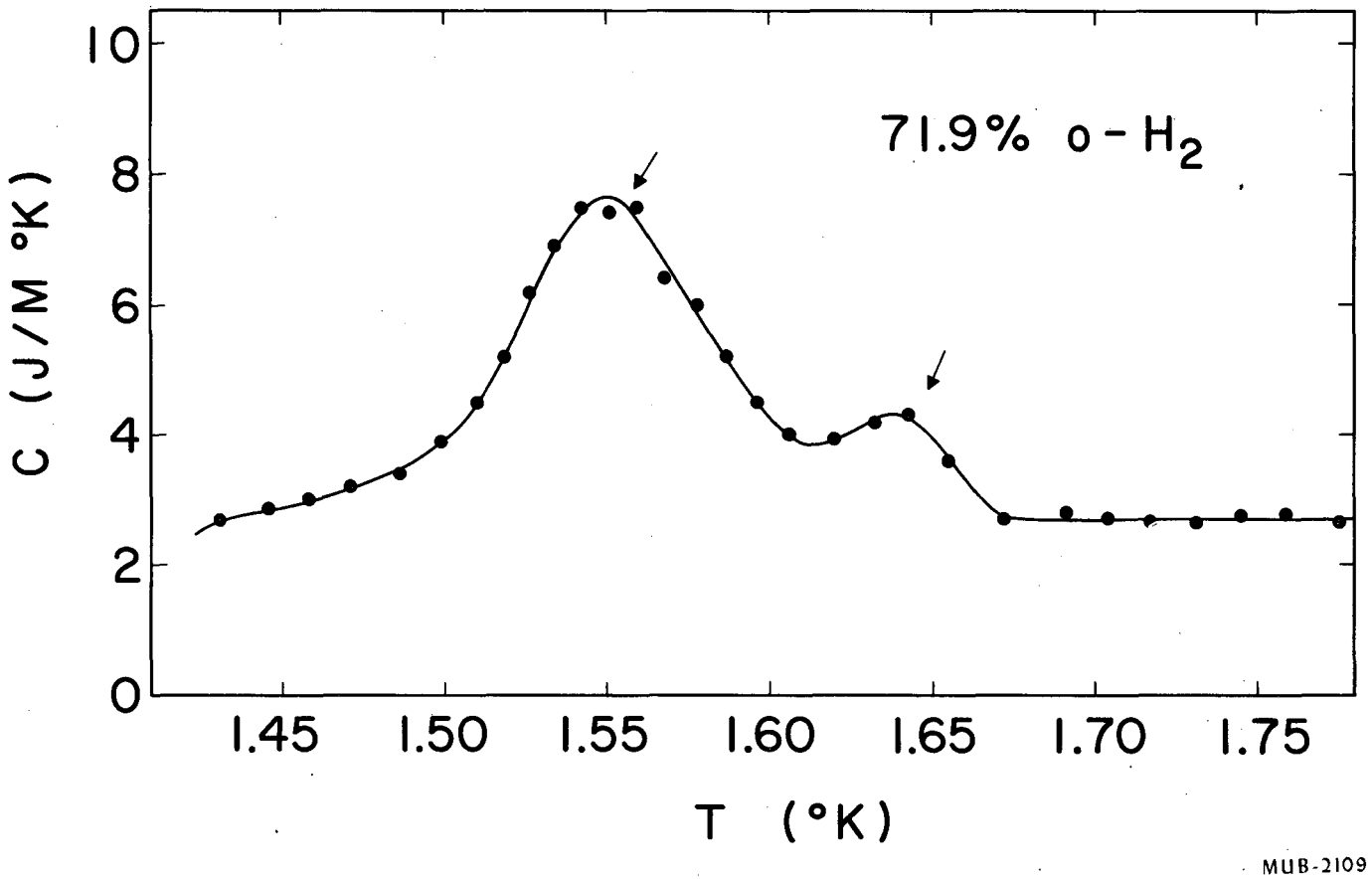


Fig. V-7. The shape of the λ anomaly at zero pressure. The arrows indicate distinguishable peaks.

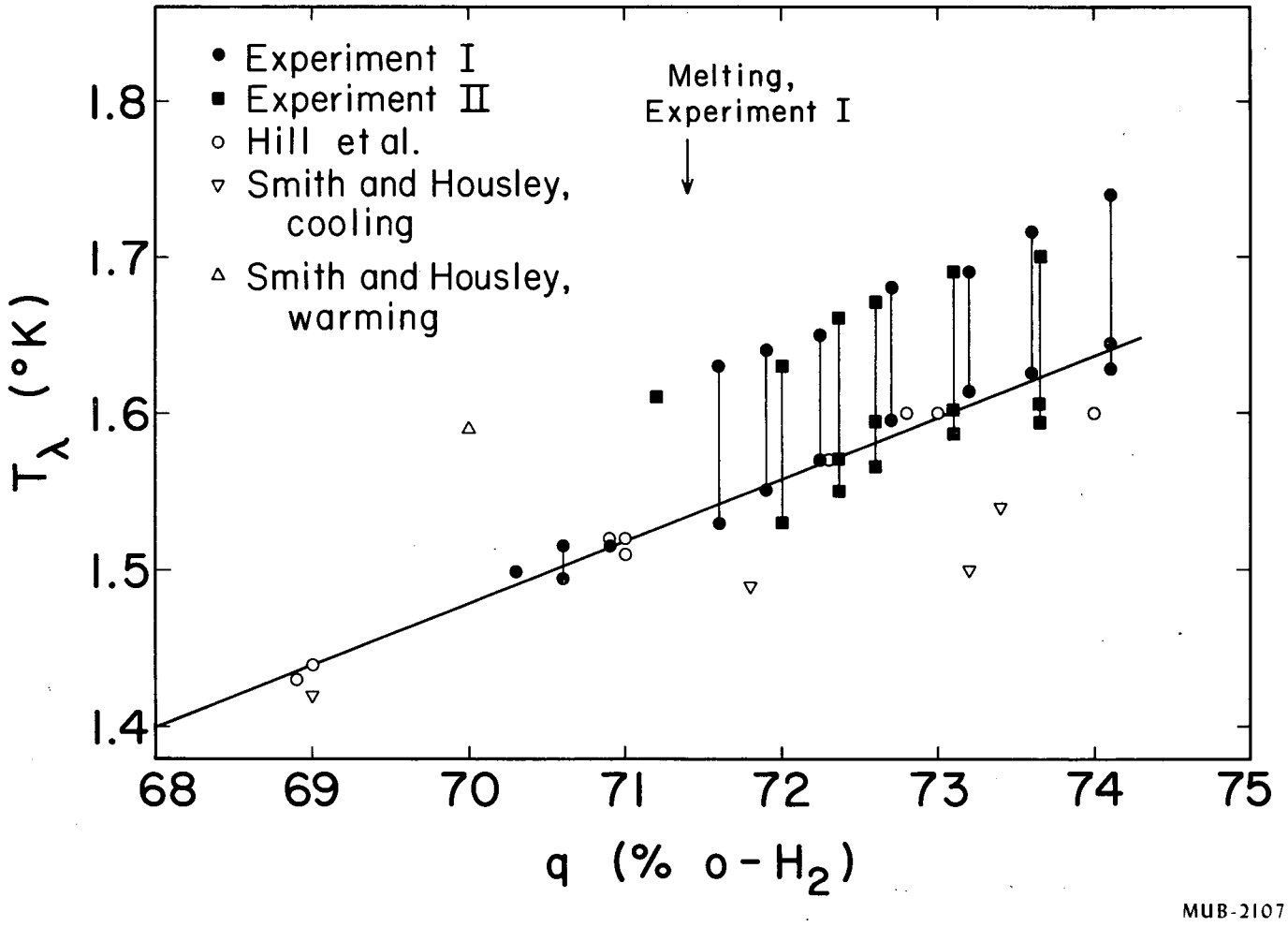


Fig. V-8. The λ temperature at zero pressure as a function of concentration. The points connected vertically are different peaks observed during the same heating.

recooled. This caused the λ anomaly to appear again, at temperatures well in line with those at higher concentrations. Hill et al. were able to observe the λ anomaly at concentrations as low as 62.7%, and in view of the present results presumably used fresh samples for each heating curve. One interesting feature of the λ anomaly after melting and recooling is that the small maximum at the highest of the three temperatures was never observed.

So far there has been essentially no information on the entropy involved in the λ anomaly. For those heating curves for which cooling well below the λ anomaly was possible, the entropy involved in the λ transition was determined by plotting the entropy above the minimum experimental temperature against temperature. In this graph the entropy above and below the λ transition can easily be extrapolated to the λ temperature, and the change in entropy due to the λ transition can thus be determined. This procedure is illustrated in Fig. V-5. Between 73 and 74% ortho hydrogen, the entropy involved in the λ anomaly amounts to about 23% of R ln 3 per mole ortho hydrogen. The contribution of the λ anomaly rapidly decreases as the concentration decreases. The relative entropy contribution of the λ anomaly is plotted against concentration of ortho hydrogen in Fig. V-9. These entropy values are those obtained from samples whose composition changed at temperatures below the minimum self-diffusion temperature, and whose original concentration was 75% ortho hydrogen. No reliable entropy values could be obtained after melting and recooling, because the λ temperature was too low.

In view of the fact that the entropy of the λ anomaly decreased much faster than the total anomalous entropy, it would be expected that the entropy of the broad anomaly would increase. No evidence for this was found at temperatures immediately above the λ temperature. Temperatures below the λ anomaly were not accessible to experimental measurement.

Little can be said about the shape of the λ anomaly. The experimental data do not portray the typical λ shape found in liquid helium, but rather look like the superposition of more or less

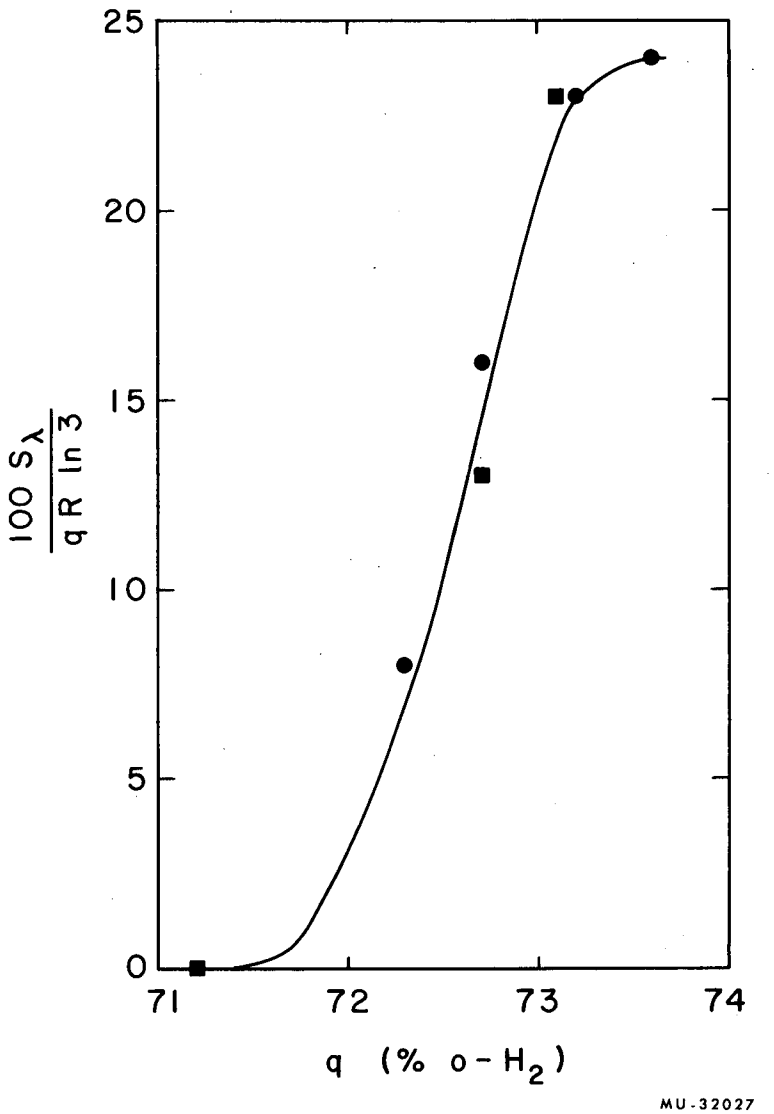


Fig. V-9. The entropy of the λ anomaly at zero pressure as a function of concentration.

symmetric peaks. But thermal nonequilibrium effects may well have altered the shape considerably. The width of the peaks varied from $2 \times 10^{-2}$ °K to $6 \times 10^{-2}$ °K at half the maximum heat capacity as the size of the anomaly decreased.

### 3. The λ Anomaly at Constant Volume

The effect of volume changes on the λ temperature was studied by McCormick.[55] He reported that at a pressure of 2300 atm (V = 15.8 cc/M) $T_\lambda$ had been raised to 3.1°K, to be compared with 1.6 °K at zero pressure. McCormick's concentration was not specified, but presumably was in the vicinity of 73% ortho hydrogen. The purpose of the present measurements was to define the volume dependence of the λ temperature more precisely, and to look for any changes in the nature of the anomaly with volume.

A number of measurements were made at several molar volumes between 22.6 and 15.8 cc/M. The measurements were in principle very similar to those at zero pressure. Some additional difficulties were experienced, however, due to the more severe experimental conditions. It was important to introduce the sample into the apparatus and to cool it below the λ temperature as rapidly as possible because of the large increase in the ortho-para conversion with decreasing molar volume. This made it necessary to use the samples directly from the hydrogen cylinder at about 100 atm, because the time involved in the initial compression of the sample would have been too long to be tolerable. The initial concentration of ortho hydrogen thus was always 75%. The sample was introduced at 78 °K. The maximum concentration at which the λ anomaly could be observed varied somewhat with molar volume, but generally was about 69% ortho hydrogen.

Because the sample size had to be as small as 0.6 cc in order to make cooling by means of the mechanical heat switch possible, any determination of the sample density by the method employed during the measurements on para hydrogen would have been subject to rather large errors. Furthermore, in order to obtain a representative sample for the ortho-para analysis, the fraction of the sample in the

capillary had to be discarded, and thus could not easily be measured in a determination of the sample volume. It was therefore not feasible to determine the density of the sample directly. An attempt to use the filling pressure and temperature to estimate the density yielded densities that seemed too low for the temperature at which the λ anomaly occurred. This is believed to be due to movement of the solid plug in the capillary when the sample was cooled below 78 °K. Because no time could be lost at high temperatures because of the change in sample composition, it was not possible to adjust experimental conditions so that no plug movement occurred in the capillary. An indirect method was therefore used to determine the molar volumes of the samples. The volume dependence of the second-order rate constant was determined in cell I, and the volumes of the samples on which the λ anomaly measurements were made was estimated from the rate constant. The determination of the volume-dependence of the rate constant is described in Sec. VI. The maximum error in any individual rate-constant determination was estimated to be ±5%. The associated maximum error in the molar volume is ±0.5 cc. For the rate-constant determinations it was found important to discard the hydrogen in the capillary. If this was not done, the rate constants generally were found to be too small. During the early experiments this was not realized, and the results of these experiments were used only for general considerations in which the molar volumes and concentrations are not critical. During the later experiments the hydrogen in the capillary was discarded by warming the sample to 14 °K, permitting the capillary plug to break, and pumping out the pressure system before the rest of the sample was expanded.

The λ temperature as a function of ortho-hydrogen concentration is given in Fig. V-10 for several molar volumes. For comparison, the data for zero pressure are also reproduced here. The solid lines go through the experimental points, and the dashed lines are based on Eq. (V-6) to be derived below. It is clear that the λ anomaly is strongly affected by changes in the molar volume. Again the changes in concentration are due to the ortho-para conversion at temperatures at which no self-diffusion occurred.

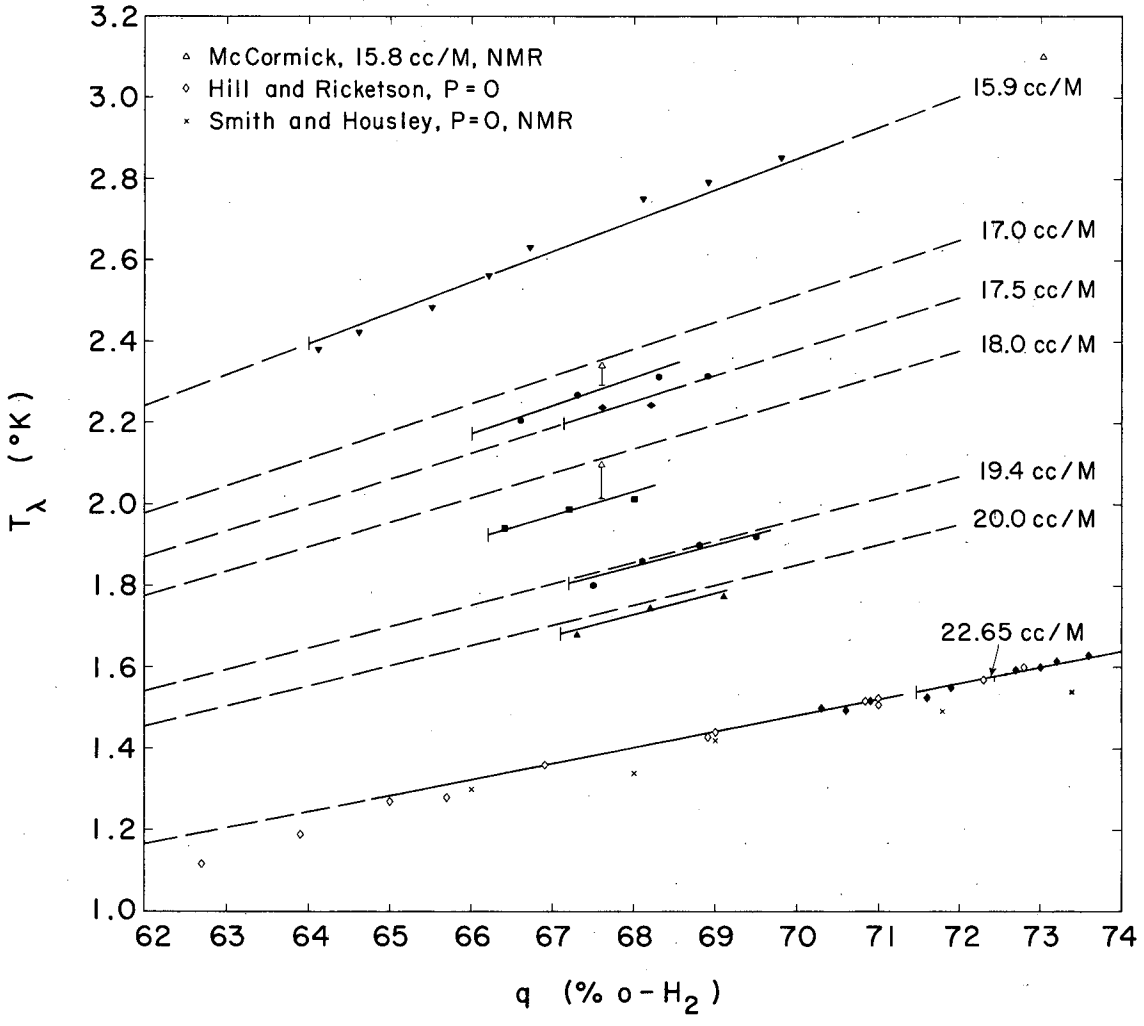


Fig. V-10. The λ temperature as a function of concentration at several molar volumes. The dashed lines correspond to Eq. (V-6) and the experimental molar volumes.

The minimum concentrations at which the $\lambda$ anomaly existed are indicated by a vertical bar. Two samples at a molar volume of about 18 cc/M were heated above their melting temperature in an attempt to regenerate the $\lambda$ anomaly. After melting, no $\lambda$ anomaly was found at a concentration of about 65%. This is quite different from that found at zero pressure. The minimum concentration at which the $\lambda$ anomaly occurs is plotted in Fig. V-11. The considerable scatter in these data is believed to be due primarily to small variations in the thermal histories of the samples. But it is apparent that the minimum concentration for the $\lambda$ anomaly decreases with decreasing molar volume.

The volume dependence of the $\lambda$ anomaly was estimated at a concentration of 68%. This concentration was chosen because data are available for all molar volumes studied. The $\lambda$ temperature at 68% ortho hydrogen is plotted against molar volume on a logarithmic scale in Fig. V-12. The $\lambda$ temperature changes with the intermolecular separation R as $R^{-5}$, with a small contribution from $R^{-n}$, where n is larger than 5. The data were fitted to an $R^{-5}$ plus an $R^{-15}$ term, using the zero pressure and 15.9 cc/M data. The choice of n cannot be made unambiguously on the basis of the experimental data, and $n = 15$ was chosen because it is the most important term besides the $R^{-5}$ term in the theoretical Hamiltonian for pair interactions between ortho molecules.[50] The concentration dependence can be expressed by a linear relation over the small concentration range of the experiments, and was estimated from the zero pressure data. These data were used because they show by far the least scatter. Within experimental error the $\lambda$ anomaly as a function of concentration and volume is given by

$$T_\lambda = (-226 + 6.93\ q)\ (V^{-5/3} + 1.20 \times 10^3\ V^{-5})\ . \qquad \text{(V-6)}$$

The lines corresponding to this equation and the estimated molar volumes of the experiments are given in Fig. V-10. The largest difference between Eq. (V-6) and the experimental data is 0.1 °K and corresponds to an error in the molar volume of 0.5 cc/M.

As was found at zero pressure, the data at smaller molar volumes also show that the $\lambda$ anomaly is not a simple maximum.

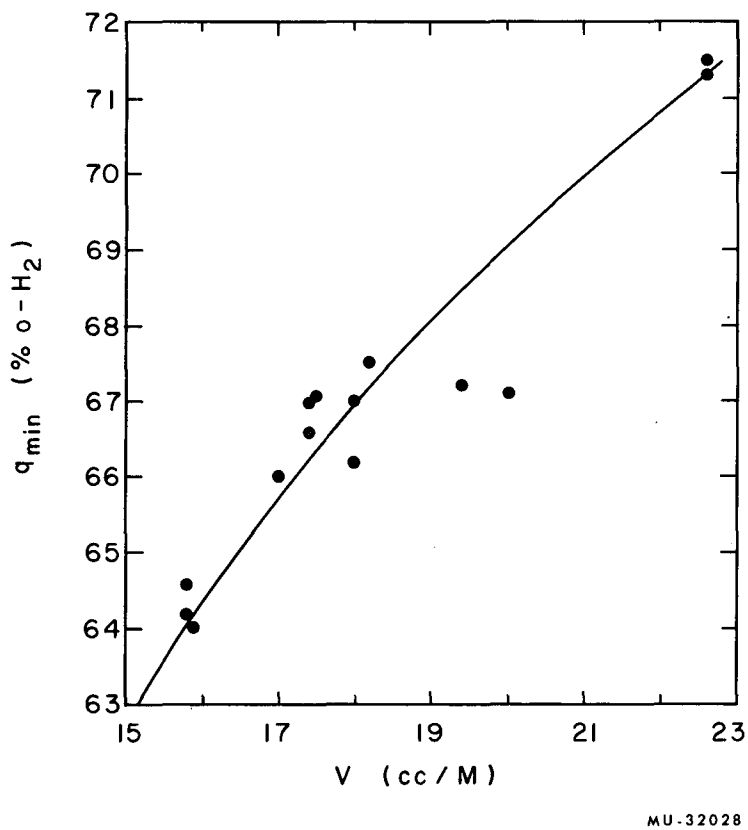


Fig. V-11. The minimum concentration of ortho hydrogen at which the λ anomaly existed as a function of molar volume.

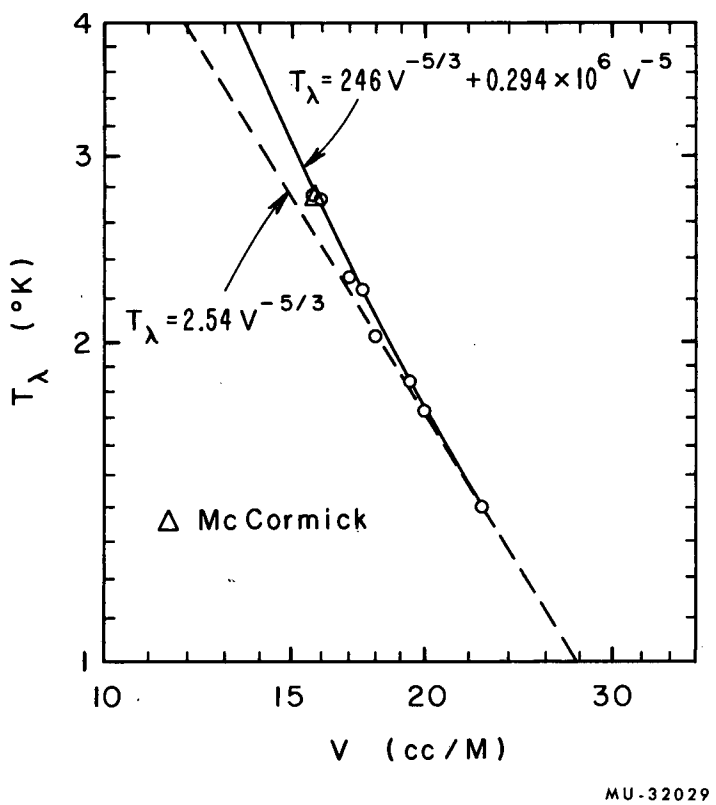


Fig. V-12. The λ temperature at 68% ortho hydrogen as a function of molar volume on a logarithmic scale.

Frequently two distinct peaks were observed. Four sets of heat capacities are shown in Fig. V-13. These data were taken in cell III, and the transitions are rather broad because of pressure gradients in the cell. This broadening lowered the maximum considerably, and makes it somewhat difficult to distinguish the two peaks. In Fig. V-14 the heat capacities for measurements under similar conditions in cell II and cell III are shown. Fig. V-14(a) clearly shows the doublet. Occasionally at the smaller molar volumes only a single peak could be observed. The relative sizes of the peaks did not seem to follow any definite pattern, and were probably affected by uncontrolled differences in thermal histories. The temperature difference between the two peaks also seemed to be affected by uncontrolled variables, but in general, increased with decreasing molar volume. At 15.9 cc/M it was of the order of 0.1 °K.

The entropy of the λ anomaly as a function of concentration could be most easily measured at zero pressure and at small molar volumes. At zero pressure no time was spent in cooling from 78 °K, and at small molar volumes less time was spent cooling to very low temperatures because the λ anomaly occurred at relatively high temperatures. The greatest concentration ranges could thus be studied at 22.65 cc/M and 15.9 cc/M. Some information was also obtained at other molar volumes. The relative contribution of the λ anomaly to the total anomalous entropy is shown in Fig. V-15. At all molar volumes studied the entropy of the λ anomaly decreased very rapidly with concentration. The decrease at the smaller molar volumes was perhaps not quite as fast as it was at zero pressure.

It was pointed out earlier that part of the entropy lost in the λ anomaly must appear in the entropy of the broad anomaly. No appreciable change in the heat capacity was ever observed at temperatures immediately above the λ anomaly. At the smallest molar volumes, the λ anomaly occurred at sufficiently high temperatures to make it possible to observe the heat capacity below the λ anomaly. In this region the heat capacity changed by about a factor of two while the λ anomaly disappeared. This change is shown in Fig. V-16 for one set of measurements at 15.9 cc/M. The dashed extrapolations of the

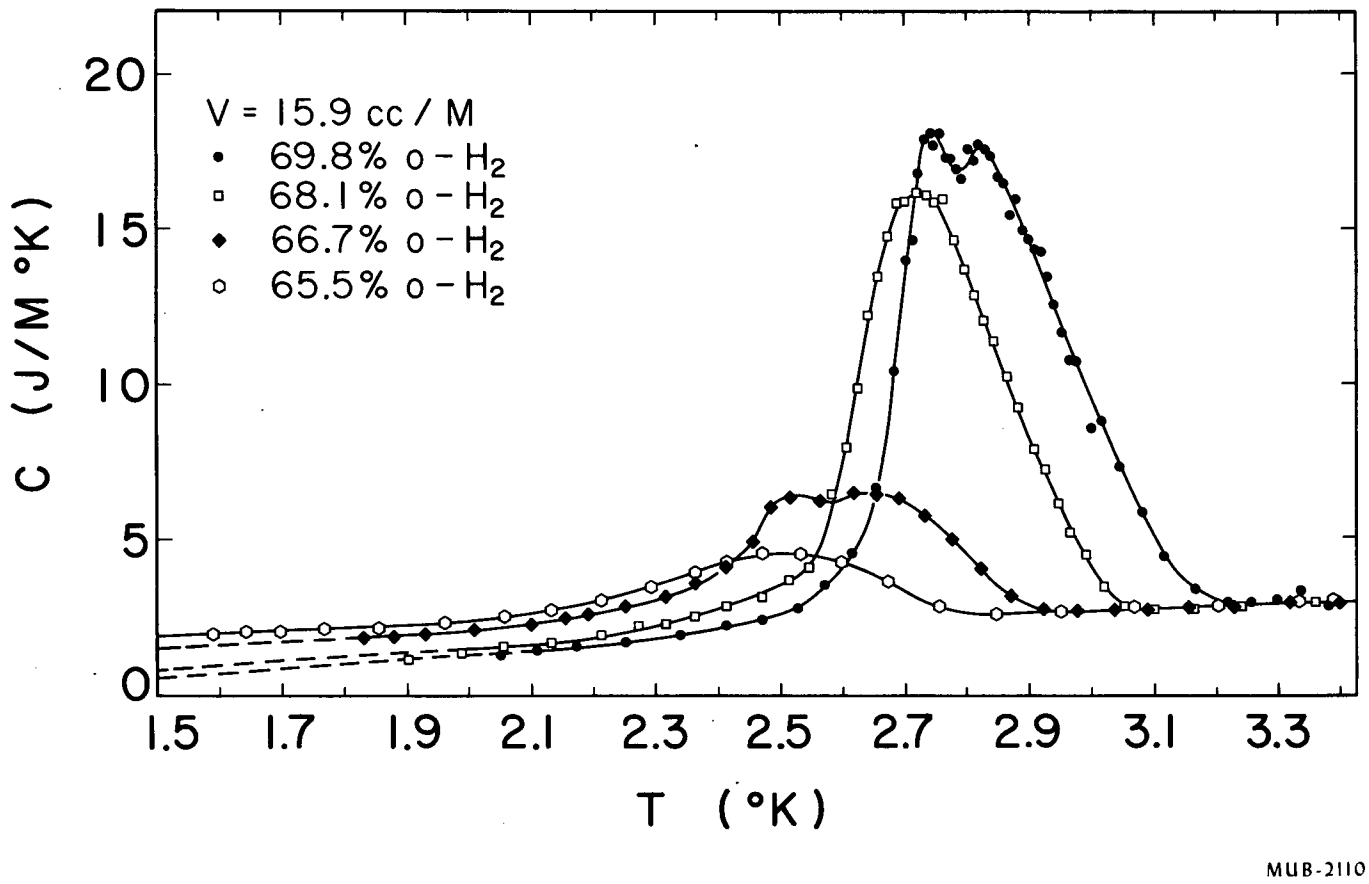


Fig. V-13. The shape of the λ anomaly at four concentrations of ortho hydrogen at 15.9 cc/M.

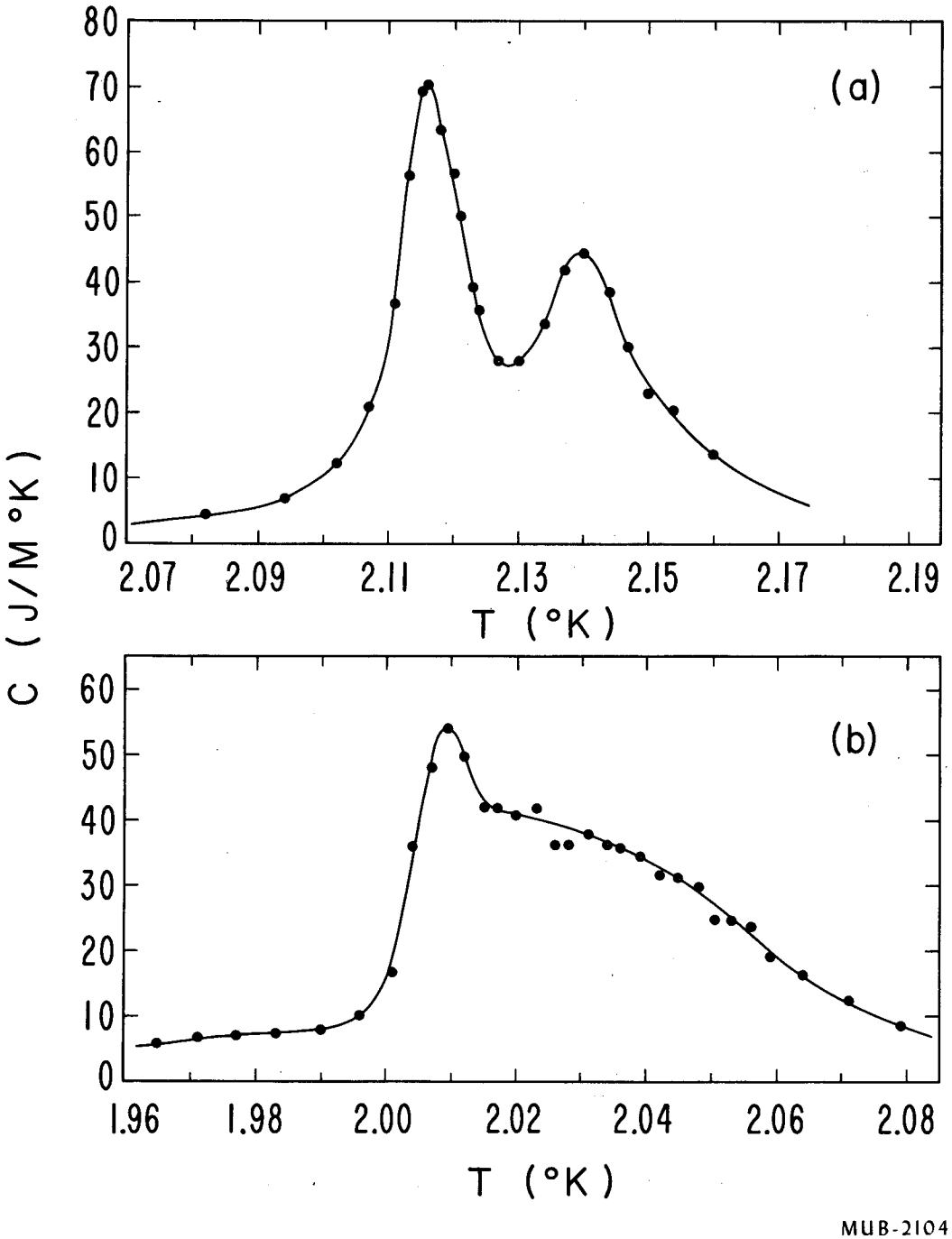


Fig. V-14. Comparison of the shape of the λ anomaly under similar conditions in cell II(a) and cell III(b). The difference in the λ temperatures is not an effect of the cell geometry, but rather is due to a difference in the molar volumes.

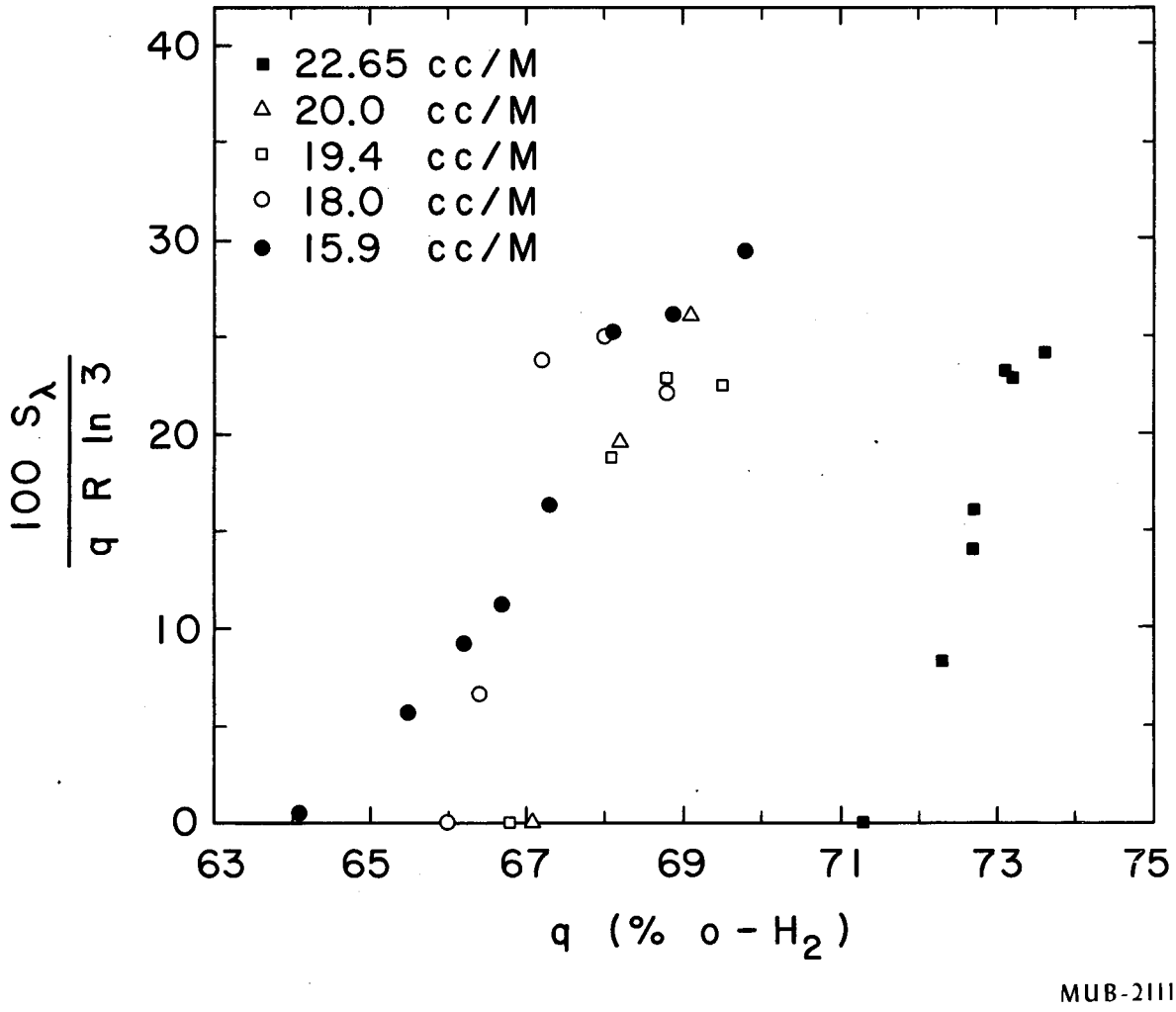


Fig. V-15. The entropy of the λ anomaly as a function of ortho-hydrogen concentration at several different molar volumes.

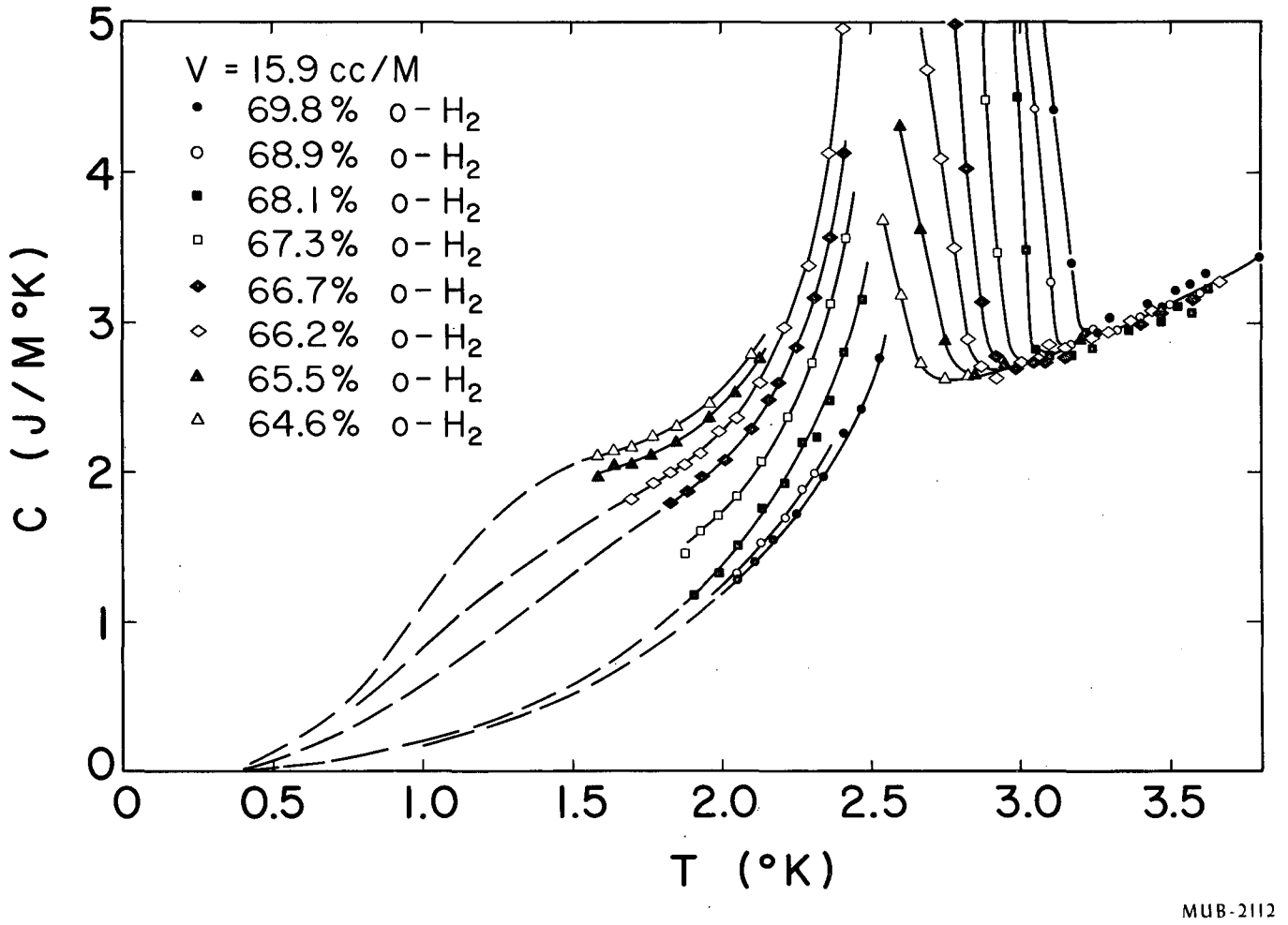


Fig. V-16. The heat capacity in the vicinity of the λ anomaly at several concentrations of ortho hydrogen and at 15.9 cc/M.

experimental data to $T = 0$ are of course only approximate, and do not permit accurate estimates of entropy changes. Entropy changes calculated from these extrapolations do, however, qualitatively correspond to the entropy lost in the $\lambda$ anomaly. The entropy as a function of temperature is shown in Fig. V-17 for three concentrations of ortho hydrogen at 15.9 cc/M. The entropy shown there includes a small contribution from the entropy of the lattice and the empty cell.

4. Discussion of Results

The volume dependence of the $\lambda$ anomaly was given by Eq. (V-6). Simple theories of cooperative phenomena indicate that the cooperative transition should have a critical temperature proportional to some linear combination of the various interactions that produce the effect. The volume dependence of $T_\lambda$ thus strongly supports the idea that the interaction primarily responsible for the anomaly is the electric quadrupole interaction.[57] At small molar volumes valence forces start to contribute to the interaction. The relative contribution of the valence forces is in qualitative agreement with what might be expected for the Hamiltonian derived by Orttung for the interaction between pairs of ortho molecules.[50]

The interpretation of the relative contribution of the $\lambda$ anomaly to the total anomalous entropy is not at all simple, and is well beyond the scope of this work. We might postulate that only certain types of configurations of $n$ ortho molecules contribute to the $\lambda$ anomaly, and that the remainder contribute to the broader anomaly. If any one of the $n$ molecules in a configuration contributing to the $\lambda$ anomaly is converted to para hydrogen, then the entire entropy ($nk\ln 3$) of that configuration is lost in the $\lambda$ anomaly, and $(n-1)k\ln 3$ is added to the entropy of the broad anomaly. This would explain the rapid decrease in the $\lambda$ anomaly in the absence of self diffusion. It does not by itself, however, explain why all the entropy of the $n-1$ remaining molecules is added at temperatures below the original $\lambda$ temperature. The energy levels of configurations that do <u>not</u> contribute to the $\lambda$ anomaly also depend on their occupation. They thus do not produce a

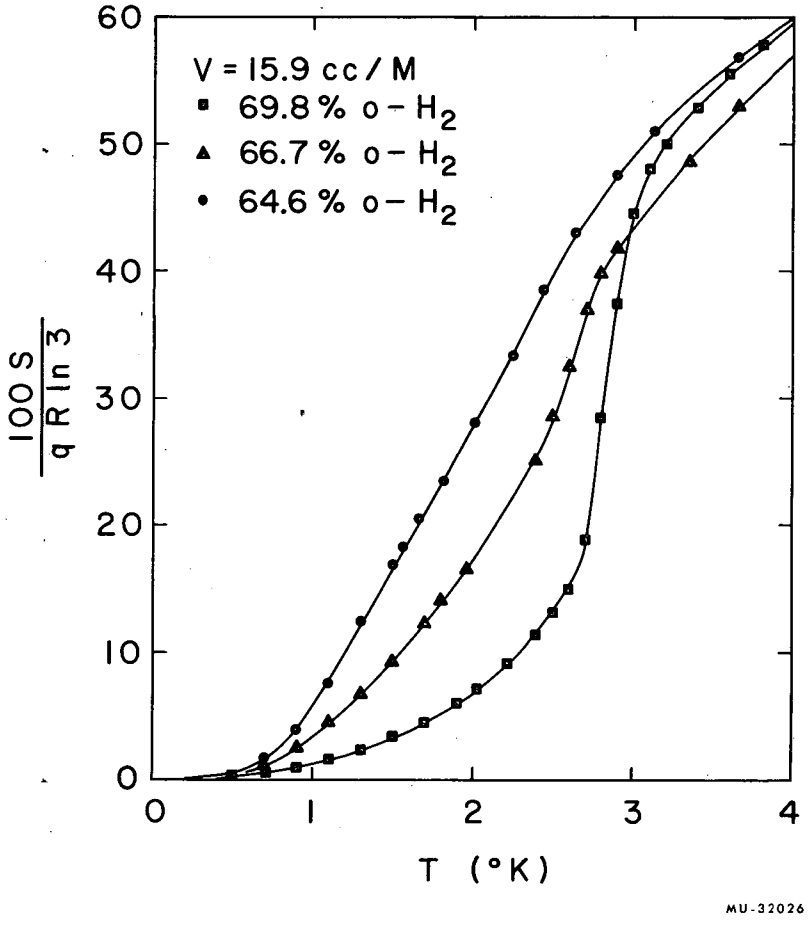


Fig. V-17. The estimated total entropy of the sample and the cell at three concentrations of ortho hydrogen at 15.9 cc/M.

heat-capacity contribution of the Schottky type, but rather a contribution compressed towards low temperature.

The interpretation of the existence of at least two distinct maxima in the λ anomaly is equally uncertain. It could be indicative of the presence of two phases. This is considered unlikely because no basic change in the doublets was observed when the molar volume was varied. Alternatively it could be due to two or more different types of configurations, all of which give rise to a λ anomaly, the λ temperature being different for the different types.

It can be concluded that the λ anomaly is much more complicated than simple order-disorder transitions, and that simple theories such as those used by Tomita[57] need considerable extension before they will be capable of explaining even the qualitative features of the anomalous heat capacity of hydrogen at high ortho concentrations.

## VI. THE KINETICS OF THE ORTHO-PARA CONVERSION

The homogeneous conversion of ortho hydrogen to para hydrogen in the liquid and solid state at zero pressure has been studied by a number of investigators.[56,58] It is generally agreed that the conversion follows a second-order rate law with a temperature-independent rate constant. In the solid state at sufficiently low temperatures, there is a deviation from second order after the conversion has progressed for about 100 h because of the formation of isolated ortho molecules.[58] McCormick determined the second-order rate constant at a molar volume of 13.7 cc by observing the change in intensity of the NMR signal with time.[55] The rate constant for the ortho-para conversion was measured during the course of this work at zero pressure and at two smaller molar volumes by permitting normal hydrogen to convert in pressure cell I for a number of hours, and then measuring the final concentration by the thermal-conductivity method. These measurements were made over a time short enough that the effect of forming isolated ortho molecules was unimportant. The molar volume of the samples was determined by the method described in Sec. III.

Some of the rate constants determined by various investigators are given in Table VI-1. They are also plotted in Fig. VI-1 as a function of molar volume on a logarithmic scale. Within experimental error the rate constants are proportional to $R^{-8}$, where R is the intermolecular separation. The rate constant appears to be unaffected by temperature.

Cremer[58] first suggested, on the basis of theoretical calculations by Wigner,[59] that the rate constant should depend on $R^{-8}$. More recently calculations were made by Motizuki and Nagamiya in which the emission of phonons is considered in some detail in the Debye approximation.[60] They show that two-phonon emission should be the dominating process for the dissipation of the energy of the conversion. A rather complicated dependence on the molar volume through the sound velocity results, and it was estimated by McCormick[55] that the rate constant should depend on $R^{-12}$. It is apparent from Fig. V-1 that this dependence is not realized.

Table VI-1. The second-order rate constant for the ortho-para conversion.

| Investigator | $k \times 10^5$ $(\% \ h)^{-1}$ | Volume (cc/M) | Temperature (°K) |
|---|---|---|---|
| Cremer (Ref. 58) | 17.5 ± 0.2 | 23.0 ± 0.1 | 11 to 12 |
| Cremer (Ref. 58) | 11.2 ± 0.1 | 28.39 ± 0.01 (liquid) | 20 |
| Smith & Housley (Ref. 56) | 18.1 | 22.64 ± 0.1 | 2 |
| McCormick (Ref. 55) | 75 | 13.7 | — |
| This work | 18.2 ± 0.3 | 22.64 ± 0.10 | 2 to 4 |
| This work | 18.2 ± 0.3 | 22.64 ± 0.10 | 2 to 4 |
| This work | 18.1 ± 0.3 | 22.64 ± 0.10 | 2 to 4 |
| This work | 29.9 ± 0.5 | 18.98 ± 0.10 | 9 to 20 |
| This work | 45.6 ± 0.5 | 16.42 ± 0.10 | 3 to 20 |

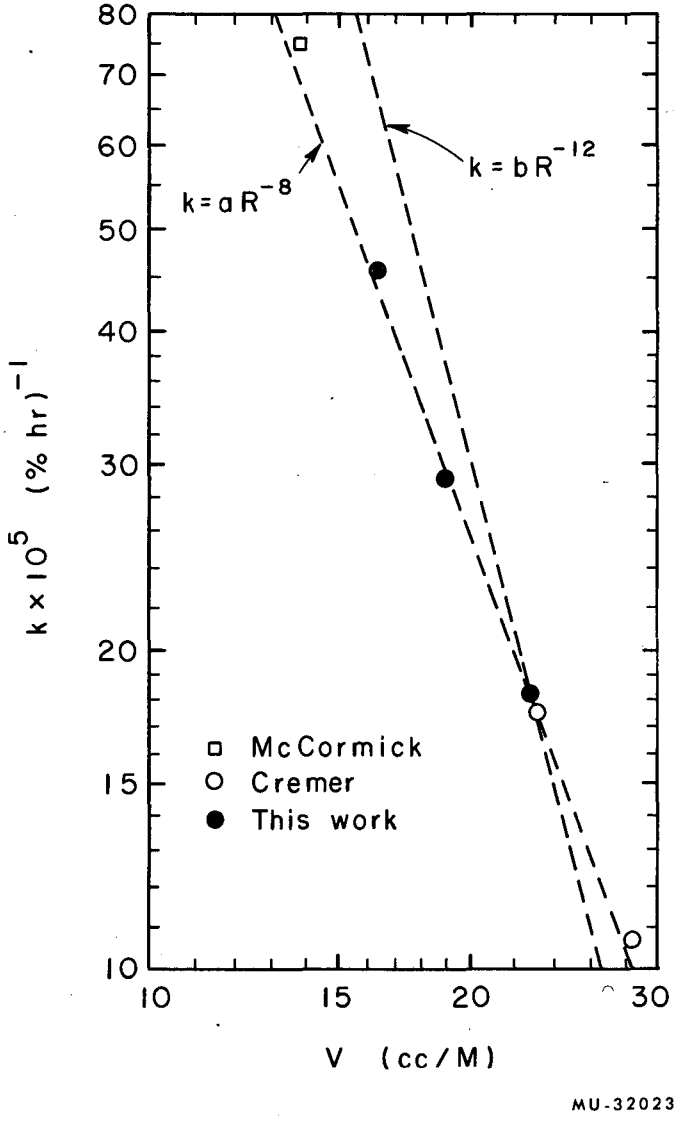


Fig. VI-1. The rate constant for the ortho-para conversion as a function of molar volume.

A logical extension of the theory of Motizuki and Nagamiya would have to permit one-phonon emission at molar volumes smaller than about 19 cc, because at smaller volumes the Debye theta becomes larger than the energy difference between the $J = 0$ and $J = 1$ states. For the para-ortho conversion in deuterium the rate was calculated with one-phonon emission,[61] and found to be an order of magnitude larger than with two-phonon emission.[62] For hydrogen, three-phonon emission is only about one tenth as efficient as two-phonon emission.[60] It can thus be expected that the theoretical rate constant for hydrogen should discontinuously increase by perhaps one order of magnitude for volumes less than 19 cc/M. No such increase is manifested by the experimental data. It is suspected that this discrepancy may be due to the deficiency of the Debye theory for the treatment of high-energy phonons in the case of solid hydrogen, for which anharmonicity effects are severe due to the large zero-point energy.

During the studies on the $\lambda$ anomaly, the rate constants of two samples with molar volumes of 19.4 and 15.9 cc were determined from the heat evolution in the samples between 1.6 and 2.7 °K and between 1.6 and 3.6 °K respectively. No temperature dependence was observed. It is estimated from the possible experimental errors that the rate constants were independent of temperature to within 10% over the respective temperature ranges.

## ACKNOWLEDGMENTS

The author is grateful to Dr. Kenneth S. Pitzer for suggesting this problem, to Dr. William H. Orttung for designing and partially constructing the apparatus, and to Dr. Norman E. Phillips for his guidance throughout the experimental work.

The author is indebted to the National Science Foundation and the General Electric Company for predoctoral fellowships during the academic years 1960-62 respectively, and to the U. S. Atomic Energy Commission for support of this project.

## REFERENCES


1. G. K. Horton and J. W. Leech, unpublished data.
2. R. H. Beaumont, H. Chihara, and J. A. Morrison, Proc. Phys. Soc. (London), 78, 1462 (1961).
3. P. Flubacher, A. J. Leadbetter, and J. A. Morrison, Proc. Phys. Soc. (London), 78, 1449 (1961).
4. R. W. Hill and B. W. A. Ricketson, Phil. Mag. 45, 277 (1954).
5. R. W. Hill, B. W. A. Ricketson, and F. Simon, International Conference on Low Temperature Physics and Chemistry (4th Conference, Paris, 1955), No. 76.
6. William H. Orttung, Thermal Properties of Solid Hydrogen under Pressure (Ph. D. Thesis), Lawrence Radiation Laboratory Report UCRL-9388, February 1961 (unpublished).
7. P. W. Bridgman, The Physics of High Pressure, (G. Bell and Sons, Ltd., London, 1958), Chapter II.
8. E. J. Walker, Rev. Sci. Instr. 30, 834 (1959).
9. W. DeSorbo and G. E. Nichols, J. Phys. Chem. Solids 6, 352 (1958).
10. Lawrence V. Gregor, The Heat Capacity of Silver Oxide at Low Temperatures (Ph. D. Thesis), Lawrence Radiation Laboratory Report UCRL-9723, May 31, 1961 (unpublished).
11. R. B. Scott and F. G. Brickwedde, J. Chem. Phys. 5, 736 (1937).
12. Harry Roger O'Neal, The Low Temperature Heat Capacity of Tin and Indium (Ph. D. Thesis), Lawrence Radiation Laboratory Report UCRL-10426, January 1963 (unpublished).
13. J. P. Franck, F. D. Manchester, and D. L. Martin, Proc. Roy Soc. (London) A263, 494 (1961).
14. Norman E. Phillips (Department of Chemistry, University of California, Berkeley, California), private communication.
15. G. Kneip, private communication.
16. J. Rayne, Australian J. Phys. 9, 189 (1956).
17. W. S. Corak, M. P. Garfunkel, C. B. Satterthwaite, and A. Wexler, Phys. Rev. 98, 1699 (1955).
18. F. J. du Chatenier and J. de Nobel, Physica 28, 181 (1962).

19. M. Giffel, R. W. Vest, and J. F. Smith, J. Chem. Phys. 27, 1267 (1957).
20. F. D. Manchester, Can. J. Physics 37, 989 (1959).
21. K. G. Ramanathan and T. M. Srinivasan, J. Sci. Ind. Res. (India) 16B, 277 (1957).
22. W. H. Keesom and A. P. Keesom, Physica 3, 105 (1936).
23. F. J. Webb, K. R. Wilkinson, and J. Wilks, Proc. Roy. Soc. (London) A214, 546 (1952).
24. J. S. Dugdale and F. E. Simon, Proc. Roy. Soc. (London) A218, 291 (1953).
25. E. C. Heltemes and C. A. Swenson, Phys. Rev. Letters 7, 363 (1961).
26. D. O. Edwards, A. S. McWilliams, and J. G. Daunt, Phys. Letters 1, 218 (1962).
27. Guenter Ahlers, Phys. Rev. Letters 10, 439 (1963).
28. E. Bartholomé and A. Eucken, Z. Elektrochem. 42, 547 (1936).
29. M. E. Hobbs, J. Chem. Phys. 7, 318 (1939).
30. H. W. Wooley, R. B. Scott, and F. G. Brickwedde, J. Res. Nat. Bur. Std. (U. S.) 41, 379 (1948).
31. H. van Dijk, M. Durieux, J. R. Clement, and J. K. Logan, Nat. Bur. Std. (U. S.) Monograph 10, June 17, 1960.
32. R. W. Hill and O. V. Lounasmaa, Phil. Mag. 4, 785 (1959).
33. E. Bartholomé, Z. Physik. Chem. B33, (Leipzig) 387 (1936).
34. R. D. Goodwin and H. M. Roder, Cryogenics 3, 12 (1963).
35. H. D. Megaw, Phil. Mag. 28, 129 (1939).
36. R. D. Goodwin, D. E. Diller, H. M. Roder, and L. A. Weber, J. Res. Nat. Bur. Std. (U. S.) 67A, 173 (1963).
37. R. D. Goodwin, D. E. Diller, H. M. Roder, and L. A. Weber, Cryogenics 1, 81 (1961).
38. R. D. Goodwin, Cryogenics 2, 353 (1962).
39. H. M. Roder, D. E. Diller, L. A. Weber, and R. D. Goodwin, Cryogenics 3, 16 (1963).
40. J. W. Stewart and C. A. Swenson, Phys. Rev. 94, 1069 (1954).
41. J. W. Stewart, Phys. Rev. 97, 578 (1955).
42. J. W. Stewart, J. Phys. Chem. Solids 1, 146 (1956).

43. K. Clusius and K. Hiller, Z. Physik. Chem. B4, (Leipzig) 158 (1929).
44. R. L. Mills and E. R. Grilly, Phys. Rev. 101, 1246 (1956).
45. G. W. Smith and C. F. Squire, Phys. Rev. 111, 188 (1958).
46. K. Clusius and E. Bartholomé, Z. Physik. Chem. (Leipzig) B30, 237 (1935).
47. O. V. Lounasmaa, J. Chem. Phys. 33, 443 (1960).
48. E. R. Grilly and R. L. Mills, Ann. Phys. (N. Y.) 18, 250 (1962).
49. J. W. Stewart, unpublished data.
50. W. H. Orttung, J. Chem. Phys. 36, 652 (1962).
51. T. Nakamura, Progr. Theoret. Phys. (Kyoto) 14, 135 (1955).
52. J. Hatton and B. V. Rollin, Proc. Roy. Soc. (London) A199, 222 (1949).
53. F. Reif and E. M. Purcell, Phys. Rev. 91, 631 (1953).
54. T. Sugawara, Y. Masuda, T. Kanda, and E. Kanda, Sci. Rept. Res. Inst. Tohoku Univ. A7, 67 (1955).
55. W. D. McCormick, Nuclear Magnetic Resonance in Solid Hydrogen at High Pressure (Ph. D. Thesis), Dept. of Physics, Duke University, Durham, North Carolina, April 24, 1959.
56. G. W. Smith and R. M. Housley, Phys. Rev. 117, 732 (1960).
57. K. Tomita, Proc. Phys. Soc. (London) A68, 214 (1955).
58. E. Cremer, Z. Physik. Chem. B39, 445 (1938).
59. E. Wigner, Z. Physik. Chem. B23, 28 (1933).
60. K. Motizuki and T. Nagamiya, J. Phys. Soc. Japan 11, 93 (1956). For Errata see ibid. 11, 656 (1956).
61. K. Motizuki, J. Phys. Soc. Japan 17, 1192 (1962).
62. K. Motizuki, J. Phys. Soc. Japan 12, 163 (1957).
63. J. W. Stewart, J. Phys. Chem. Solids 1, 146 (1956).

This report was prepared as an account of Government sponsored work. Neither the United States, nor the Commission, nor any person acting on behalf of the Commission:

A. Makes any warranty or representation, expressed or implied, with respect to the accuracy, completeness, or usefulness of the information contained in this report, or that the use of any information, apparatus, method, or process disclosed in this report may not infringe privately owned rights; or

B. Assumes any liabilities with respect to the use of, or for damages resulting from the use of any information, apparatus, method, or process disclosed in this report.

As used in the above, "person acting on behalf of the Commission" includes any employee or contractor of the Commission, or employee of such contractor, to the extent that such employee or contractor of the Commission, or employee of such contractor prepares, disseminates, or provides access to, any information pursuant to his employment or contract with the Commission, or his employment with such contractor.